

University of Windsor

Scholarship at UWindor

Electronic Theses and Dissertations

Theses, Dissertations, and Major Papers

1992

Geology, hydrothermal activity and gold mineralization in the Gemmell Lake area of the Early Proterozoic, Lynn Lake greenstone belt, Manitoba.

George R. Sherman
University of Windsor

Follow this and additional works at: <https://scholar.uwindsor.ca/etd>

Recommended Citation

Sherman, George R., "Geology, hydrothermal activity and gold mineralization in the Gemmell Lake area of the Early Proterozoic, Lynn Lake greenstone belt, Manitoba." (1992). *Electronic Theses and Dissertations*. 2223.

<https://scholar.uwindsor.ca/etd/2223>

This online database contains the full-text of PhD dissertations and Masters' theses of University of Windsor students from 1954 forward. These documents are made available for personal study and research purposes only, in accordance with the Canadian Copyright Act and the Creative Commons license—CC BY-NC-ND (Attribution, Non-Commercial, No Derivative Works). Under this license, works must always be attributed to the copyright holder (original author), cannot be used for any commercial purposes, and may not be altered. Any other use would require the permission of the copyright holder. Students may inquire about withdrawing their dissertation and/or thesis from this database. For additional inquiries, please contact the repository administrator via email (scholarship@uwindsor.ca) or by telephone at 519-253-3000ext. 3208.



National Library
of Canada

Bibliothèque nationale
du Canada

Canadian Theses Service

Service des thèses canadiennes

Ottawa, Canada
K1A 0N4

NOTICE

The quality of this microform is heavily dependent upon the quality of the original thesis submitted for microfilming. Every effort has been made to ensure the highest quality of reproduction possible.

If pages are missing, contact the university which granted the degree.

Some pages may have indistinct print especially if the original pages were typed with a poor typewriter ribbon or if the university sent us an inferior photocopy.

Reproduction in full or in part of this microform is governed by the Canadian Copyright Act, R.S.C. 1970, c. C-30, and subsequent amendments.

AVIS

La qualité de cette microforme dépend grandement de la qualité de la thèse soumise au microfilmage. Nous avons tout fait pour assurer une qualité supérieure de reproduction.

S'il manque des pages, veuillez communiquer avec l'université qui a conféré le grade.

La qualité d'impression de certaines pages peut laisser à désirer, surtout si les pages originales ont été dactylographiées à l'aide d'un ruban usé ou si l'université nous a fait parvenir une photocopie de qualité inférieure.

La reproduction, même partielle, de cette microforme est soumise à la Loi canadienne sur le droit d'auteur, SRC 1970, c. C-30, et ses amendements subséquents.

Geology, Hydrothermal Activity and Gold Mineralization
in the Gemmell Lake Area of the Early Proterozoic,
Lynn Lake Greenstone Belt, Manitoba

by

George R. Sherman

A Thesis

Submitted to the Faculty of Graduate Studies and Research
through the Department of Geology
in Partial Fulfillment of the Requirements for the
Degree of Master of Science at the
University of Windsor

Windsor, Ontario, Canada
1992



National Library
of Canada

Bibliothèque nationale
du Canada

Canadian Theses Service Service des thèses canadiennes

Ottawa, Canada
K1A 0N4

The author has granted an irrevocable non-exclusive licence allowing the National Library of Canada to reproduce, loan, distribute or sell copies of his/her thesis by any means and in any form or format, making this thesis available to interested persons.

The author retains ownership of the copyright in his/her thesis. Neither the thesis nor substantial extracts from it may be printed or otherwise reproduced without his/her permission.

L'auteur a accordé une licence irrévocable et non exclusive permettant à la Bibliothèque nationale du Canada de reproduire, prêter, distribuer ou vendre des copies de sa thèse de quelque manière et sous quelque forme que ce soit pour mettre des exemplaires de cette thèse à la disposition des personnes intéressées.

L'auteur conserve la propriété du droit d'auteur qui protège sa thèse. Ni la thèse ni des extraits substantiels de celle-ci ne doivent être imprimés ou autrement reproduits sans son autorisation.

ISBN 0-315-72807-8

Canada

© George Randolph Sherman 1992

ABSTRACT

Gold mineralization in the Gemmell Lake area of the Early Proterozoic, Lynn Lake greenstone belt is hosted by the northeast-striking, brittle-ductile, Finlay McKinlay shear zone. The shear zone is characterized by early mylonites which are crosscut by two vein sets and late, pseudotachylyte-bearing faults. Grain-size reduction and alteration of metamorphic minerals indicate that the mylonites formed after the peak of regional metamorphism. Kinematic indicators of the mylonites indicate sinistral reverse oblique displacement.

Gold mineralization in the Finlay McKinlay shear zone occurs in the second of two vein sets. These veins are characterized by vein breccia, vein ribbons and secondary veinlets. Four stages of veinlets have been recognized. In order of formation, these are: 1) epidote-clinzoisite-magnetite; 2) pyrite-chalcopyrite-pyrrhotite; 3) native gold-galena-pyrite-chalcopyrite-galena-hessite-tellurobismuth and 4) sphalerite-covellite.

Fluid inclusion data indicate that four types of fluids infiltrated the Finlay McKinlay shear zone. These are: 1) low density aqueous vapours; 2) moderate to low salinity aqueous fluids; 3) low salinity, H₂O-CO₂ fluids with minor CH₄ and N₂ (< 12 mole % CH₄.) and 4) a high salinity, aqueous fluid, (29 to 30 wt % NaCl + CaCl₂ equiv.).

Fluid inclusion data indicate that moderate salinity aqueous fluids (12 to 14 wt% NaCl +CaCl₂) were trapped in vein set 1; lower salinity aqueous fluids (4 to 8 wt% equiv. NaCl + CaCl₂); occur in both vein sets and the lowest salinity aqueous fluid (0 to 3 wt % equiv. NaCl + CaCl₂) occur only in vein set 2. This data indicates that the salinity of the aqueous fluids decreased with time.

Gold mineralization occurs in veinlets in vein set 2 quartz. The lowest salinity aqueous fluids appear to be the mineralizing fluids.

ACKNOWLEDGEMENTS

I would like to thank Lynngold Resources, specifically, Jim Chornaby and Phil Wright, who provided access to the Shoe-Lace claim group, company reports of exploration along the Johnson shear zone, support during the field season, and financial assistance through summer employment.

I would also like to thank the Manitoba Department of Energy and Mines for supplying equipment and additional financial assistance. I would like to thank Dr. Mark Fedikow and Dr. David Baldwin of the Geological Services Branch for initiating the project and providing insight prior to and during field work in the Gemmell Lake area.

I would like to thank Dr. Iain Samson of the Department of Geology, University of Windsor for his guidance during the course of this thesis. I would also like to recognize the direction and support provided by Dr. Paul Holm of the Department of Geology, University of Windsor.

I would like to thank Hank Jones of the University of Michigan for his assistance and expertise with quadrupole mass spectrometry.

Finally, I would like to thank Susan Temporal for her assistance in preparing the final draft of this thesis. I don't know where I would be without her.

TABLE OF CONTENTS

ABSTRACT	iv
ACKNOWLEDGEMENTS	vi
LIST OF FIGURES	x
LIST OF TABLES	xiii
CHAPTER 1 INTRODUCTION	1
CHAPTER 2 REGIONAL GEOLOGY OF THE LYNN LAKE GREENSTONE BELT	
2.1 Introduction	8
2.2 Wasekwan Group	8
2.3 Sickle Group	8
2.4 Intrusive Rocks	10
2.5 Metamorphism	10
2.6 Deformation	11
Folds	11
Shear Zones	12
CHAPTER 3 GEOLOGY OF THE GEMMELL LAKE AREA	
3.1 Introduction	13
3.2 Wasekwan Group	13
Felsic Metavolcanic Flows and Pyroclastic Rocks (Unit 1)	
Mafic Metavolcanic Flows and Metasedimentary Rocks (Unit 2)	
Metasedimentary Rocks (Unit 3)	
3.3 Sickle Group	17
3.4 Intrusive Rocks	18
3.5 Discussion	19
3.6 Metamorphism	20
3.7 Regional Fabrics	22
CHAPTER 4 DEFORMATION ZONES AND GOLD MINERALIZATION IN THE GEMMELL LAKE AREA	
4.1 Introduction	25
4.2 PROSPECTOR DEFORMATION ZONE	27
4.2.1 Folds (F ₂)	27
4.2.2 Crenulation Cleavage (S ₂)	29
4.2.3 Veins	29
1) Quartz-Carbonate Veins	
2) Folded Quartz Veins	
3) Quartz Veins	

4.2.4	Fault Zones	31
4.2.5	Sequence of Events	34
4.3	FINLAY MCKINLAY DEFORMATION ZONE	37
4.3.1	Tonalite	37
4.3.2	Mylonites	37
	Protomylonite	
	Mylonite	
	Ultramylonite	
4.3.3	Kinematic Indicators	40
	Planar (S ₂) and Linear Fabric (L ₂)	
	Shear Bands	
	Porphyroclast/Tail Systems	
	Fractured and Displaced Grains	
4.3.4	Mineralogical Changes Accompanying	
	Mylonitization	46
4.3.5	Veins	48
	1) NE-SW striking quartz veins	
	2) N-S striking Quartz ± Sulphide Veins	
	Vein Breccia	
	Vein Ribbons	
	Veinlets	
	Tourmaline-Epidote-Clinzoisite-Magnetite	
	Veinlets	
	Sulphide Veinlets	
	Native Gold Tellurides	
	Sphalerite-Covellite	
	Hydrothermal Alteration	
4.3.6	Faults	56
4.3.7	Sequence of Events	57
4.4	Comparison of the Finlay McKinlay and	
	Prospector Deformation Zones.....	60
4.5	Comparison of the Finlay McKinlay and	
	Johnson Shear Zones	62

CHAPTER 5 FLUID INCLUSIONS IN THE FINLAY MCKINLAY
 DEFORMATION ZONE

5.1	Introduction	64
5.2	Characteristics of Fluid Inclusions in the	
	Finlay McKinlay Deformation Zone	65
5.3	Fluid Inclusion Compositions	69
5.3.1	Aqueous, Liquid-Vapour Inclusions (Type 1) ...	69
5.3.2	Vapour-rich Inclusions (Type 2)	71
5.3.3	Aqueous-Carbonic Inclusions (Type 3)	71
5.3.4	Aqueous, Liquid-only Inclusions (Type 4).....	79
5.4	Fluid Evolution	81

CHAPTER 6	DISCUSSION	
6.1	Gold Transport Mechanisms	88
6.1.1	Sulphide Complexes.....	88
6.1.2	Chloride Complexes	89
6.2	Mechanisms of Gold Deposition	90
	1) Wall Rock Interaction	
	2) Solution Mixing	
	3) Boiling/CO ₂ Effervescence	
6.3	Comparison of Gold Mineralization in the Finlay McKinlay Occurrence and the Agassiz Metallotect	92
6.3.1	MacLellan Deposit	92
6.3.2	Farley Lake Deposits	96
6.3.3	Discussion	97
6.4	Gold Mineralization in the Central Metavolcanic Belt, LaRonge Domain	97
6.4.1	Star Lake Lode Gold Deposits	98
6.4.2	Discussion	99
CHAPTER 7	CONCLUSIONS	101
REFERENCES	103
APPENDICES	117
VITA AUCTORIS	147

LIST OF FIGURES

Figure 1	Generalized subdivisions of Archean, Early Proterozoic, and Middle Proterozoic terranes in North America.	2
Figure 2	Main geologic subdivisions of the Early Proterozoic rocks in the Saskatchewan-Manitoba section of the Trans-Hudson orogenic belt.	3
Figure 3	Generalized regional geology of the Lynn Lake greenstone belt showing the location of the study area relative to the Agassiz metallotect (A) and Johnson shear zone (J).....	5
Figure 4	Major stratigraphic subdivisions of the Lynn Lake greenstone belt.	9
Figure 5	Geology of the Gemmell Lake area.	14
Figure 6	Equal area stereonet projection of: (a) poles to S_1 foliation and (b) L_1 lineation in the Wasekwan Group; (c) poles to S_1 foliation and (d) L_1 lineation in the Sickie Group.	23
Figure 7	Location of the Prospector and Finlay McKinlay Deformation Zones in the Gemmell Lake area.	26
Figure 8	Equal area stereonet projection in the Prospector Deformation Zone of (a) Minor F_2 fold axes (dots) and poles to S_2 crenulation cleavage (asterisks); (b) Contoured equal area stereonet projection of the minor F_2 fold axes. (c) Equal area stereonet projection of the pole to fault planes (dots) and pseudotachylyte injection veins (asterisks); (d) Contoured equal area stereonet projection of the poles to fault planes and pseudotachylyte injection veins.	28
Figure 9	(a) vein sets 1 and 2; (b) boudinaged vein set 2 in a F_2 fold; (c) vein set 3 crosscuts minor F_2 fold; and (d) boudinaged and folded vein set 2 crosscut by a fault.	30

Figure 10	(a) Fault and injection vein relationships of pseudotachylyte; (b) Geometric relationships of pseudotachylyte veins.	33
Figure 11	Relative sequence of events in the Prospector deformation zone.	35
Figure 12	Equal area stereonet projection in the Finlay McKinlay shear zone of: (a) poles to the S_2 foliation; (b) L_2 lineation; (c) poles to fault planes and (d) poles to fault planes with pseudotachylyte.	41
Figure 13	Kinematic indicators of ductile deformation in the Finlay McKinlay shear zone: (a) Horizontal view of a shear band perpendicular to L_2 lineation; (b) Vertical view of a shear band perpendicular to S_2 foliation; (c) Porphyroclast and tails; (d) Fractured and displaced grains.	44
Figure 14	Sketch of the outcrop which hosts the gold mineralization in the Finlay McKinlay shear zone.	49
Figure 15	(a) Equal area stereonet projection of poles to veins; (b) Contoured equal area stereonet of poles to veins, point concentrations indicate the average orientation of Vein Set 1 (227/75 NW) and Vein Set 2 (187/78 W).	50
Figure 16	Paragenesis of veinlets in vein set 2. Four episodes of veining are represented by (I-IV)..	53
Figure 17	Relative sequence of events in Finlay McKinlay deformation zone.	58
Figure 18	Comparison of the relative sequence of events in the Prospector and Finlay McKinlay deformation zones.	61
Figure 19	Fluid inclusions in Vein Set 1	66
Figure 20	Fluid inclusions in Vein Set 2	67
Figure 21	Th vs TmICE diagram for aqueous, Type 1 inclusions in vein sets 1 and 2.	70
Figure 22	ThCO ₂ vs TmCO ₂ diagram for mixed H ₂ O-CO ₂ , Type 3 inclusions.	72

Figure 23	Estimates of X_{CH_4} in mixed H_2O-CO_2 , Type 3 inclusions using the diagram of Heyen et al. (1982).	75
Figure 24	T_h vs T_{mICE} diagram for aqueous, Type 4 inclusions in vein set 2.	80
Figure 25	Evolution of fluids in the Finlay McKinlay shear zone.	82
Figure 26	Limiting isochores of the fluid inclusions in the Finlay McKinlay shear zone.	84
Figure 27	Pressure-Temperature paths of fluids in the Finlay McKinlay shear zone.	85
Figure 28	Location of the MacLellan (M) and the Farley Lake (F) deposits along the Agassiz metathrust (A) relative to the Johnson shear zone (J) and study area (Square).	93
Figure 29	Surficial geology map of the MacLellan Deposits.	94

LIST OF TABLES

TABLE 1	Bulk Compositions of Aqueous-Carbonic Inclusions.	77
TABLE 2	Equations for Calculating Bulk Compositions of Mixed Aqueous-Carbonic Inclusions (Type 3)	78
TABLE 3	Quadrupole Mass Spectrometry Analysis of Vein Quartz.	79

CHAPTER 1

1.1 INTRODUCTION

The Lynn Lake greenstone belt lies within the LaRonge-Lynn Lake domain of the Early Proterozoic, Trans-Hudson orogenic belt which is confined between the Archean cratons of the Superior province and the Hearne province (Gilbert et al., 1980; Hoffman, 1989). In northern Manitoba and Saskatchewan, the Trans-Hudson Orogen is subdivided into two regions, known as the Cree Lake Zone and the Reindeer Lake Zone (Figure 1), the geology of which has been described by numerous authors including Lewry and Sibbald (1980), Lewry (1981), Lewry et al. (1981), Ray and Wanless, (1980), Stauffer (1984), Green et al. (1985), Van Schmus et al. (1986) and MacDonald (1987).

The LaRonge-Lynn Lake Domain lies within the Reindeer Lake Zone of the Trans-Hudson orogenic Belt. It is a northeast-southwest trending belt of dominantly metavolcanic rocks and plutons which extends for over 500 km from northeast Manitoba to beneath the Phanerozoic cover in central Saskatchewan (Figure 2).

The Lynn Lake greenstone belt is one of three early Proterozoic, greenstone terranes within the La Ronge-Lynn Lake domain (Figure 2). The Lynn Lake belt comprises a sequence of metamorphosed volcanic, sedimentary and plutonic rocks which attain a maximum strike length of 130 km and a width of 60 km (Gilbert et al. 1980) (Figure 3). The Rusty Lake greenstone belt is located to the southeast (Steeves

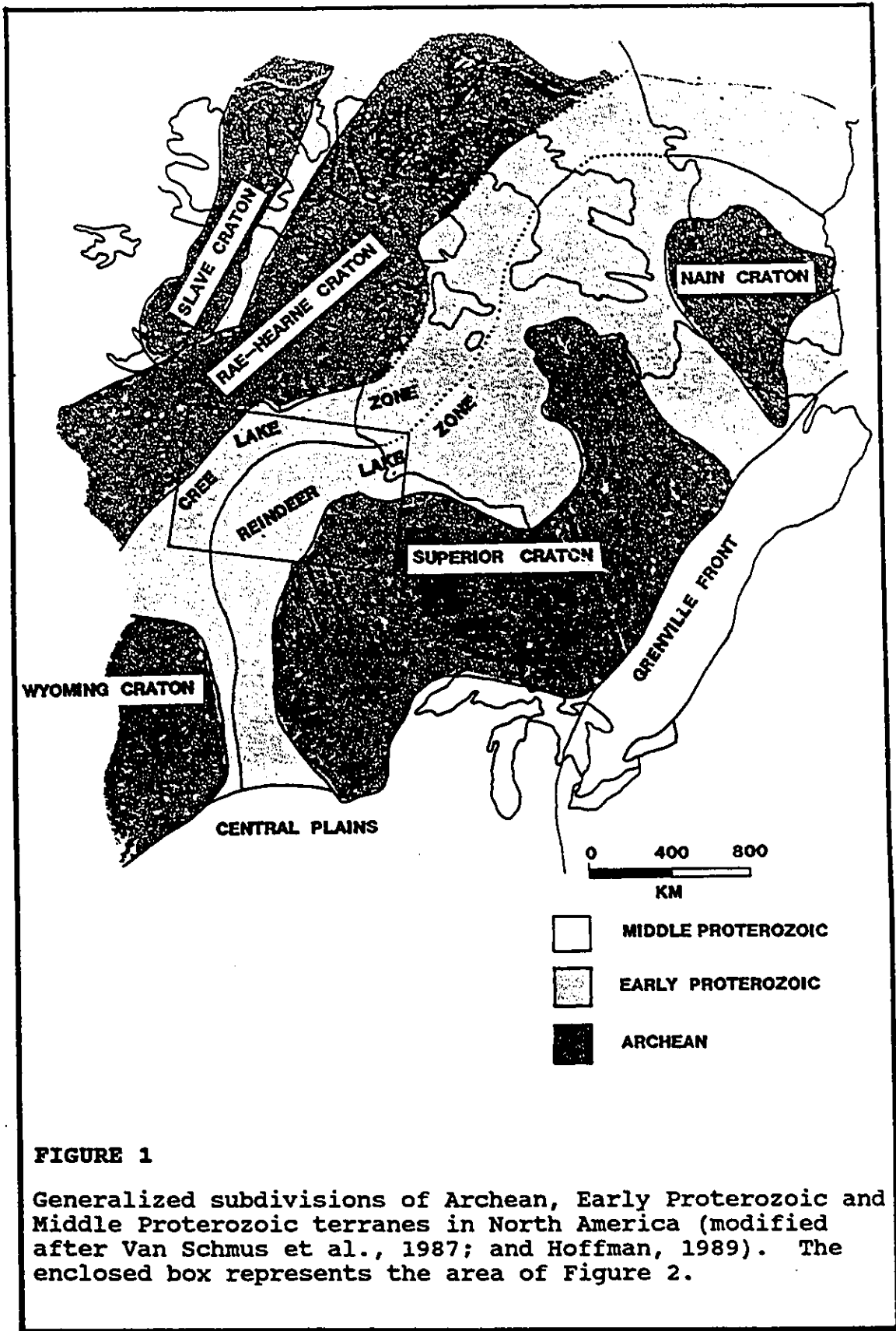


FIGURE 1

Generalized subdivisions of Archean, Early Proterozoic and Middle Proterozoic terranes in North America (modified after Van Schmus et al., 1987; and Hoffman, 1989). The enclosed box represents the area of Figure 2.

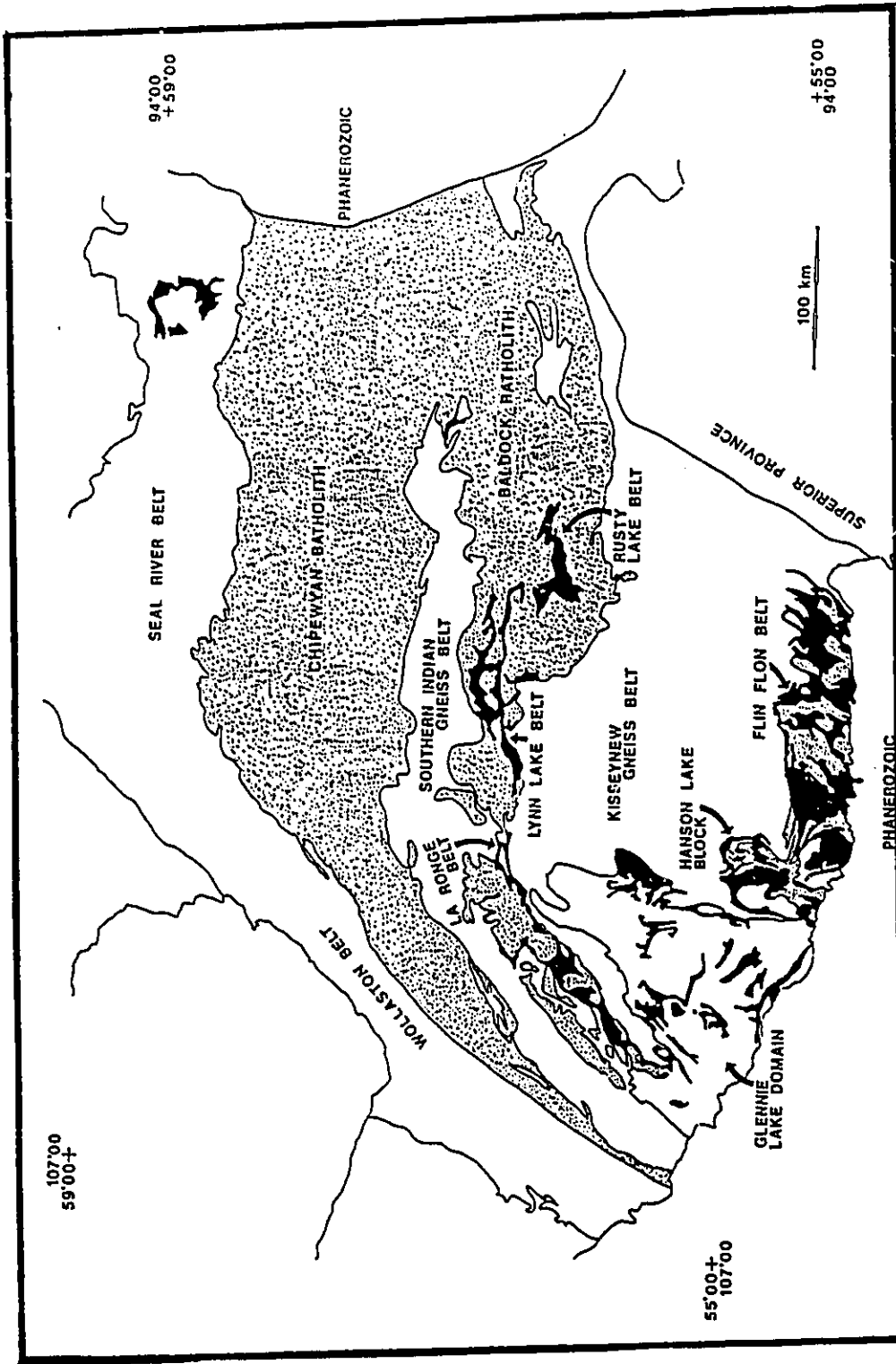


Figure 2 Main geologic subdivisions of the Early Proterozoic rocks in the Saskatchewan-Manitoba section of the Trans-Hudson orogenic belt. Areas of dominantly volcanic origin are shown in black, major plutonic areas are stippled, metasedimentary rocks and orthogneisses are white (modified after Baldwin, 1987).

and Lamb, 1972), and the Central Metavolcanic belt is located to the southwest, in Saskatchewan (Lewry et al 1981:) (Figure 2).

Gold deposits and occurrences in the Lynn Lake greenstone belt define two 'gold camps' or districts which are referred to as the Agassiz metallotect and the Johnson shear zone (Figure 3).

Agassiz Metallotect

The Agassiz metallotect, located in the northern part of the Lynn Lake greenstone belt, contains stratiform gold mineralization hosted by a sequence of dominantly mafic metavolcanic rocks that have been traced along strike for 70 km (Fedikow et al., 1986; Parbary, 1989; Gagnon, 1991).

Johnson Shear Zone

The Johnson shear zone (JSZ) is a 35-40 km long, east-west striking deformation zone which extends westward from One Island Lake to Franklin Lake in the southern part of the Lynn Lake greenstone belt. The deformation zone is up to 1.0 km wide and along most of its extent defines the southern boundary of the Lynn Lake greenstone belt.

The Johnson shear zone has been traditionally regarded as a zone of intense deformation (Milligan, 1960; Gilbert et al., 1980; Fedikow et al., 1986). Deformation in the JSZ truncates lithologic units and obliterates primary igneous, volcanic and sedimentary structures that are preserved in the adjacent rocks, and is characterized by schistosity, folds, crenulation cleavage, and quartz veins (Fedikow et

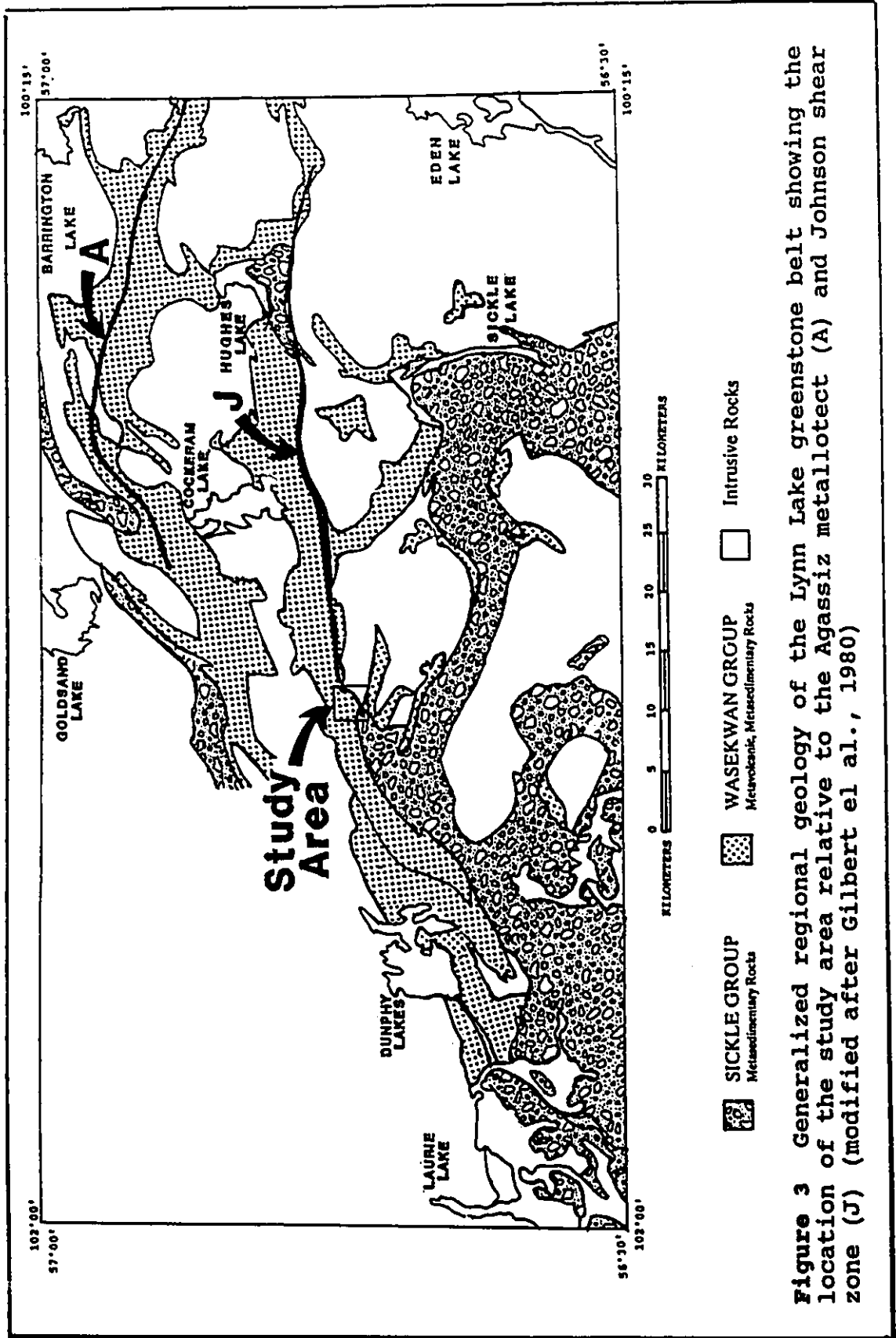


Figure 3 Generalized regional geology of the Lynn Lake greenstone belt showing the location of the study area relative to the Agassiz metallotect (A) and Johnson shear zone (J) (modified after Gilbert et al., 1980)

al., 1986). Previous work has suggested that the JSZ is the result of a distinct shearing event (Fedikow et al., 1986), however, shear zones have not been defined. Recently, the origin of the deformation and interpretation of the JSZ has been questioned. Peck (1984, 1985) suggested that deformation in the zone may have been the result of differential movement at the contact between rocks with contrasting ductility during regional deformation and metamorphism.

Most of the gold occurrences associated with the Johnson shear zone are quartz veins or stockworks which are hosted by a diverse assemblage of mafic to felsic metavolcanic, metasedimentary and intrusive rocks (Fedikow et al., 1986; Baldwin, 1987). Individual quartz veins may contain significant concentrations of gold and silver over narrow widths, ranging from 0.2 to 10.9 g of Au/tonne and from trace to 124.1 g of Ag/tonne (Fedikow et al., 1986). Individual quartz veins contain pyrite and native gold with variable amounts of galena, sphalerite, pyrrhotite, chalcopyrite, bornite and arsenopyrite (Milligan, 1960; Fedikow et al., 1986; Richardson and Ostry, 1987). Previous studies of the gold occurrences along the JSZ have concentrated on the geologic setting, petrography and geochemistry of the host rocks (Kenlay, 1982; Peck 1984, 1985, 1986; Ferreira, 1986; Fedikow et al., 1986). No previous work exists on either the style of deformation and its relationship to gold mineralization or on the nature,

composition and origin of the hydrothermal fluids associated with the gold deposits along the JSZ.

This study was initiated to investigate gold mineralization related to the JSZ in the Gemmell Lake area, which is located at the western end of the Johnson shear zone (Figure 3).

The main objective of the study was to understand the nature and timing of gold mineralization relative to the intrusive, metamorphic, deformation, and hydrothermal fluid history of the study area.

CHAPTER 2

REGIONAL GEOLOGY OF THE LYNN LAKE GREENSTONE BELT

2.1 Introduction

The Lynn Lake greenstone belt has been stratigraphically subdivided into a lower, dominantly volcanic, sequence (the Wasekwan Group) and an upper sedimentary sequence (the Sickie Group) (Figure 4) (Norman, 1933; Bateman, 1945; Milligan, 1960 and Gilbert et al. 1980). Similar subdivisions have been made in the Central Metavolcanic belt (Lewry et al., 1981), the Rusty Lake greenstone belt (Steeves and Lamb, 1972) and the Flin Flon and Snow Lake greenstone belts (Stauffer, 1984).

2.2 Wasekwan Group

The Wasekwan Group consists of metamorphosed mafic to felsic volcanic rocks with subordinate volcanoclastic and sedimentary rocks. The majority of the Wasekwan Group rocks occupy two northeast-striking belts which are referred to as the southern and northern belts. The geology, distribution and geochemistry of the Wasekwan Group rocks have been described in detail by Gilbert et al. (1980) and Syme (1985).

2.3 Sickie Group

The Sickie Group comprises a sequence of metamorphosed conglomerates and sandstones which unconformably overlie the Wasekwan group and a variety of mafic to felsic intrusions (Gilbert et al., 1980). The base of the Sickie Group consists of a polymictic conglomerate with sub-rounded

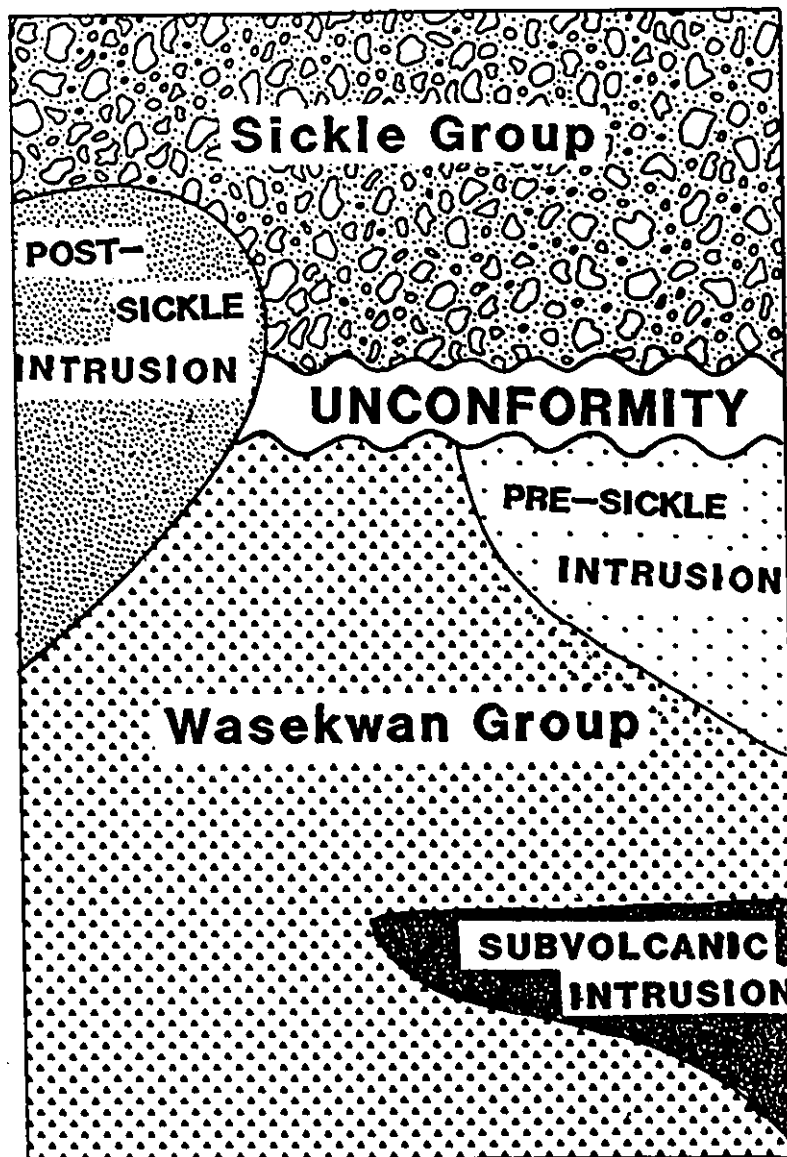


Figure 4 Major stratigraphic subdivisions of the Lynn Lake greenstone belt (modified after Gilbert et al., 1980; and Gagnon, 1991)

boulders, pebbles and cobbles consisting mainly of the various pre-Sickle volcanic and intrusive rocks, with rare clasts of chert or iron formation (Gilbert et al., 1980). Overlying, and/or interlayered with, the conglomerates are medium-grained to pebbly arkosic sandstones (Gilbert et al., 1980).

2.4 Intrusive Rocks

Numerous intrusive rocks occur throughout the Lynn Lake greenstone belt. These intrusions have been subdivided into pre- and post-Sickle suites (Milligan, 1960). The oldest intrusions consist of small, pre-Sickle, mafic to felsic sills and dykes which are similar in composition to their volcanic host rocks (Gilbert et al., 1980; Peck, 1986). Other pre-Sickle intrusions consist of composite plutons of diorite to granite and isolated plutons of gabbro, norite and minor ultramafic rocks (Milligan, 1960; Gilbert et al., 1980; Pinsent, 1980). A younger group of post-Sickle intrusions form plutons of gabbro, diorite, tonalite and granite (Milligan, 1960). Post-Sickle intrusions also include smaller bodies of pegmatites, graphic granite and quartz-feldspar porphyry (Milligan, 1960).

2.5 Metamorphism

The grade of regional metamorphism in the Lynn Lake greenstone belt varies from upper greenschist in the east to upper amphibolite facies in the west, however, most of the belt is characterized by lower to middle amphibolite facies mineral assemblages (Gilbert et al., 1980).

2.6 Deformation

Two periods of regional deformation are thought to have occurred in the Lynn Lake greenstone belt. D_1 deformation occurred during and after the deposition of the Wasekwan Group and D_2 deformation occurred after the deposition of the Sickle Group (Milligan, 1960).

Folds

Major, east to northeast-trending, tight to isoclinal folds (F_1) and a regional, axial planar foliation (S_1), which is generally developed parallel to the primary layering (S_0), are common in both the Wasekwan Group and the Sickle Group (Milligan, 1960; Gilbert et al., 1980). Major F_1 fold closures are difficult to identify and minor F_1 folds are generally absent (Milligan, 1960; Gilbert et al., 1980).

The southern belt is dominated by east to northeast-trending isoclinal, F_1 folds with vertical to steeply dipping (NW) axial planes that are spaced over 2 km apart (Gilbert et al., 1980). The structure of the northern belt, with the exception of some east to southeast-trending isoclinal F_1 folds in the eastern part of the belt, is dominated by a monoclinial sequence with a northwards younging direction (Gilbert et al., 1980). Superimposed on the earlier isoclinal F_1 folds are locally-developed, open F_2 folds with northeast-trending axial traces and an associated axial planar foliation (S_2) which has been observed within the Wasekwan Group, the Sickle Group and the

early plutons (Gilbert et al., 1980).

Shear Zones

East to northeast and north to northwest striking shear zones have been identified throughout the southern part of the Lynn Lake greenstone belt (Milligan, 1960; Gilbert et al., 1980). There has, however, been no previous work on the nature or geometry of these shear zones.

CHAPTER 3

GEOLOGY OF THE GEMMELL LAKE AREA

3.1 Introduction

The Gemmell Lake area is located approximately 14 kilometers southwest of the town of Lynn Lake, Manitoba at latitude 56°00'45" north and longitude 101°00'15" west (Figure 3). A study area in the Gemmell Lake area, approximately 1 km in width and 1.5 km in length, was mapped by the author during the summer of 1988 at a scale of 1:2400. The geologic mapping utilized an existing 200 foot grid which was cut for Shoe-Lace claim block 7811.

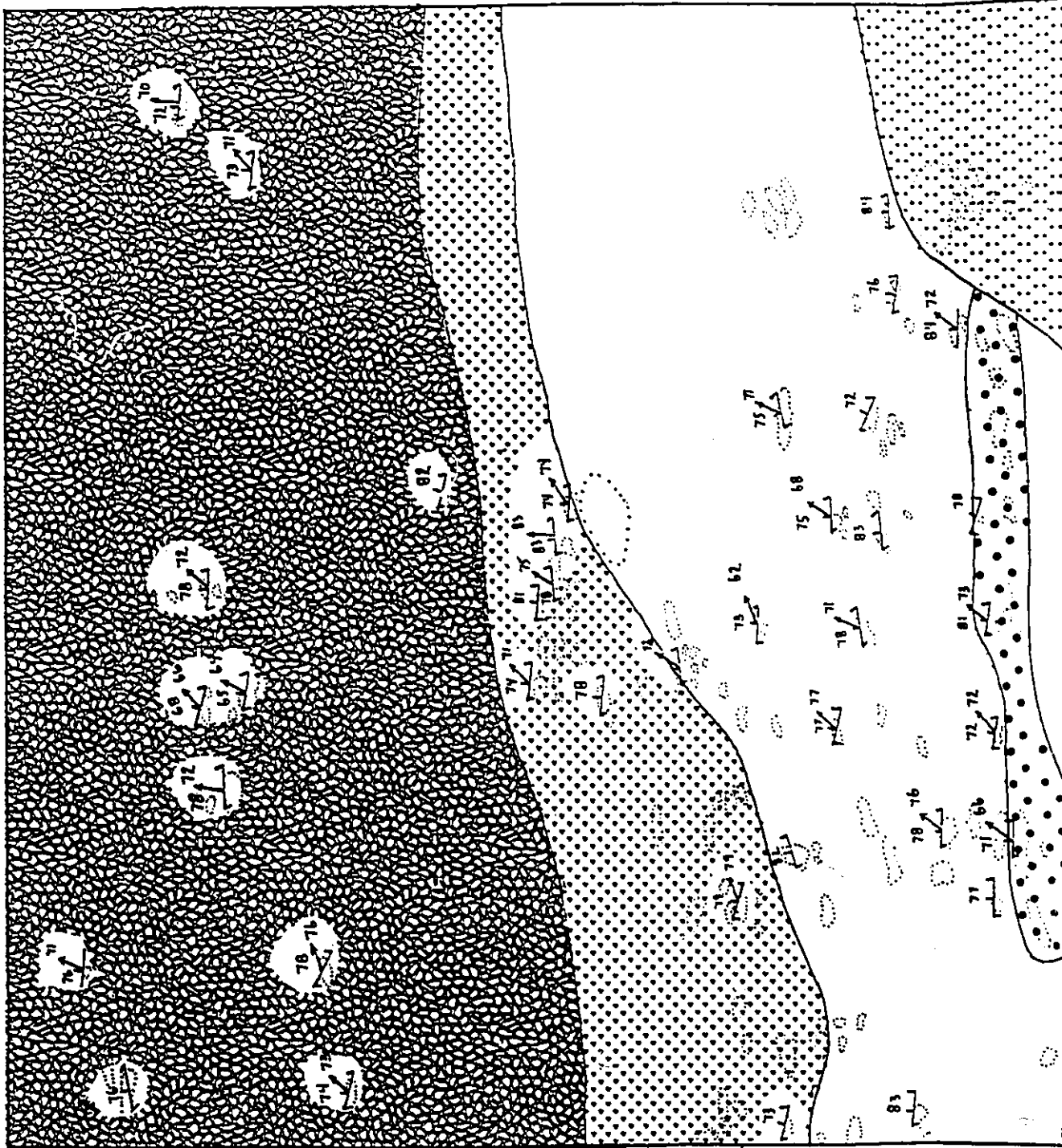
The rocks in the Gemmell Lake area comprise a sequence of Wasekwan Group rocks which are separated from the Sickle Group to the south by a large tonalite pluton (Figure 5). This chapter describes the geology of the Gemmell Lake area and compares the local stratigraphy, metamorphism and fabrics to the regional geology.

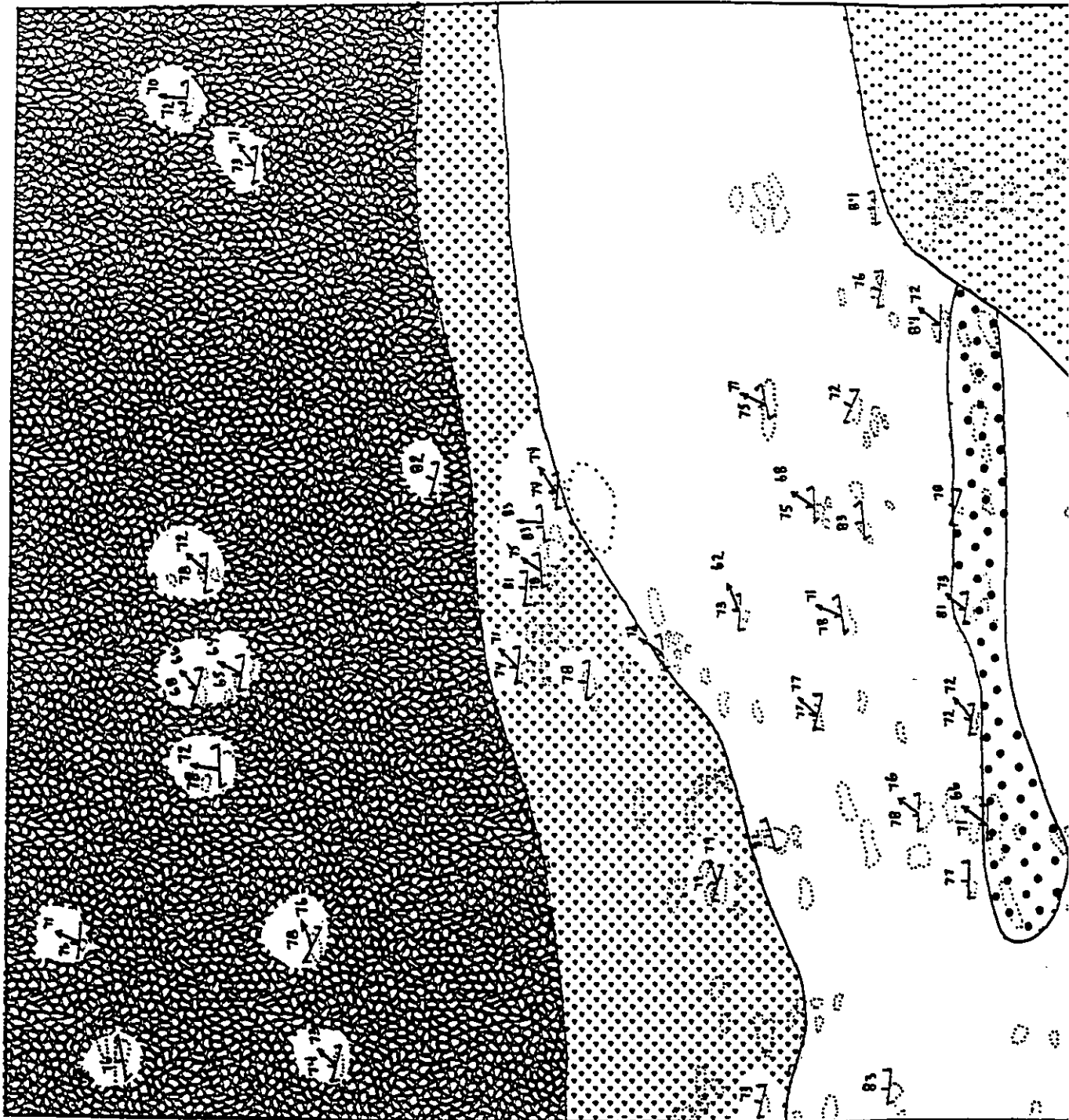
3.2 Wasekwan Group

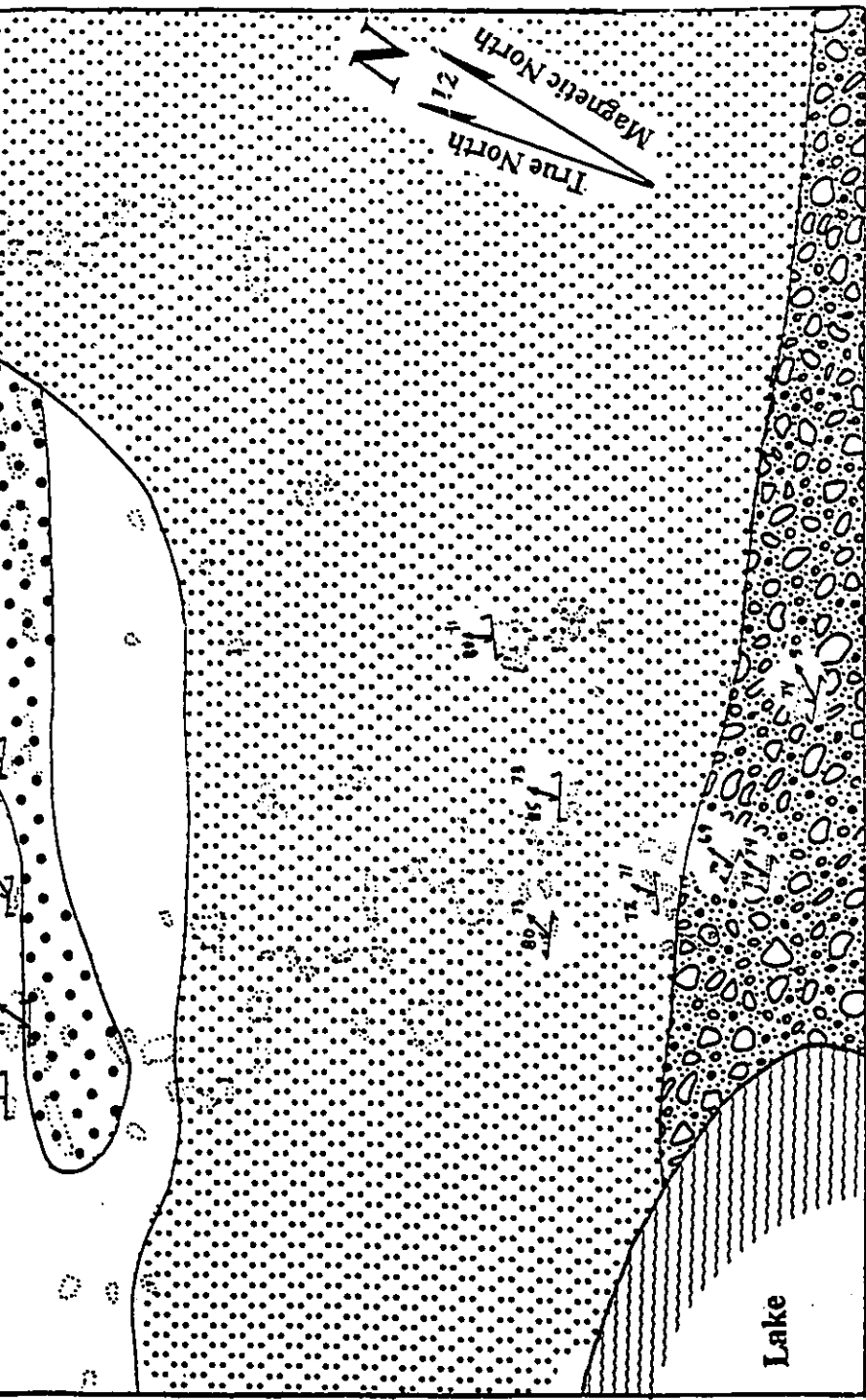
The Wasekwan Group in the Gemmell Lake area may be subdivided into three lithologic units that form a conformable stratigraphic sequence. Individual units strike east-west and dip steeply to the north at 70 to 80°.

Felsic Metavolcanic Flows and Pyroclastic Rocks (Unit 1)

The lower part of the sequence in the Gemmell Lake area is dominated by felsic metavolcanic rocks. Felsic metavolcanic flows vary in thickness from 10 to 30 m and have irregular upper contacts which are marked by an







INTRUSIVE ROCKS

SICKLE GROUP

WASEKWAN GROUP









-  Gabbro
-  Tonalite, Granodiorite
-  Metasedimentary Rocks
-  Unit 3 Metasedimentary Rocks
-  S₁ Foliation
-  Unit 2 mafic Metavolcanic Rocks
-  L₁ Lineation
-  Unit 1 Felsic Metavolcanic Rocks



Figure 5 Geology of the Gemmell Lake area.

oligomictic breccia. The flows and breccias consist of grey to white, massive to porphyritic rocks which contain grey-blue quartz phenocrysts (2-3 mm) (< 15 %), and porphyroblasts of garnet (1-2 mm) (< 5%) set in an aphanitic to fine-grained matrix consisting of quartz, feldspar, biotite and muscovite. Some of the flows contain fine-grained, disseminated (1-2 %) pyrite, pyrrhotite and chalcopyrite. The breccia comprises angular to subrounded felsic clasts, that range in size from 5 to 30 cm, and which are set in a predominantly felsic matrix.

In places, the felsic flows are overlain by, and intercalated with, discontinuous units of coarse-grained, crystal-lapilli tuff. The crystal-lapilli tuff comprises a banded, buff to grey brown, weak to moderately foliated quartzite which dominantly consists of grain-supported quartz phenocrysts (3-4 mm) with minor green hornblende, biotite and garnet.

Overlying the felsic flows and pyroclastic rocks, discontinuous felsic flows, generally less than 5 m thick, are interbedded with thinly bedded (4-5 cm to 1 m), mafic to quartzo-feldspathic schists. The felsic flows are pink to red, aphanitic to porphyritic rocks comprising phenocrysts of plagioclase and alkali feldspar in a banded, aphanitic to fine-grained, siliceous matrix with minor biotite and disseminated magnetite. Some of the quartzo-feldspathic schists contain pink, rounded to angular fragments, which are similar in composition to the felsic flows. These

fragments vary in size from 1 to 15 cm and are generally flattened in the plane of the foliation from 4:1 to 6:1. The quartzo-feldspathic schists are probably pyroclastic or epiclastic in origin.

Overlying the felsic flows is a thin sequence of chemical metasediments which contains beds of chert and rare beds of oxide-facies iron formation. The chert beds are massive to laminated, brown to buff coloured, and contain minor disseminated magnetite. The iron formation forms thin black layers (less than 2 cm thick) which are composed of massive magnetite.

Mafic Metavolcanic Flows and Metasedimentary Rocks (Unit 2)

In the Gemmell Lake area, a thick, heterogeneous unit of mafic metavolcanic rocks (Unit 2) overlies the felsic metavolcanic and metasedimentary rocks of Unit 1. The base of the unit predominantly consists of banded (2 cm to 1 m) mafic schists comprising fine-grained hornblende, quartz, biotite, and magnetite. Overlying and intercalated with these rocks is a sequence of massive mafic flows and breccias with minor pillowed and plagioclase-porphyrific flows. The mafic flows are generally massive, consisting of medium to coarse-grained hornblende porphyroblasts in a finer-grained matrix of hornblende, plagioclase and biotite. The pillowed mafic flows contain individual pillows which range in size from 12 to 30 cm that are defined by 2-3 cm wide, amphibole-rich selvages. The porphyritic mafic flows are characterized by euhedral plagioclase phenocrysts which

vary in size from 0.8 to 1 cm, set in an aphanitic to fine-grained, hornblende-chlorite matrix. The volcanic breccias form thin units (1 to 3 m thick) which contain heterolithic, rounded, felsic clasts (2 to 15 cm diameter) set in a well-foliated hornblende-biotite schistose matrix.

Metasedimentary Rocks (Unit 3)

The youngest unit of the Wasekwan Group predominantly consists of biotite-rich, quartzo-feldspathic schists which most likely represent a metasedimentary sequence. The base of the unit consists of a schistose, polymictic metaconglomerate containing pebble to cobble-sized clasts of granite and felsic to intermediate metavolcanic and metasedimentary rocks. The clasts are generally flattened and elongated in the plane of the foliation with aspect ratios of up to 10:1. These rocks grade upwards into a fine- to medium-grained quartzite which is interpreted as a metagreywacke or subarkosic metasandstone.

3.3 Sickle Group

Exposures of the Sickle Group occur in the southern part of the study area and represent the youngest lithologic unit in the area (Sherman et al., 1988; Gilbert et al., 1980). The base of the Sickle Group consists of a poorly-sorted, matrix-supported, polymictic metaconglomerate. The conglomerate clasts are well- to subrounded, range in size from boulders (30 x 20 cm) to pebbles, and include felsic, intermediate and mafic volcanics, granite, syenite, tonalite, quartz diorite, quartz, and magnetite-rich chert.

The schistose matrix is quartzo-feldspathic and contains abundant biotite, muscovite and/or magnetite. Interbedded with the metaconglomerate are thin beds (< 30 cm thick) of coarse-grained, quartzo-feldspathic metasandstone.

3.4 Intrusive Rocks

An intrusion separates the rocks of the Wasekwan Group from those of the Sickle Group. The intrusion grades from tonalite to granodiorite towards its northern contact and is characterized by coarse to medium-grained hornblende and anhedral, blue, quartz grains, set in a fine-grained plagioclase-hornblende-biotite matrix.

The northern contact with the Wasekwan Group is a sharp intrusive contact. The intrusive nature of the northern contact is supported by the presence of numerous mafic xenoliths which consist of hornblende and plagioclase. Milligan (1960) made similar observations and suggested that the xenoliths represent Wasekwan Group supracrustal rocks or inclusions of earlier gabbro or diorite.

The southern contact with the Sickle Group strikes at 255°, and dips to the north at 74°. The Sickle conglomerate contains clasts of tonalite and the matrix contains blue quartz grains which are typical of the intrusive rock. The presence of this material within the conglomerate suggests that the felsic intrusive rock pre-dates the deposition of the conglomerate. As a result, the contact between the Sickle Group and the tonalite intrusion appears to represent a nonconformity.

Mafic dykes and sills intrude the Wasekwan Group rocks and the tonalite pluton. No dykes were observed within the Wasekwan Group conglomerate or the Sickle Group. The mafic dykes are fine-grained, massive to weakly-foliated rocks and comprise prismatic hornblende with interstitial, anhedral plagioclase. In places, they contain minor disseminated pyrite and chalcopyrite. Contacts are generally sharp and chilled margins vary in width up to 5 cm.

3.5 Discussion

In the Gemmell Lake to Fox Mine section of the Lynn Lake greenstone belt the Wasekwan group has been subdivided into five stratigraphic units (Gilbert et al., 1980). The Wasekwan Group sequence consists of 1) the Fox Lake porphyritic basaltic suite, at the base of the sequence, overlain by 2) the Snake Lake dacites and rhyolites, 3) the Fox Mine succession, 4) the Fox Road turbidites and 5) the Wilmot Lake basaltic suite (Gilbert et al, 1980).

Geologic mapping in the Gemmell Lake area has identified three stratigraphic units. The base of the sequence is dominated by felsic metavolcanic rocks (unit 1) which are overlain by a heterogeneous sequence of mafic metavolcanic and metasedimentary rocks (unit 2). At the top of the Wasekwan Group is a fine-grained to conglomeratic metasedimentary rock (unit 3). The stratigraphy of the Wasekwan Group in the Gemmell Lake area appears to correlate with the Snake Lake dacites and rhyolites, Fox Mine Succession and the Fox Road Turbidites.

The fine-grained to conglomeratic metasediments of the Wasekwan Group (Unit 3) may represent a turbidite sequence. However, sedimentary structures which are typical of a turbidite sequence were not observed in the Gemmell Lake area. Gilbert et al. (1980) indicated that the fine-grained to conglomeratic metasediments in the Gemmell Lake area may represent Sickle Group metasediments. The lower contact of these metasediments was not observed by the author and may or may not form an angular unconformity with the underlying Wasekwan Group rocks.

3.6 Metamorphism

In a regional study of the Lynn Lake greenstone belt, Gilbert et al. (1980) indicated that much of the belt was subjected to lower to middle amphibolite facies metamorphism (medium grade of metamorphism as defined by Winkler, 1979). Milligan (1960) indicated that the prograde regional metamorphism throughout the Lynn Lake greenstone belt is not uniform and isograds are difficult to trace because of a lack of outcrop, the distribution of suitable rock types and the absence of diagnostic indicator minerals in the mafic rocks. In general, the metamorphic grade increases from upper greenschist facies in the east to upper amphibolite facies in the west.

The grade of regional metamorphism in the Gemmell Lake area was evaluated using the mineral assemblages of the mafic metavolcanic rocks and the tonalite intrusion. The mafic metavolcanic rocks of the Wasekwan Group dominantly

comprise poikilitic, blue-green hornblende with inclusions of quartz, magnetite and ilmenite, which are set in a matrix of brown to reddish-brown biotite, plagioclase and granoblastic quartz.

In contrast, the tonalite is dominated by plagioclase and quartz with variable amounts of hornblende, biotite and ilmenite. Plagioclase varies in composition from oligoclase to andesine. Quartz occurs either as a granoblastic groundmass or as rounded, anhedral, polycrystalline grains. Blue-green hornblende is interstitial to the plagioclase and occurs with intragranular biotite and quartz. The hornblende has a poikiloblastic texture and contains abundant inclusions of quartz, with lesser epidote, ilmenite and magnetite.

The mineral assemblages of the mafic metavolcanic rocks and the tonalite are consistent with the lower to middle amphibolite facies assemblage described by Gilbert et al., (1980).

The medium grade mineral assemblages described above are selectively altered to chlorite, carbonate, muscovite, clinozoisite and epidote. Hornblende and biotite are altered to chlorite, carbonate and rarely to muscovite along cleavage traces, grain boundaries and fractures. In contrast, plagioclase is altered to fine-grained muscovite, carbonate, epidote, clinozoisite and chlorite. The secondary mineral assemblages generally represent only a minor component of the rocks. They are more abundant near

fractures which cross cut the metamorphic textures.

Prograde metamorphic minerals such as hornblende and biotite define well-developed planar and linear fabrics, suggesting that peak metamorphism was coeval with regional deformation.

3.7 Regional Fabrics

As noted above, the southern belt is dominated by east to northeast-trending isoclinal folds with vertical to steeply dipping (NW) axial planes (Gilbert et al., 1980). Although no isoclinal folds have been identified in the Gemmell Lake area, some of the Wasekwan and Sickle Group rocks are characterized by a planar fabric (S_1) and a linear fabric (L_1). The S_1 planar fabric is defined by a penetrative schistosity which is developed parallel to bedding within both the Wasekwan and Sickle Groups. The planar surfaces generally display an L_1 lineation which is defined by the elongation of sedimentary clasts, mineral aggregates or grains, and the alignment of metamorphic minerals; predominantly hornblende. The average L_1 lineation trends 000° and plunge 72° to the north in both the Wasekwab and Sickle Groups (Figure 6 b and d). The S_1 and L_1 fabrics are well developed in the mafic metavolcanic rocks, moderately well developed within the metasedimentary rocks and poorly developed within the felsic metavolcanic and plutonic rocks.

The orientation of the schistosity and lineation within both the Wasekwan and Sickle Groups are similar

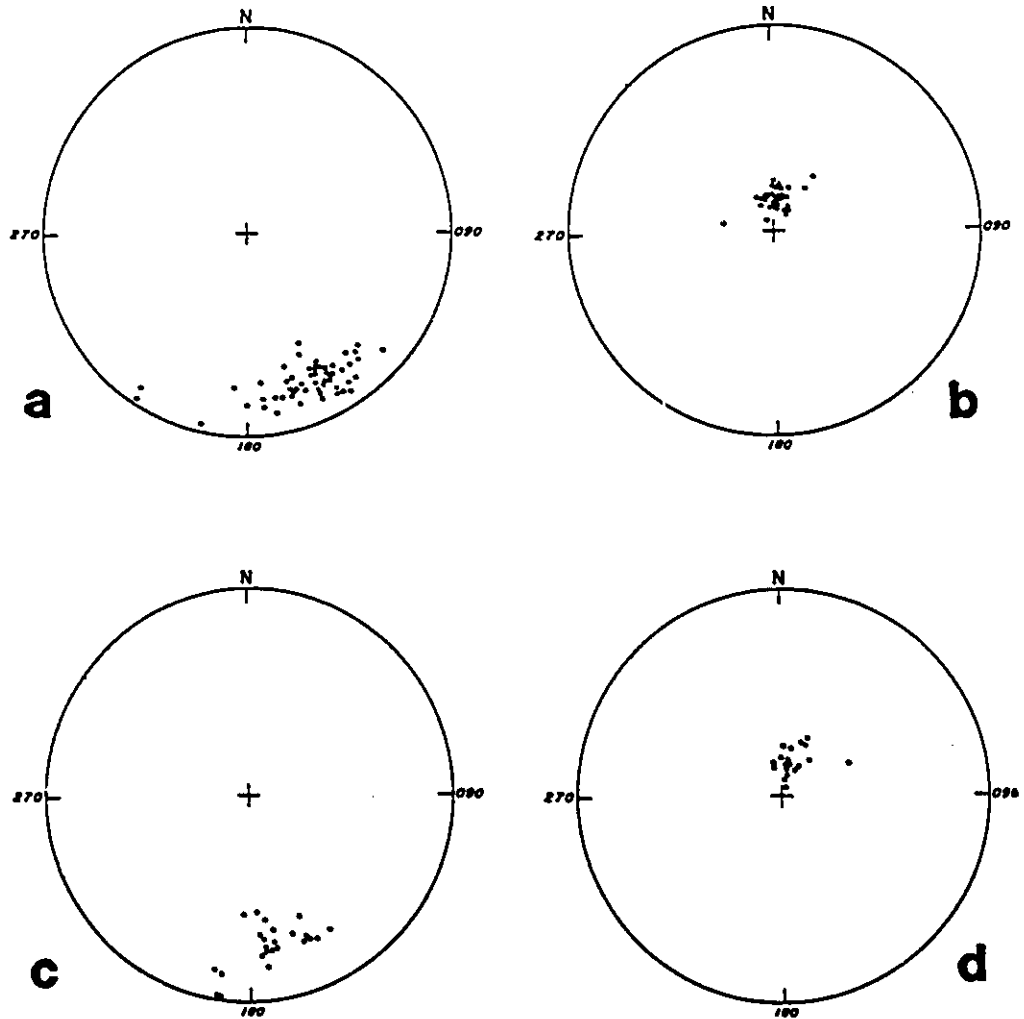


Figure 6 Equal area stereonet projection of: (a) poles to S_1 foliation and (b) L_1 lineation in the Wasekwan Group; (c) poles to S_1 foliation and (d) L_1 lineation in the Sickle Group.

(Figure 6). The schistosity in the Wasekwan and Sickle Groups have an average strike and dip of 262/67 N and 245/79 N respectively (Figure 6 a and c). The orientation of the schistosity is consistent with an axial planar foliation associated with east to northeast trending isoclinal folds.

CHAPTER 4

DEFORMATION ZONES AND GOLD MINERALIZATION IN THE GEMMELL LAKE AREA

4.1 Introduction

Gold mineralization in the Gemmell Lake area of the Lynn Lake greenstone belt was discovered in 1986 by Sherrit Gordon Mines (Lynngold Resources Inc.) during exploration of the Shoe-Lace claim blocks (C.B. 7810-7812). The gold mineralization is located approximately seven kilometers west of the known extent of the Johnson shear zone.

Two zones of deformation and veining were identified by Baldwin (1987) during geologic mapping in the Gemmell Lake area. These zones are referred to as the Prospector deformation zone and Finlay McKinlay deformation zone. The Prospector deformation zone lies directly along strike from the Johnson Shear Zone and may represent the westward extension of the zone through the Gemmell Lake area. The Finlay McKinlay deformation zone is hosted by the tonalite intrusion, approximately 300 metres south of the Prospector deformation zone (Figure 7).

The main objective of this chapter is to establish the timing of gold mineralization relative to deformation and veining in the Prospector and Finlay McKinlay deformation zones. The Prospector and Finlay McKinlay deformation zones were mapped by the author at a scale of 1:100.

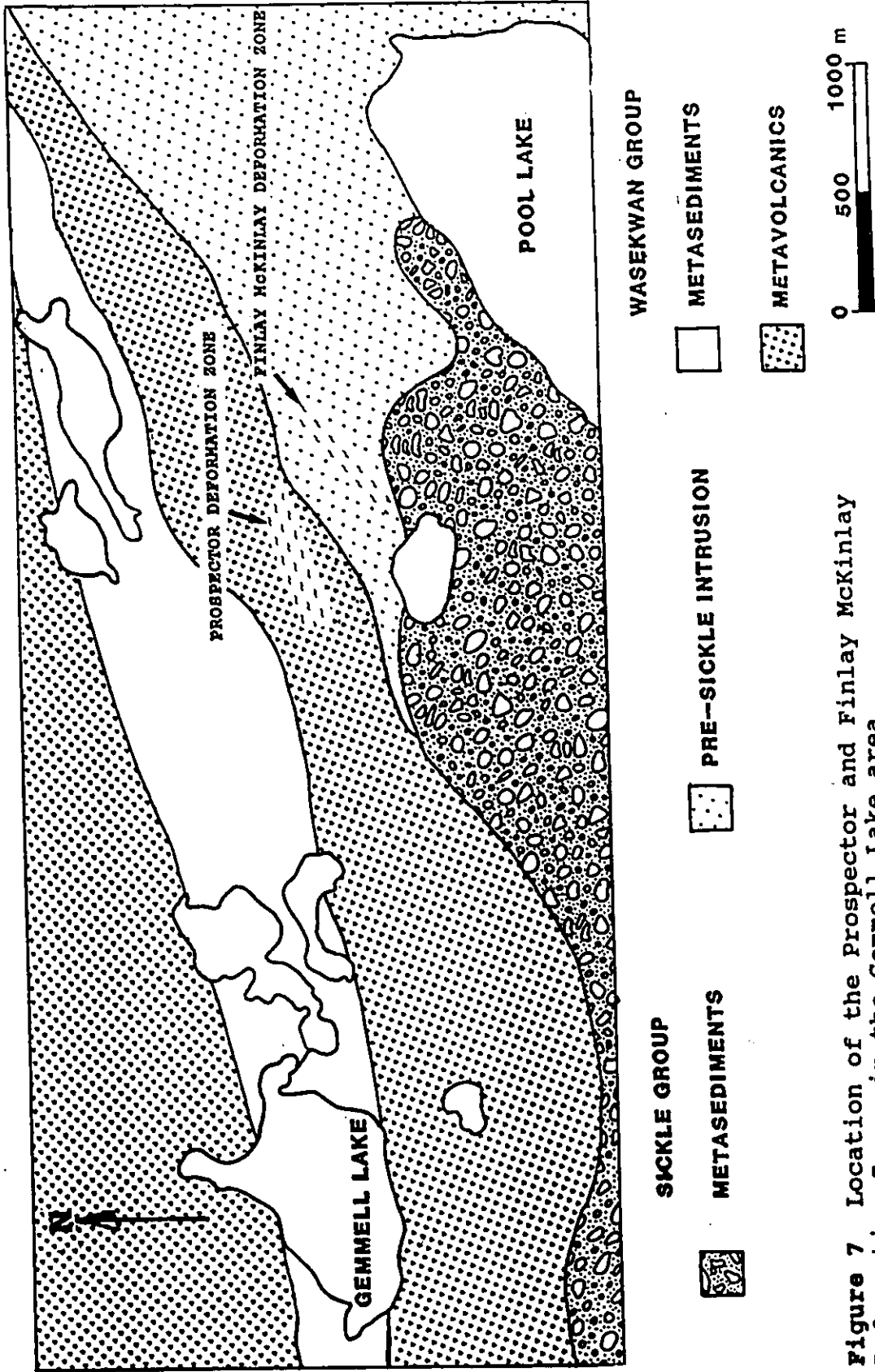


Figure 7 Location of the Prospector and Finlay McKinlay Deformation Zones in the Gemmell Lake area.

4.2 PROSPECTOR DEFORMATION ZONE

The Prospector deformation zone is a 75 m wide, east-west striking zone of intense ductile and brittle deformation within the Wasekwan Group rocks. The host lithologies to the Prospector deformation zone predominantly consist of quartzo-feldspathic schists. Deformation in the Prospector zone is characterized by abundant F_2 folds, a crenulation cleavage (S_2), boudinaged and folded quartz veins, and brittle fault zones. The contacts of the zone are gradational and are marked by a decrease in the number of faults within the felsic metavolcanic flows of unit 1 and the mafic metavolcanic flows and sediments of unit 2.

4.2.1 Folds (F_2)

The F_2 folds are defined by the S_1 foliation and in some places, by layers of boudinaged metasedimentary rocks and by early quartz veins. The average orientation of the fold axes of the F_2 folds trends 002° and plunges 66° to the north (Figure 8a). Axial planes of F_2 folds strike to the northeast (15 to 40°) and vary in dip from 60 to 80° to the northwest or 70 to 90° to the southeast. The F_2 folds are dominantly open to tight, asymmetric Z-folds or symmetric M-folds. No large-scale F_2 folds were identified from the minor fold relationships in the Prospector deformation zone.

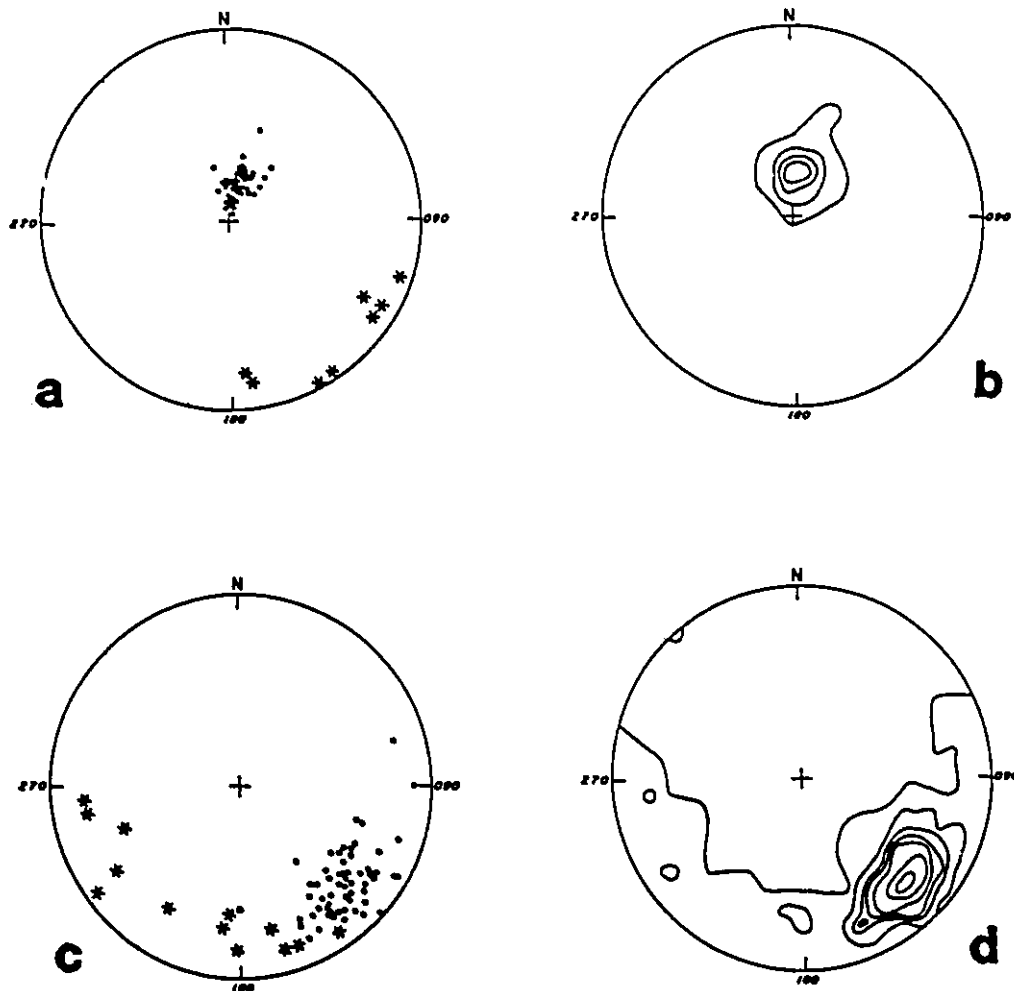


Figure 8 Equal area stereonet projection in the Prospector Deformation Zone of (a) Minor F_2 fold axes (dots) and poles to S_2 crenulation cleavage (asterisks); (b) Contoured equal area stereonet projection of the minor F_2 fold axes. Point concentration indicates the average orientation of the F_2 folds (002° at 66° N). Contours equal 1, 20, 30, 40 and $n = 71$. (c) Equal area stereonet projection of the pole to fault planes (dots) and pseudotachylite injection veins (asterisks); (d) Contoured equal area stereonet projection of the poles to fault planes and pseudotachylite injection veins. Point concentration indicate the average orientation of faults ($228^\circ/76^\circ$ N and $250^\circ/79^\circ$ N) and injection veins ($273/72^\circ$ N, $373/79^\circ$ N and $321/72^\circ$ N). Contours equal 1, 2, 4, 6, 9, 12, 14 and $n = 73$.

4.2.2 Crenulation Cleavage (S_2)

Superimposed on the S_1 foliation is a crenulation cleavage (S_2) which generally consists of poorly defined crenulations of the S_1 fabric. The S_2 cleavage is northeast-striking and may represent an axial planar cleavage to the minor F_2 folds (Figure 8a). S_2 crenulation cleavage occurs sporadically, but was never observed in direct association with the F_2 folds.

4.2.3 Veins

The Prospector deformation zone contains abundant deformed quartz veins which have been subdivided into three vein sets on the basis of mineralogy and cross-cutting relationships.

1) Quartz-Carbonate Veins

These veins form a stockwork and comprise fine-grained, granular, white quartz with minor carbonate. Individual veins are thin (< 2 cm in width) with greenish alteration halos. The alteration halos vary in thickness from 1 to 4 cm and consist of chlorite, epidote, quartz and carbonate. These veins and their alteration halos generally form isolated, rounded boudins which were always oriented parallel to the S_1 foliation (Figure 9a).

2) Folded Quartz Veins

This vein set comprises veins (< 3 cm in width) of fine-grained, granular, highly fractured white quartz with no visible alteration halos. These veins are boudinaged and/or folded by F_2 folds (Figure 9 a, b, d).

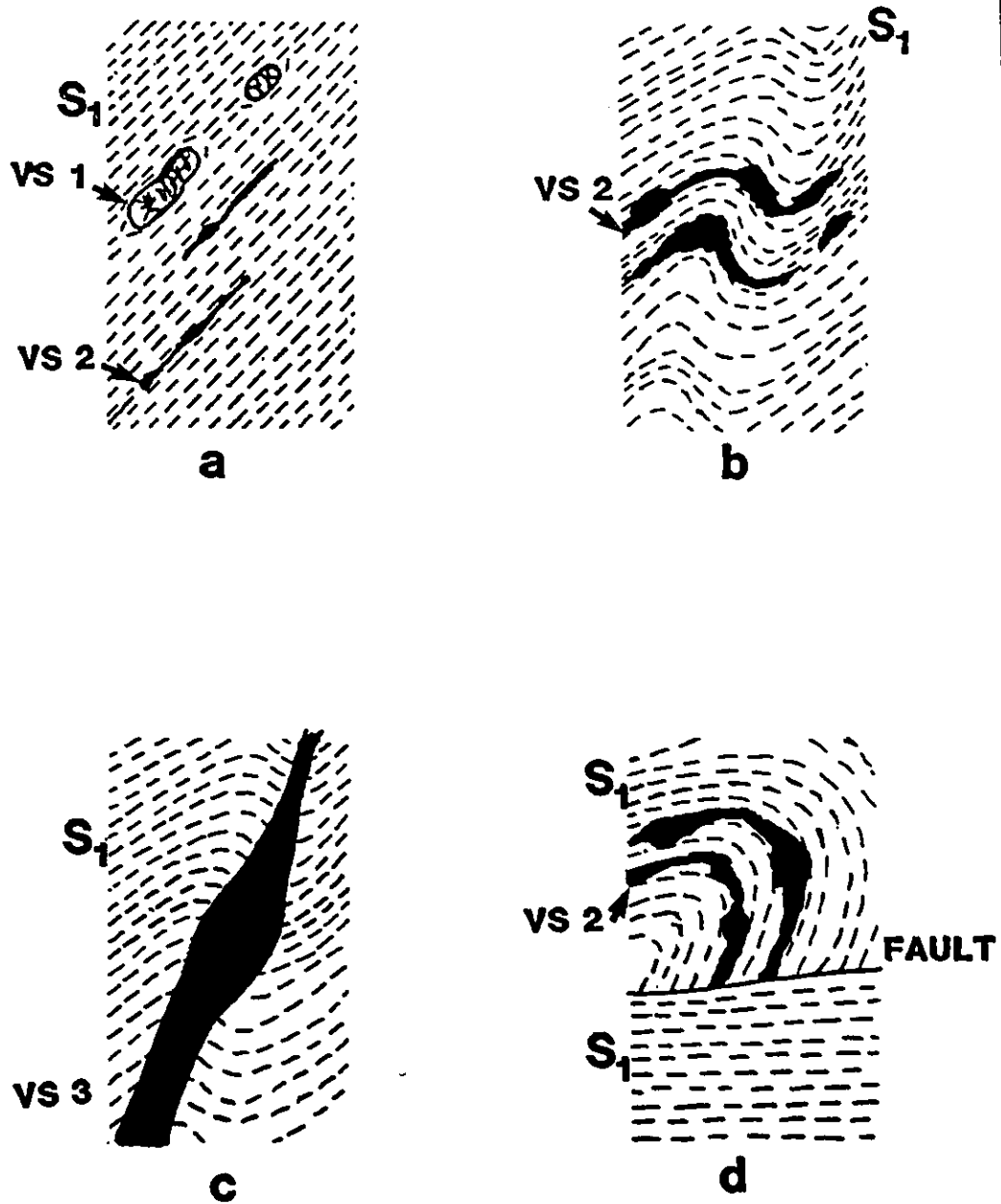


Figure 9 (a) vein sets 1 and 2; (b) boudinaged vein set 2 in a F_2 fold; (c) vein set 3 crosscuts minor F_2 fold; and (d) boudinaged and folded vein set 2 crosscut by a fault.

3) Quartz Veins

The veins that comprise the third vein set are much larger than those in sets 1 and 2. These veins occur as north-south trending, asymmetrically boudinaged quartz veins, which vary from < 10 cm to 3 m in width, and up to 5 m in length. Individual veins are dominated by highly fractured, coarse-grained white to gray quartz with minor carbonate, tourmaline, biotite, chlorite and muscovite. Alteration halos vary up to 10 cm in width and consist of variable amounts of chlorite, quartz, biotite, tourmaline, carbonate, garnet, pyrite, chalcopyrite, pyrrhotite and magnetite. Some of these veins cross-cut the earlier veins and the minor folds, subparallel to the axial traces (Figure 8 c).

4.2.4 Fault Zones

Brittle faults in the Prospector zone are concentrated in several fault zones. These fault zones are discontinuous, irregular in shape and are up to 20 m in width.

The faults cross-cut and offset the S_1 foliation, minor F_2 folds, crenulation cleavage (S_2) and boudinaged and folded quartz veins (Figure 8d). In one of the fault zones, the average orientation of the S_1 foliation changes from $245^\circ/79^\circ$ N in the Wasekwan Group to $228^\circ/80^\circ$ N within the zone. There is no change in the orientation of the L_1 lineation within the fault zone.

The faults within the zones can be subdivided into

layer-parallel faults and oblique faults. Layer parallel faults are oriented sub-parallel to the lithologic boundaries and to the S_1 foliation. Oblique faults are oriented at a high angle to the lithologic boundaries and to the S_1 foliation. Many of the layer-parallel and oblique faults are characterized by the development of pseudotachylyte, a black to reddish brown, aphanitic, glassy material. The layer-parallel faults contain fault veins (Figure 10a; Sibson, 1975) consisting of planar veins or curving lenses of pseudotachylyte that pinch and swell. These veins vary from less than 2 mm to 2 cm in width and from less than 10 cm up to 60 cm in length. Injection veins (Figure 10a; Sibson, 1975) are generally wider than the fault veins and can sometimes be traced back to a parental fault vein. They vary in thickness from 0.3 mm to 3 cm with the longest injection vein of pseudotachylyte having a length of 47 cm. The oblique faults may also contain veins of pseudotachylyte which cross-cut the S_1 foliation but generally do not cross-cut lithologic boundaries.

The layer-parallel and oblique faults often form a network which isolates individual blocks of country rock. Breccias with a pseudotachylyte matrix generally develop where two relatively close (within several centimeters), parallel faults are connected by numerous injection veins. The breccia fragments are generally angular, and the orientation of the fragments in the blocks indicates rotation.

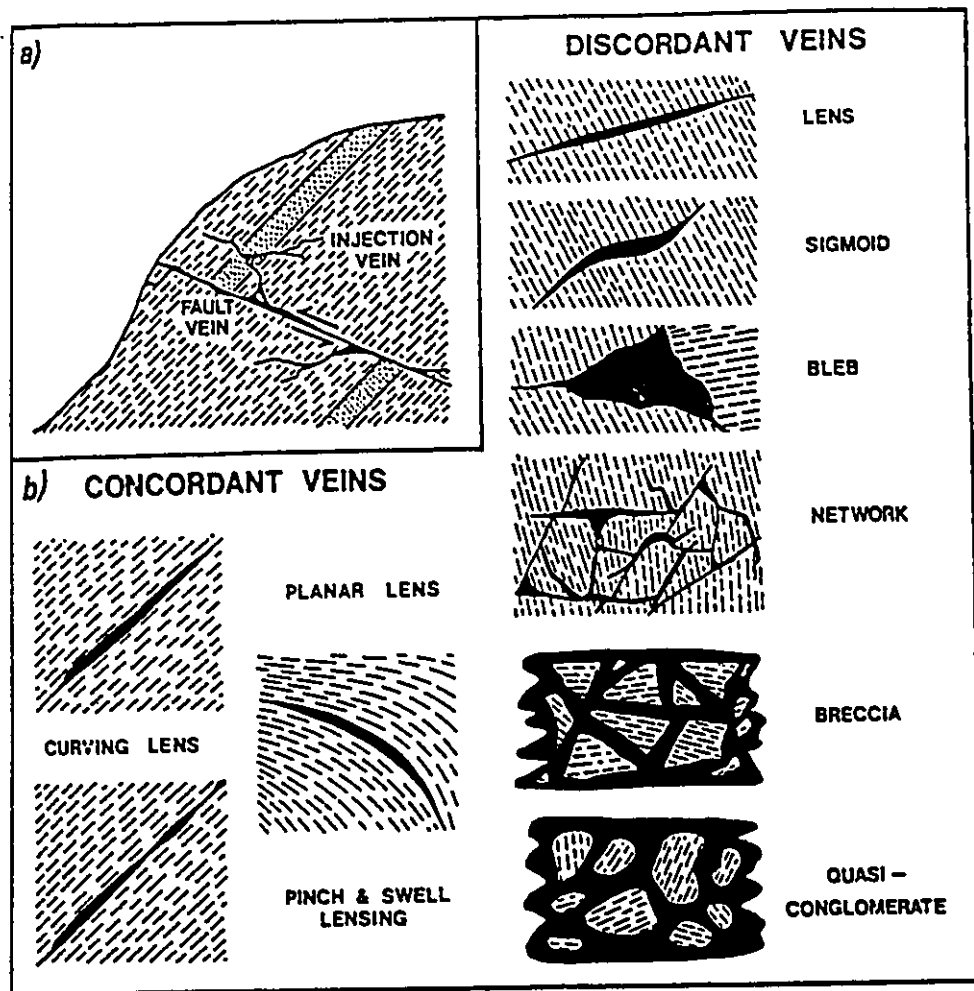


Figure 10 (a) Fault and injection vein relationships of pseudotachylite; (b) Geometric relationships of pseudotachylite veins (taken from Sibson, 1975).

The layer-parallel faults, oblique faults and injection veins of pseudotachylyte define five different orientations (Figure 8 c, d). The layer-parallel faults and fault veins of pseudotachylyte can be subdivided into two groups. A large number strike at approximately 228° and dip at 76° N, which is parallel to the S_1 foliation. A smaller number strike at 250° and dip at 79° N, which is similar to the orientation of lithologic contacts. In contrast, the oblique faults and the injection veins define a group at 273°/72° N and at 353°/79° N, and a third group which strikes 321° and dips 72° N.

The sense of displacement on oblique faults is generally provided by the offset of lithologic layers, quartz veins and folds. Observed displacement on oblique faults vary from 1.5 cm to a maximum of 18 cm. The sense of movement on the oblique faults varies with their orientation such that faults oriented at 273°/72° N indicate sinistral displacement and those oriented at 353°/79° N indicate dextral movement.

4.2.5 Sequence of Events

The field relationships described above indicate the following relative sequence of events for the Prospector deformation zone (Figure 11).

- 1) Formation of vein sets 1 and 2. The exact relationship of the formation of the early vein sets to the development of the S_1 and L_1 fabric is unclear. Vein set 1 comprises quartz-carbonate veins with alteration halos of

Sequence of Events

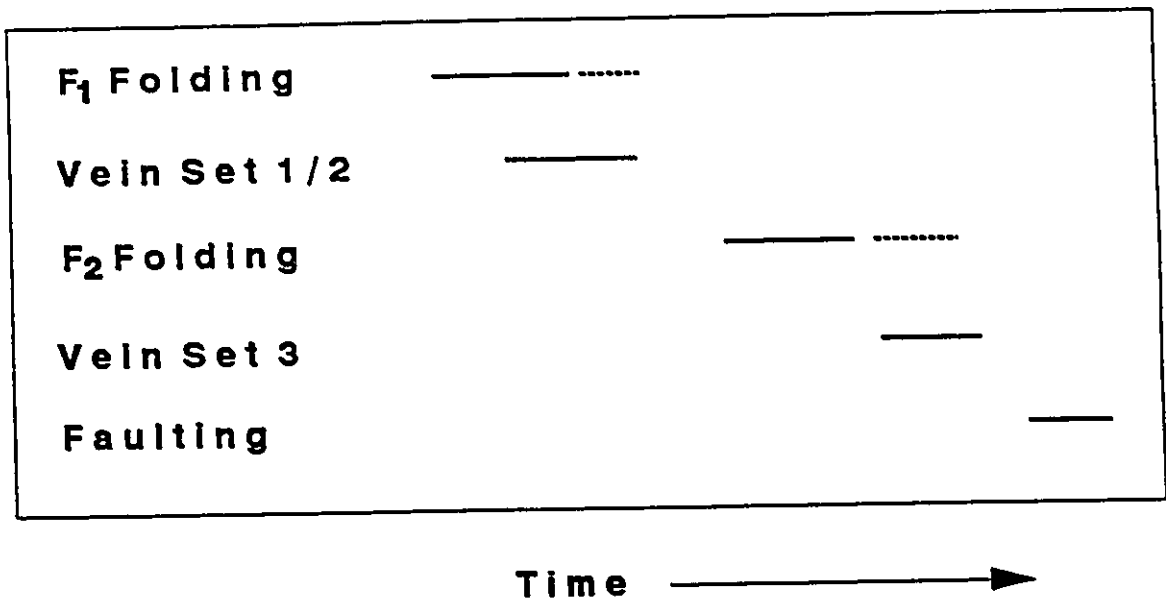


Figure 11 Relative sequence of events in the Prospector deformation zone.

chlorite, epidote, quartz and carbonate. This hydrothermal alteration mineralogy suggests that these veins formed after the lower amphibolite regional metamorphism. However, both vein sets are boudinaged and lie parallel to the S_1 foliation, which suggests that these veins formed prior to deformation and were rotated into parallelism with the S_1 foliation.

2) Ductile deformation and formation of the F_2 folds and the crenulation cleavage (S_2). The S_1 foliation and boudinaged quartz veins are both folded to form F_2 folds. This indicates that the F_2 folds post-date the development of the S_1 and L_1 fabric and the formation of the early quartz veins.

3) Formation of vein set 3, which cross-cuts the earlier veins (sets 1 and 2) and the minor F_2 folds.

4) Ductile deformation occurred after the formation of these later veins as is indicated by the boudinaged veins of set 3.

5) These events were followed by brittle faulting and the associated development of pseudotachylyte, which disrupted the S_1 foliation, minor F_2 folds, crenulation cleavage (S_2) and all of the vein sets.

4.3 FINLAY MCKINLAY DEFORMATION ZONE

The Finlay McKinlay deformation zone is a 10 m wide northeast-striking, steeply dipping (70-75°NW) deformation zone characterized by mylonites and brittle faults. The zone can be followed along strike for 100 m within the tonalite, to the contact with the Sickle Group.

4.3.1 Tonalite

The tonalite is dominated by plagioclase and quartz with lesser amounts of hornblende, biotite, ilmenite and magnetite. Anhedral to subhedral plagioclase varies in composition from oligoclase to andesine and exhibits mottled to granoblastic textures. These textures suggest that the plagioclase feldspars have been recrystallized. Quartz occurs either as rounded, anhedral polycrystalline grains or as a granoblastic groundmass. Poikilitic blue-green hornblende contains inclusions of quartz, epidote, ilmenite and magnetite.

Outside the deformation zone, the tonalite is generally massive. However, in places a weak, spaced schistosity is defined by biotite. This weak foliation is subparallel to the regional S_1 foliation.

4.3.2 Mylonites

Within the deformation zone, the tonalite has been transformed into protomylonite, mylonite and ultramylonite. The deformation is marked by a change in mineralogy, grain size reduction and the development of a schistosity (S_2) and a linear fabric (L_2).

Protomylonite

A protomylonite is defined by Sibson (1977) as a foliated rock comprising 50 to 90 % of the original protolith. In the Finlay McKinlay deformation zone, the protomylonite comprises quartz, hornblende and plagioclase porphyroclasts set in a fine-grained granoblastic matrix of quartz and plagioclase with subordinate biotite, muscovite, epidote and apatite. Protomylonite is characterized by the development of a weak S_2 - L_2 fabric in the tonalite which is generally defined by wispy seams of biotite and chlorite that curve around elongated hornblende, quartz and plagioclase porphyroclasts.

Quartz and plagioclase porphyroclasts vary from 1.0 to 2.1 mm in width and from 4.0 to 6.0 mm in length. The quartz porphyroclasts consist of polycrystalline grains that display strong undulose extinction and deformation bands. They have coarse, granoblastic to sutured cores with finer grained boundaries. Plagioclase porphyroclasts are rounded, finer-grained toward the grain boundaries, and partially altered to biotite. Rare fractures within the plagioclase grains offset twin lamellae within the cores of the grains and may contain chlorite, calcite and muscovite. Blue-green hornblende porphyroclasts become elongate and are replaced by chlorite, calcite, and brown to reddish-brown biotite. The original textures of the tonalite are partially retained despite the mineralogical and textural changes noted above.

Mylonite

A mylonite is defined by Sibson (1977) as a strongly foliated and lineated rock comprising 10 to 50 % of the original protolith. In the Finlay McKinlay deformation zone, the transition from protomylonite to mylonite is abrupt. Mylonite occurs as discrete bands, less than several centimeters in thickness, which anastomose through zones of protomylonite. The original textures of the tonalite, which were partially preserved in the protomylonite, are not present in the mylonite.

Quartz porphyroclasts become the dominant clasts over plagioclase porphyroclasts in the mylonite, and are set in a fine-grained matrix of quartz, plagioclase, muscovite and biotite. The quartz porphyroclasts form elongate, polycrystalline ribbons that vary in width from 0.5 to 1.0 mm and attain lengths of 0.4 to 2.0 cm. The plagioclase porphyroclasts occur as elongate or rounded grains which vary in width from 0.1 to 0.4 cm and in length from 0.1 to 1.0 cm. All of the hornblende in the protomylonite has been replaced in the mylonite, predominantly by biotite.

The mylonite is characterized by a penetrative S_2-L_2 fabric that deflects around the porphyroclasts. The foliation is defined by wispy to planar seams of biotite and aligned quartz, plagioclase and muscovite.

Ultramyylonite

An ultramyylonite is defined by Sibson (1977) as strongly foliated and lineated rock which contains less than 10 % of the original protolith. The mylonite in the Finlay McKinlay deformation zone grades into narrow bands of ultramyylonite which anastomose through the mylonite. These bands of ultramyylonite vary in width from 10 to 37 cm and have a minimum length of 1.5 m.

The ultramyylonite is characterized by quartz porphyroclasts, with rare plagioclase porphyroclasts, and a strong planar and linear fabric. The quartz porphyroclasts consist of individual crystals or polycrystalline aggregates, which generally form rounded and elongate grains that vary from 0.2 to 0.9 mm in width and from 0.3 to 1.5 cm in length. The matrix of the ultramyylonite consists of very fine-grained quartz, feldspar, biotite and muscovite. A penetrative planar fabric is defined by continuous planar seams of biotite that deflect only slightly around the porphyroclasts.

4.3.3 Kinematic Indicators

Planar (S_2) and Linear Fabric (L_2)

The protomyylonite, mylonite and ultramyylonite in the Finlay McKinlay deformation zone are associated with the development of planar and linear fabrics. The average orientation of the S_2 foliation in the mylonite and

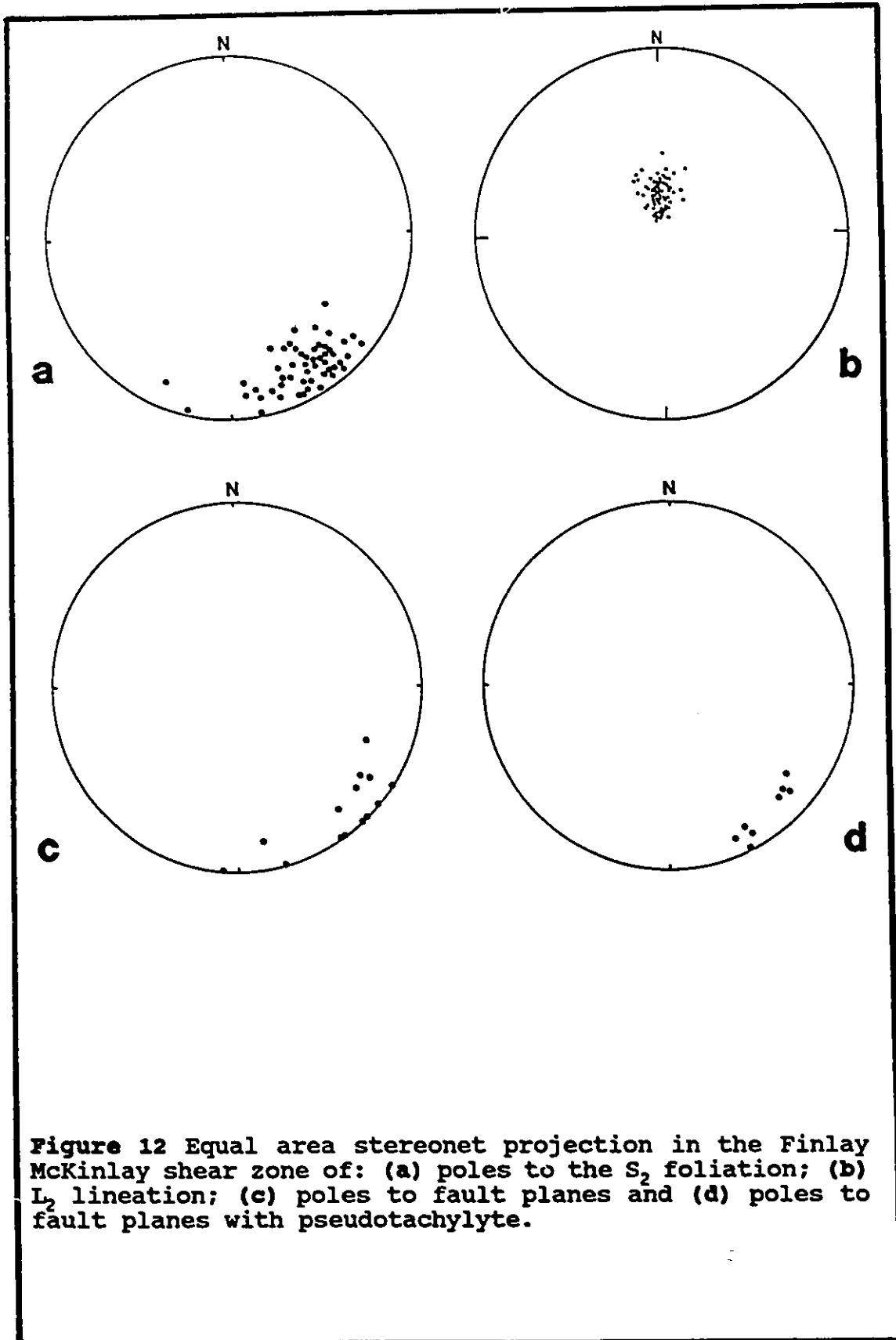


Figure 12 Equal area stereonet projection in the Finlay McKinlay shear zone of: (a) poles to the S_2 foliation; (b) L_2 lineation; (c) poles to fault planes and (d) poles to fault planes with pseudotachylyte.

ultramylonite strikes at 227° and dips at 70° N (Figure 12a). In contrast, the average orientation of the foliation in the less deformed protomylonite and mylonite to the south and north has a strike and dip of 245°/71° N and 231°/74° N respectively. The linear fabric (L_2) within the zone is defined by elongate quartz porphyroclasts on the foliation surfaces. The lineation, which develops parallel to the displacement direction in ductile shear zones (Ramsay, 1980; Ramsay and Huber, 1987), has an average trend of 358° and plunges 74° to the north (Figure 12b). The orientation of the lineation and the progressive change in orientation of the foliation indicates reverse-oblique movement across the width of the Finlay McKinlay shear zone (Ramsay and Huber, 1984, 1987).

Shear Bands

Bands of higher strain occur in places throughout the protomylonite and mylonite. These zones are generally less than a centimeter in width, display a finer grain size, are northeast striking, and dip to the northwest ($\approx 70^\circ$).

The bands of higher strain in the mylonite and protomylonite may represent shear bands. Shear bands are defined as narrow zones of high strain which develop within a major shear zone (Simpson, 1986). They usually occur as evenly-spaced, subparallel zones (one to ten centimeters apart) which deflect some pre-existing planar fabric (such as bedding or a foliation) with a consistent sense of shear (Simpson, 1986).

The geometry of the planar fabrics associated with shear bands can provide a sense of shear for the shear zone (Simpson, 1986). The sense of shear is determined by the movement indicated by earlier foliations or S-planes which curve into C-planes or shear bands (Simpson, 1986, Ramsay and Huber, 1987).

The S_2 foliation in the protomylonite or mylonite in the Finlay McKinlay deformation zone in places deflects into the shear bands. The sense of deflection of the S_2 foliation in the shear bands indicate that the northwest-side moved up relative to the southeast-side indicating reverse movement (Figure 13a and b).

Porphyroclasts/Tail Systems

Quartz porphyroclasts in the mylonite and the ultramylonite were used as kinematic indicators in the field and in oriented thin section cut parallel to the L_2 lineation and perpendicular to the S_2 foliation. Some quartz porphyroclasts form σ -type porphyroclast/tail systems (Simpson, 1986). The asymmetric tails consist of finer-grained, recrystallized quartz and the sense of shear indicates that the north-side moved up relative to south-side, indicating reverse displacement (Figure 13c).

Fractured and Displaced Grains

Some quartz porphyroclasts in the Finlay McKinlay zone are fractured and displacement has occurred along these fractures suggesting that the north side moved up relative to the south side (Simpson, 1986; Ramsay and Huber, 1987)

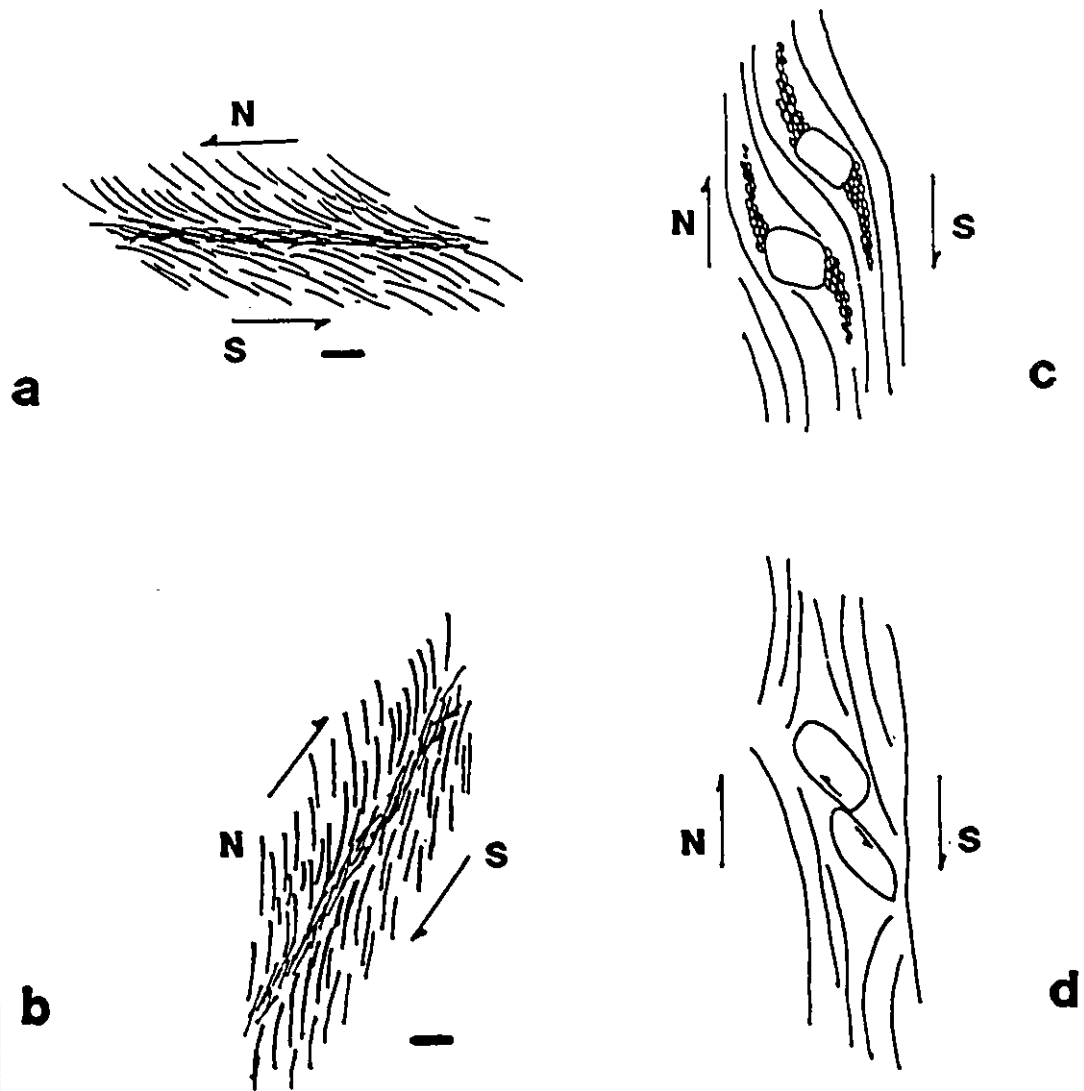


Figure 13 Kinematic indicators of ductile deformation in the Finlay McKinlay shear zone: (a) Horizontal view of a shear band perpendicular to L_2 lineation; (b) Vertical view of a shear band perpendicular to S_2 foliation; (c) Porphyroclast and tails; (d) Fractured and displaced grains.

(Figure 13d).

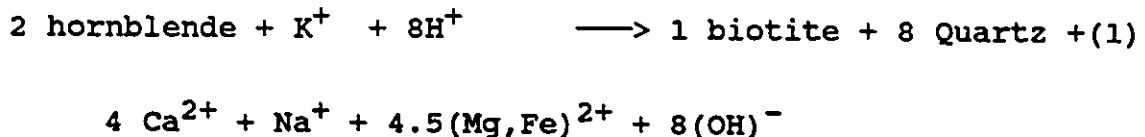
In summary, kinematic indicators in the Finlay McKinlay shear zone are all consistent and indicate that the ductile deformation which formed mylonites was the result of sinistral-reverse oblique displacement.

4.3.4 Mineralogical Changes Accompanying Mylonitization

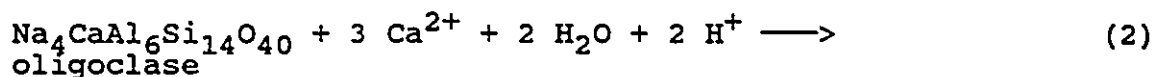
The tonalite in the Finlay McKinlay deformation zone has been transformed from a rock dominated by plagioclase and quartz with hornblende and biotite to a mylonite dominated by quartz, biotite, epidote, clinozoisite and tourmaline with minor plagioclase and no hornblende.

The presence of recrystallized plagioclase feldspar in the tonalite indicates that regional metamorphism was a precursor to its mechanical breakdown in the Finlay McKinlay shear zone. The plagioclase feldspar underwent dominantly ductile deformation, forming elongate, recrystallized grains in the mylonites and ultramylonites.

Biotite increase in abundance from the protomylonite, mylonite and ultramylonite and in the protomylonite, replaces hornblende. This suggests that chemical and mechanical alteration at an early stage of mylonitization was responsible for the breakdown of hornblende in the mylonites. Therefore, a reaction converting hornblende to biotite most likely operated in the mylonites of the Finlay McKinlay shear zone. Such a reaction might be (Beach, 1976):



A secondary mineral assemblage of tourmaline, epidote and clinozoisite is disseminated throughout the mylonite and ultramylonite. Epidote and clinozoisite replace feldspar which may be illustrated by following reaction:



These reactions require water, calcium and potassium and loss of alkalis and silica. The breakdown of plagioclase to form epidote could be represented by reaction 2 with the addition of iron from the fluid. A possible source of iron may be the breakdown of hornblende (reaction 1).

Tourmaline, epidote and clinozoisite generally have a preferred orientation, parallel to the mylonitic fabric. However, in places, these minerals have a random orientation which suggests that they post-date the mylonite.

4.3.5 Veins

Quartz veins in the Finlay McKinlay deformation zone have been subdivided into two sets:

1) NE-S7 striking quartz veins

These veins consist of light gray to yellow-brown, fine to medium-grained quartz with minor tourmaline, biotite, and chlorite (Figure 14). The average strike and dip of these veins ($227^{\circ}/79^{\circ}$ N) is parallel to the orientation of the shear zone ($227^{\circ}/70^{\circ}$ N) (Figure 15). Individual veins vary from < 1 cm to 10 cm in width and from 1 to 10 m in length. A number of smaller, south-trending branch veins extend away from the larger veins. These smaller branch veins have a sigmoidial shape and terminate to the south, away from the parent vein. All of the veins decrease in width toward the southwest and terminate before the Sickie unconformity.

Individual veins of the first vein set generally consist of massive quartz and lack any internal structure. Anhedral, coarse-grained (> 4 mm) crystals of quartz typically comprise greater than 90 to 95 % of the vein. Some veins have a narrow zone in their centre which consists of tourmaline, biotite and chlorite.

Most of the veins in the first set have sharp contacts and cross-cut the mylonite at a low angle to the foliation. Some of the veins display 1-2 cm wide, hydrothermal alteration halos of fine-grained chlorite, biotite and tourmaline.

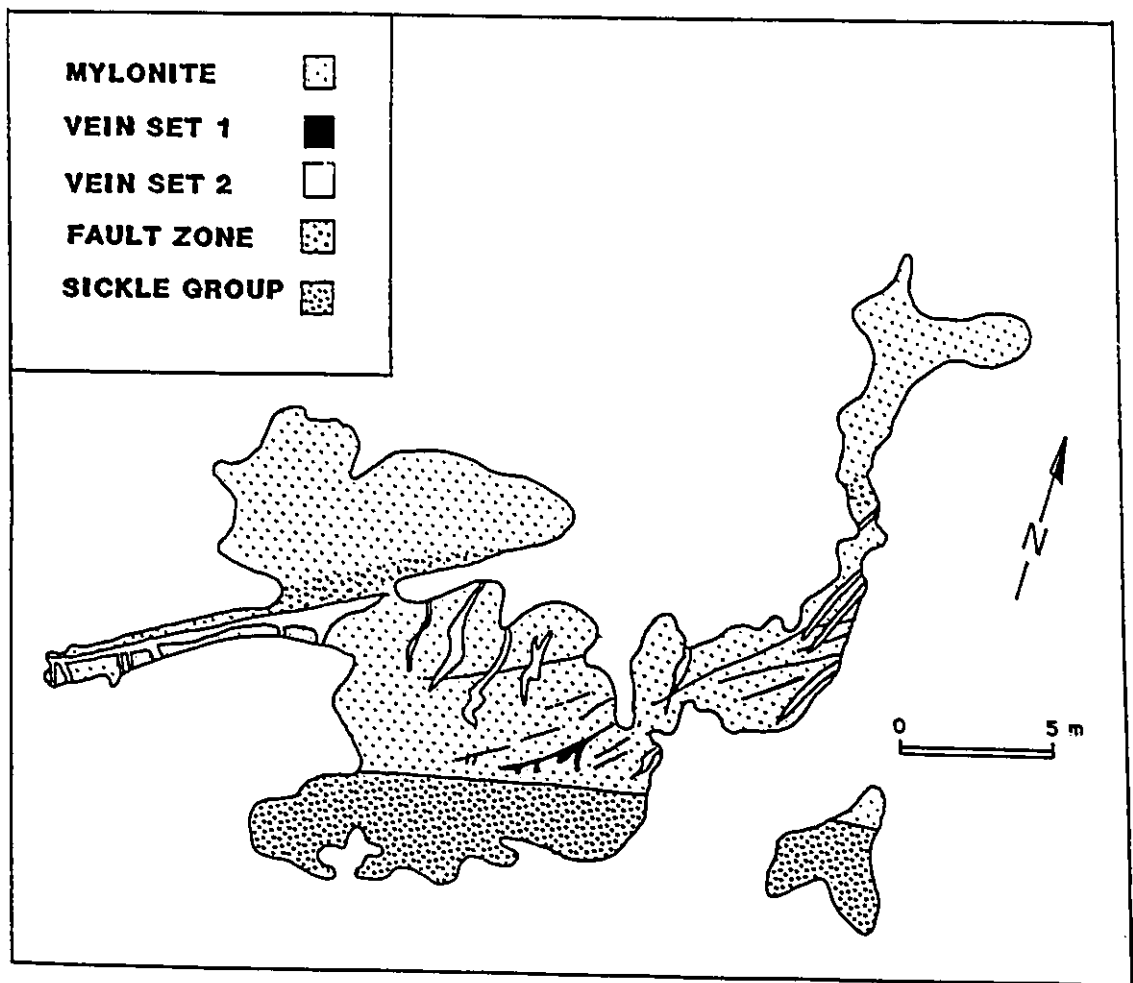
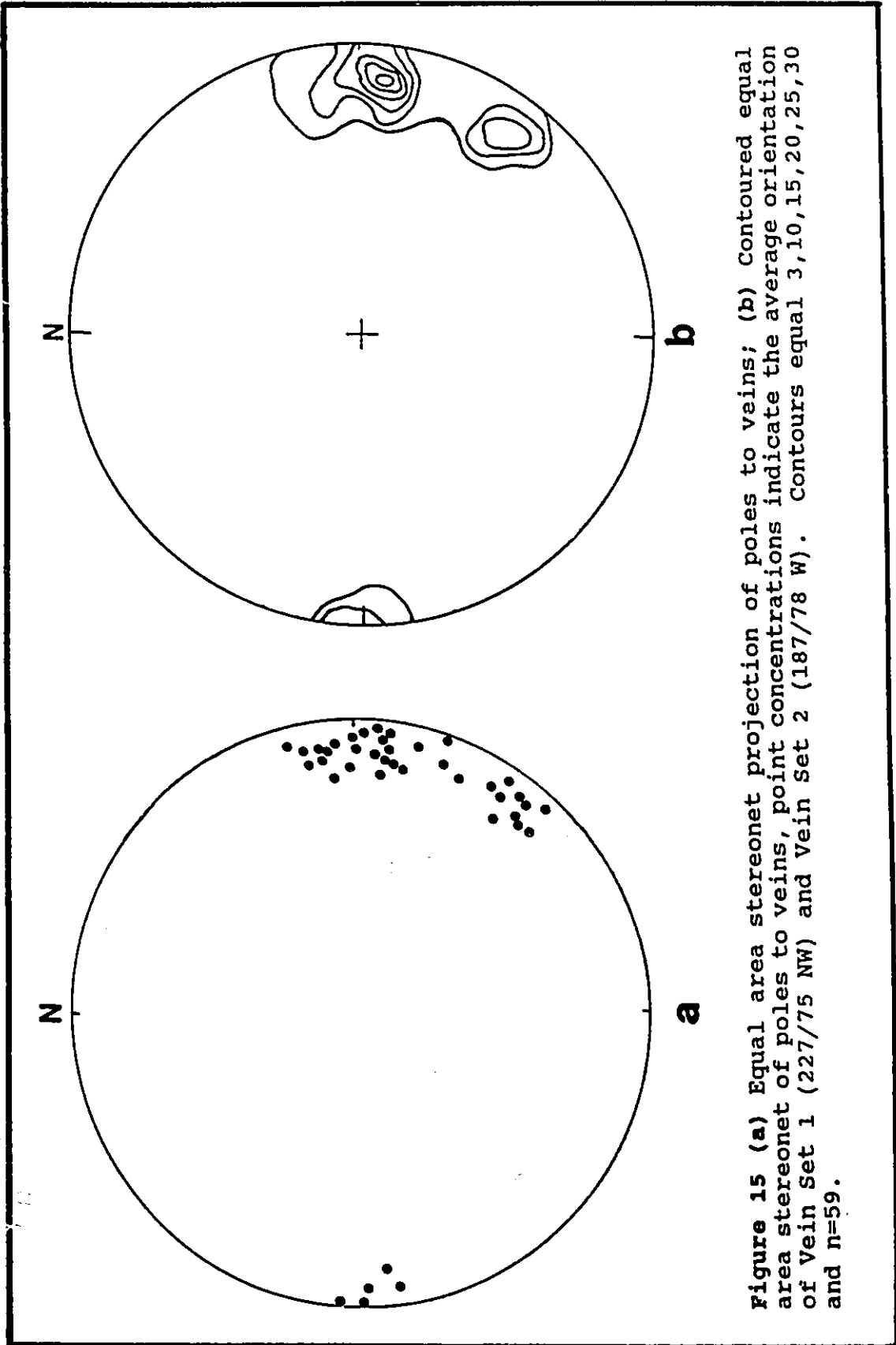


Figure 14 Sketch of the outcrop which hosts the gold mineralization in the Finlay McKinlay shear zone.



2) N-S striking Quartz ± Sulphide Veins

The N-S striking quartz ± sulphide veins generally cross-cut the NE-SW striking quartz veins of set 1. Veins of set 2 predominantly consist of gray to white, anhedral, coarse-grained, strongly fractured quartz with variable amounts of tourmaline, biotite, chlorite, carbonate, sulphides, tellurides and native gold.

The veins have an average strike of 187° and a dip of 78° W (Figure 15), and vary in width from < 1 cm to 46 cm and in length from < 1 m to 7 m. All of the veins decrease in width toward the southwest and terminate before the Sickie Group unconformity. The largest vein occurs near the centre of the Finlay McKinlay deformation zone (Figure 14). The vein has a length of approximately 12 m and varies in width from 8 to 40 cm. The orientation of the vein varies from 219 to 225° and dips steeply to the northeast at 85°. There are a number of smaller veins which vary in width from 3 to 26 cm that are similar to the central vein. These smaller veins branch to the south off of the larger quartz vein.

Vein contacts are generally sharp. Alteration halos range up to 2 cm in thickness and comprise epidote, clinozoisite and tourmaline. The mineralogy of the alteration halos are similar to the secondary mineral assemblages noted in the mylonite and ultramylonite.

Vein set 2 also contains a vein breccia, vein ribbons and includes veinlets that postdate the quartz, all of which

are described below.

Vein Breccia

The large vein in the centre of the Finlay McKinlay deformation zone contains a vein breccia which comprise angular fragments of mylonite, partially altered to tourmaline, set in a quartz matrix. In the breccia fragments, mylonite porphyroclasts of recrystallized quartz are set in a matrix of massive tourmaline. The fragments vary in size from less than 5 cm up to 20 cm and show no evidence of rotation.

Vein Ribbons

The second vein set contains tourmaline aggregates (5 to 10 %) intergrown with quartz and calcite. The tourmaline aggregates generally form layers or ribbons in the veins. They are less than 1 cm in thickness and between 10 and 15 cm in length. The veins frequently contain several ribbons, which lie parallel to the vein walls. The tourmaline occurs as euhedral crystals encased in quartz, indicating that deposition of the tourmaline was closely followed by quartz deposition. Therefore, each new vein opening started with tourmaline deposition followed by quartz deposition.

Veinlets

Numerous veinlets occur in the second vein set and adjacent alteration halos. The mineralogy and temporal relationships of the veinlets indicate at least four episodes of veinlet formation. Paragenesis of the veinlets is shown in Figure 16.

	I	II	III	IV
Quartz	—	—		
Tourmaline	—		—	
Epidote	—			
Magnetite	—			
Clinozoisite	—			
Calcite		—	—	
Muscovite			—	
Chalcopyrite		—	—	
Pyrite		—	—	
Pyrrhotite		—		
Galena			—	
Gold			—	
Hessite			—	
Tellurobismuth			—	
Covellite				—
Sphalerite				—

Figure 16 Paragenesis of veinlets in vein set 2. Four episodes of veining are represented by (I-IV)

Tourmaline-Epidote-Clinzoisite-Magnetite Veinlets

Coarse-grained tourmaline, epidote, clinzoisite and magnetite occur as irregular veinlets (2-4 mm wide) in the quartz. The epidote and clinzoisite may contain some inclusions of quartz and tourmaline. The magnetite contains inclusions of quartz, epidote, clinzoisite and tourmaline.

Sulphide Veinlets

These veinlets contain variable amounts of quartz, carbonate, pyrite, and chalcopyrite, with lesser chlorite, muscovite and pyrrhotite. The quartz consists of very fine-grained ($< 0.5 \mu\text{m}$) crystals, and has a weak undulose extinction. The carbonate consists of fine-grained to microcrystalline calcite. Some of the veinlets contain microbreccias composed of quartz fragments set in a microcrystalline matrix of quartz and calcite.

Veinlets containing dominantly chalcopyrite and pyrite are common. The chalcopyrite forms anhedral grains which rim fractured, euhedral to subhedral pyrite. The pyrite contain abundant inclusions of tourmaline, chalcopyrite and pyrrhotite. However, the textures indicate that chalcopyrite and pyrrhotite replace the pyrite and are therefore genetically younger than the pyrite.

These veinlets generally cross-cut the tourmaline-epidote veinlets described above; fractures in the magnetite of the first set of veinlets often contain pyrite, chalcopyrite and minor pyrrhotite.

Native Gold-Tellurides

Native gold occurs in late veinlets associated with quartz, calcite, chlorite, muscovite, tourmaline, galena, chalcopyrite, pyrite, hessite and tellurobismuth. These veinlets may range up to 0.5 mm in width and up to 10 mm in length.

Most of the gold occurs as irregular aggregates that range from 1 to 10 μm in size and which occur interstitially to fine-grained tourmaline and muscovite. Individual grains of gold are generally less than 10 μm in size. Some native gold forms rounded grains and occurs along grain boundaries and in fractures in recrystallized quartz.

Native gold is also associated with hessite. Gold and hessite form intergrowths with textures that indicate the minerals were in equilibrium and were co-precipitated.

Tellurobismuth was observed as rims around hessite and gold or as intergrowths with hessite. However, gold was never observed in contact with tellurobismuth which suggests that tellurobismuth may slightly post-date gold deposition.

The veinlets with native gold cross-cut the vein quartz and earlier sulphide veinlets. This indicates that gold mineralization was deposited after the early epidote-clinozoisite-tourmaline-magnetite veinlets and the sulphide veinlets.

Sphalerite-Covellite

Anhedral, fine-grained aggregates of sphalerite, which is colourless to yellow, occurs in the veinlets as coatings which partially replace pyrite, chalcopyrite, galena, hessite and tellurobismuth. Covellite also occurs as rims around chalcopyrite. In places, sphalerite, with inclusions of covellite, occur as rims around hessite and tellurobismuth. This indicates that sphalerite and covellite post-date the sulphide and gold-telluride veinlets.

Hydrothermal Alteration

The veinlets within the second vein set are associated with a second alteration assemblage which consists of chlorite, muscovite and calcite. The veinlets cross-cut the alteration halos associated with the second vein set. In the halos around the second vein set, chlorite and muscovite replace biotite and tourmaline respectively. In some cases, the muscovite and chlorite occur in veinlets and in patches with calcite. Calcite also occurs in veinlets in, and along grain boundaries between epidote and clinozoisite.

4.3.6 Faults

A brittle fault zone occurs within the central portion of the Finlay McKinlay deformation zone. The fault zone is approximately 1 m in width and can be followed for approximately 15 m along strike.

Deformation of the mylonite within the fault zone

consists of fracturing, faulting and brecciation. Small faults often contain brown to black, aphanitic, pseudotachylyte, which occurs as concordant and discordant veins. The pseudotachylyte veins attain a maximum thickness of 18 mm. Small, fragment-supported breccia zones consist of angular mylonite fragments, up to several centimeters wide, in a pseudotachylyte matrix.

Faults also occur away from the main fault zone where they crosscut protomylonite, mylonite, and quartz veins. These small faults vary in strike from 200° to 255° and dip steeply to the northeast (Figure 12 c, d). Displacements associated with individual faults indicate sinistral offsets of up to 0.5 cm.

The faults crosscut, and clearly post-date, the formation of both vein sets in the Finlay McKinlay deformation zone.

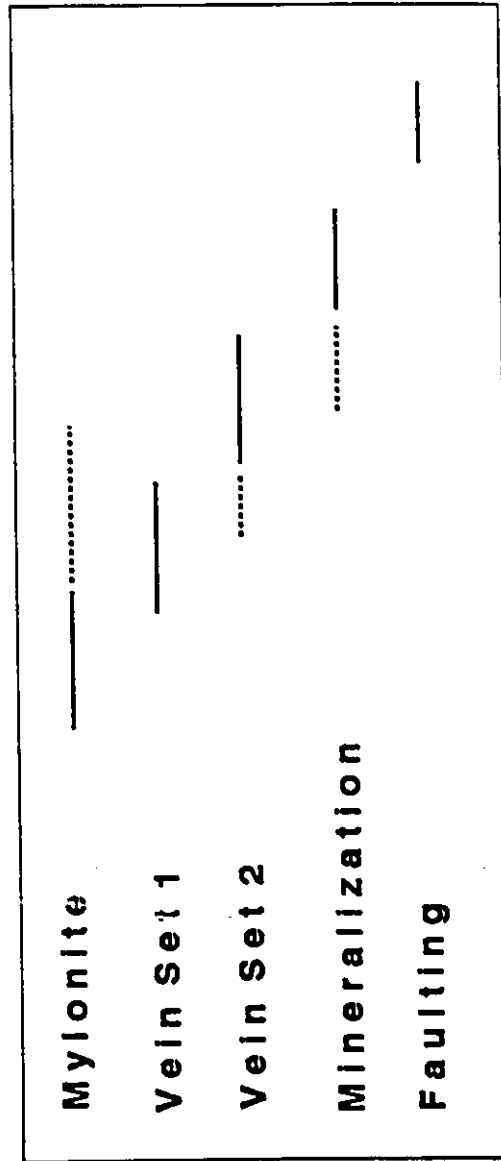
4.3.7 Sequence of Events

The field and petrographic relationships described above from the Finlay McKinlay deformation zone indicate the following sequence of events (Figure 17):

- 1) Heterogeneous ductile deformation in the tonalite resulted in the development of protomylonite, mylonite, and ultramylonite.

- 2) Formation of vein set 1, sub-parallel to the orientation of the shear zone. The veins cross-cut the mylonite fabric at a low angle to the foliation which indicates that they post-date mylonitization.

Sequence of Events



Time →

Figure 17 Relative sequence of events in Finlay McKinlay deformation zone.

3) Formation of vein set 2. These veins cross-cut the early veins and the mylonites at a high angle to the foliation. Vein set 2 is characterized by a vein breccia, vein ribbons and veinlets that cross-cut the vein quartz. These vein textures and structures are not present in the first vein set. Secondary mineral assemblages in the mylonites and hydrothermal alteration of vein set 2 are similar. The secondary minerals in the mylonite display a preferred orientation parallel to the foliation in the mylonite. This may suggest that ductile deformation in the mylonites continued after formation of vein set 2.

4) Brittle fracturing, veining and mineralization in the veins and the mylonites occurred after the cessation of ductile deformation. Multiple episodes of fracturing are indicated by cross-cutting veinlets with different mineral assemblages. The mineral assemblages in the veinlets represent individual stages in the paragenesis. These include tourmaline-epidote-clinozoisite-magnetite, pyrite-chalcopyrite-pyrrhotite, native gold-tellurides-pyrite-chalcopyrite-galena, and sphalerite-covellite.

5) Brittle faulting with associated brecciation and pseudotachylyte development.

4.4 Comparison of the Finlay McKinlay and Prospector Deformation Zones

Ductile deformation in the Finlay McKinlay deformation zone is characterized by mylonites and the development of a strong S-L fabric. These features are characteristic products of ductile shear zones (Sibson, 1977; Ramsay and Huber, 1987). No mylonites have been identified in the Prospector deformation zone (Figure 18). In contrast, ductile deformation in the Prospector deformation zone is characterized by minor F_2 folds and crenulation cleavage. The Prospector deformation zone occurs within well foliated and layered, Wasekwan Group metavolcanic and metasedimentary rocks. Whereas, the Finlay McKinlay occurs within a massive pre-Sickle tonalite. The different lithologies (well layered versus massive) may explain the ductile deformation (folds vs mylonites) in the Prospector and Finlay McKinlay zones.

All of the veins in the Prospector deformation zone have been affected by ductile deformation and subsequently cross-cut by later faults. Veins in the Finlay McKinlay deformation zone post-date ductile deformation which produced the mylonites but pre-date late faulting (Figure 18).

Gold mineralization occurs in the second vein set of the Finlay McKinlay deformation zone. Gold mineralization may occur as native gold in isolated veinlets or in veinlets associated with pyrite, chalcopyrite, galena, hessite,

SEQUENCE OF EVENTS

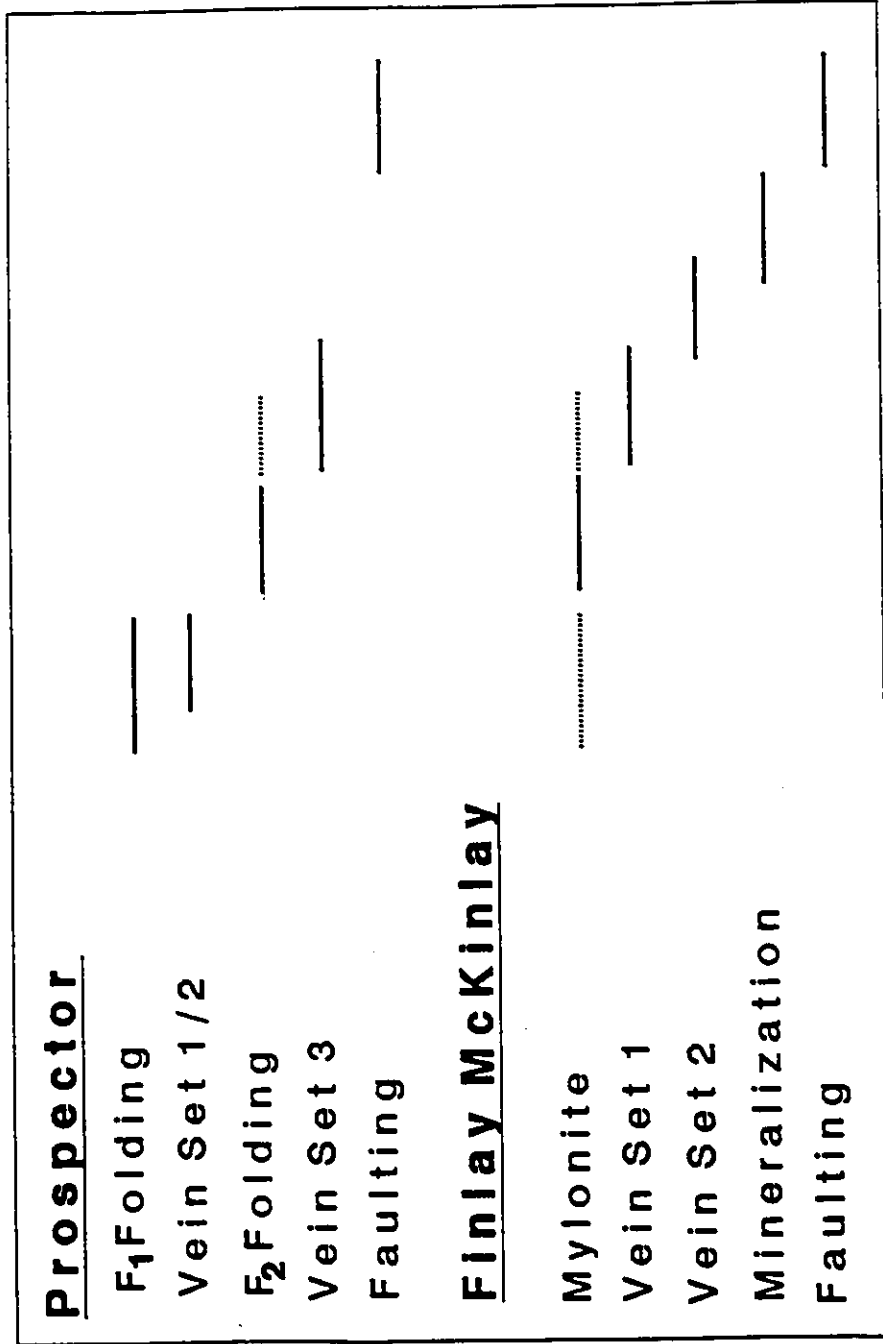


Figure 18 Comparison of the relative sequence of events in the Prospector and Finlay McKinlay deformation zones.

tellurobismuth, muscovite, carbonate and tourmaline. These veinlets suggest that gold mineralization post-dates formation of the second vein set. However, if the veinlets are genetically unrelated to vein set 2 then they should also occur in vein set 1. The second vein set is characterized by vein breccia, vein ribbons and veinlets that cross-cut the vein quartz. These textures and the mineralization have not been observed in any other veins in either the Prospector or Finlay McKinlay deformation zones. It would therefore appear that gold mineralization is genetically linked to the formation of the second vein set in the Finlay McKinlay deformation zone.

4.5 Comparison of the Finlay McKinlay/Prospector Zones to the Johnson Shear Zone

The Prospector deformation zone is a 75 m wide, east-west trending deformation zone which lies directly along strike from the westward end of the Johnson Shear Zone (JSZ), and therefore probably represents the western extension of the JSZ through the Gemmell Lake area. The Finlay McKinlay deformation zone is a 10 m wide, northeast trending zone which occurs approximately 300 m to the south of the Prospector deformation zone.

Deformation features in the Prospector zone and the JSZ are similar, in that both zones are characterized by strongly foliated rocks, crenulation cleavages and minor folds (Fedikow et al., 1986; Richardson and Ostry, 1987). Numerous faults have also been described from the JSZ and

occur as closely spaced faults, breccia zones and fault gouge. In contrast, deformation in the Finlay McKinlay zone is characterized by the development of mylonites which are cross-cut by later faults. Mylonitic textures in the Johnson shear zone are rare, but have been identified in some coarser-grained host lithologies (Kenlay, 1981; Peck, 1986).

Most of the gold occurrences along the length of the Johnson shear zone occur as quartz veins or stockworks (Fedikow et al., 1986; Baldwin, 1987). These veins commonly contain veinlets which contain native gold and pyrite with variable galena, sphalerite, pyrrhotite, chalcopyrite, bornite and arsenopyrite (Milligan, 1960; Fedikow et al., 1986; Richardson and Ostry, 1987). Deformation and gold mineralization in the Johnson shear zone is similar to that found in the Finlay McKinlay shear zone. It may therefore be concluded that the nature of gold mineralization and deformation in both the Finlay McKinlay and the Johnson shear zones are similar and that the relationship of mineralization to deformation in the Gemmell Lake area may also apply to the rest of the JSZ.

CHAPTER 5

FLUID INCLUSIONS IN THE FINLAY MCKINLAY DEFORMATION ZONE

5.1 Introduction

Fluid inclusions have been used extensively in the study of lode gold deposits to determine the nature of the hydrothermal fluids associated with gold mineralization. Roedder (1984) provides a summary of the fluid inclusion literature pertinent to lode gold deposits. Examples of relevant fluid inclusion studies include those by Krupka et al. (1977), English (1981), Guha et al. (1982), Lakind and Brown, (1984), Smith et al. (1984), Brown (1985), Ho et al. (1985), Brown and Lamb (1986), Wood et al. (1986) and Robert and Kelly (1987). Most lode gold deposits are characterized by low salinity, aqueous fluids (1 to 6 wt. % NaCl equiv.) which contain CO₂ (< 15 to 25 mole %) and in some cases, minor amounts of CH₄ (< 5 mole %). Homogenization temperatures of fluid inclusions in lode gold deposits generally range from 200° to 400°C. These temperatures provide minimum formation temperatures; the actual temperatures of formation may have been higher (Roedder, 1984; Colvine et al., 1988). Fluids associated with lode gold deposits are considered to be relatively reducing with neutral to slightly alkaline pH.

The objectives of this portion of the study are to determine the nature of hydrothermal fluids that permeated the Finlay McKinlay zone and to identify the fluids responsible for gold deposition.

5.2 Characteristics of Fluid Inclusions in the Finlay McKinlay Deformation Zone

Fluid inclusions in the two vein sets were classified according to the nature and proportion of phases present at room temperature. The quartz in both vein sets contains abundant secondary inclusions. No primary fluid inclusions have been identified.

Fluid inclusions in the two vein sets have been classified into four types: Type 1) aqueous, liquid-vapour inclusions, Type 2) vapour-rich inclusions, Type 3) mixed aqueous-carbonic inclusions and Type 4) aqueous, liquid-only inclusions.

The distribution of the above fluid inclusions between the two vein sets is distinctive (Figures 19 and 20). Most of the fluid inclusions are small, less than 10 μm .

Aqueous, liquid-vapour inclusions (Type 1) and mixed aqueous-carbonic inclusions (Type 3) are present in both vein sets. Type 1 inclusions in vein set 1 occur along short secondary or pseudosecondary planes which generally do not cross quartz grain boundaries. In contrast, Type 1 inclusions in the second vein set occur along secondary planes which cross-cut grain boundaries. Type 3 inclusions occur in both vein sets along short secondary planes and appear to be more abundant in vein set 1.

The vapour-rich inclusions (Type 2) occur in long secondary planes in vein set 1 but are rare in vein set 2, where they occur along short secondary planes. Aqueous,

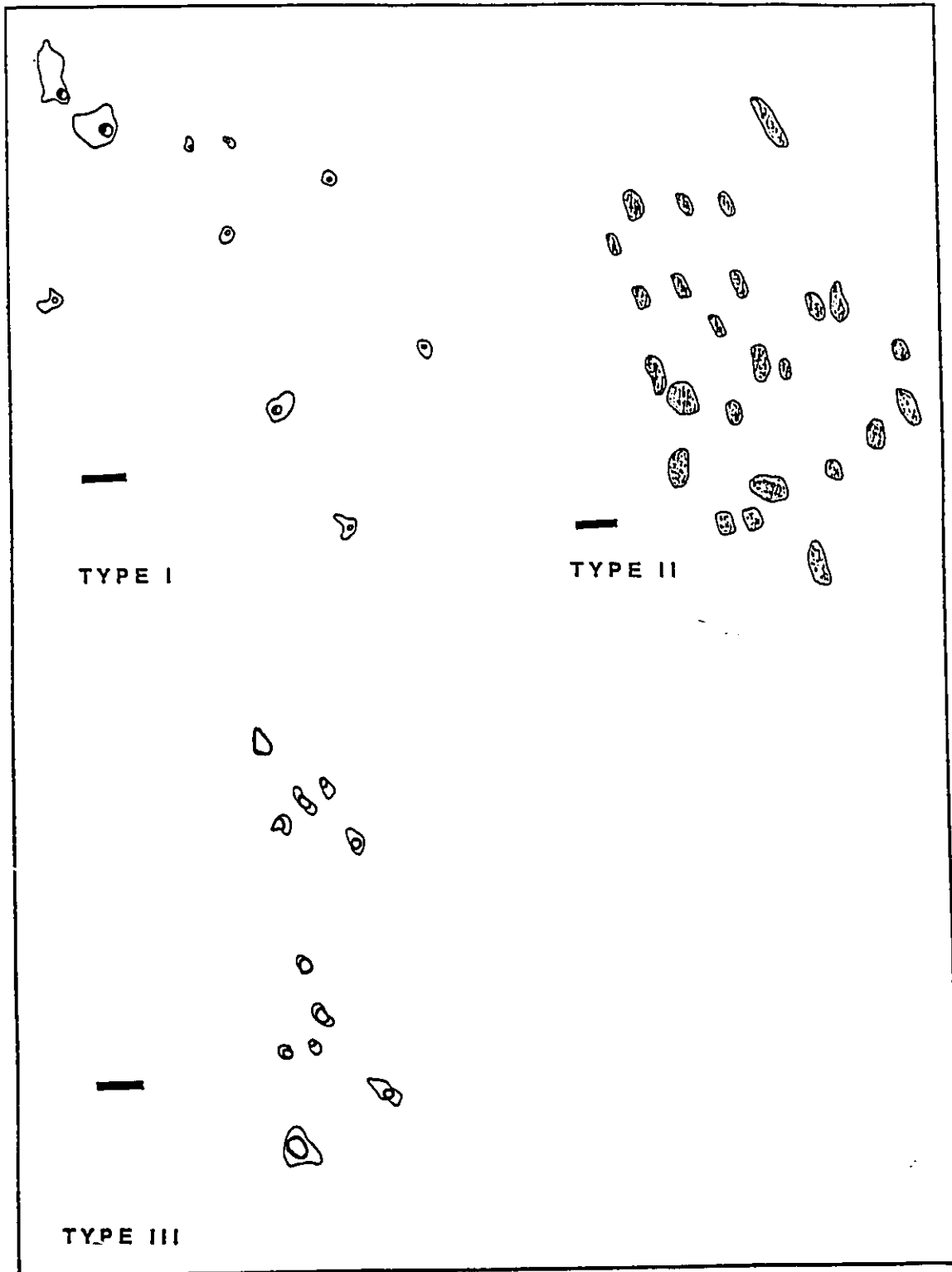


Figure 19 Fluid inclusions in Vein Set 1. Scale bars are 10 μm in length.

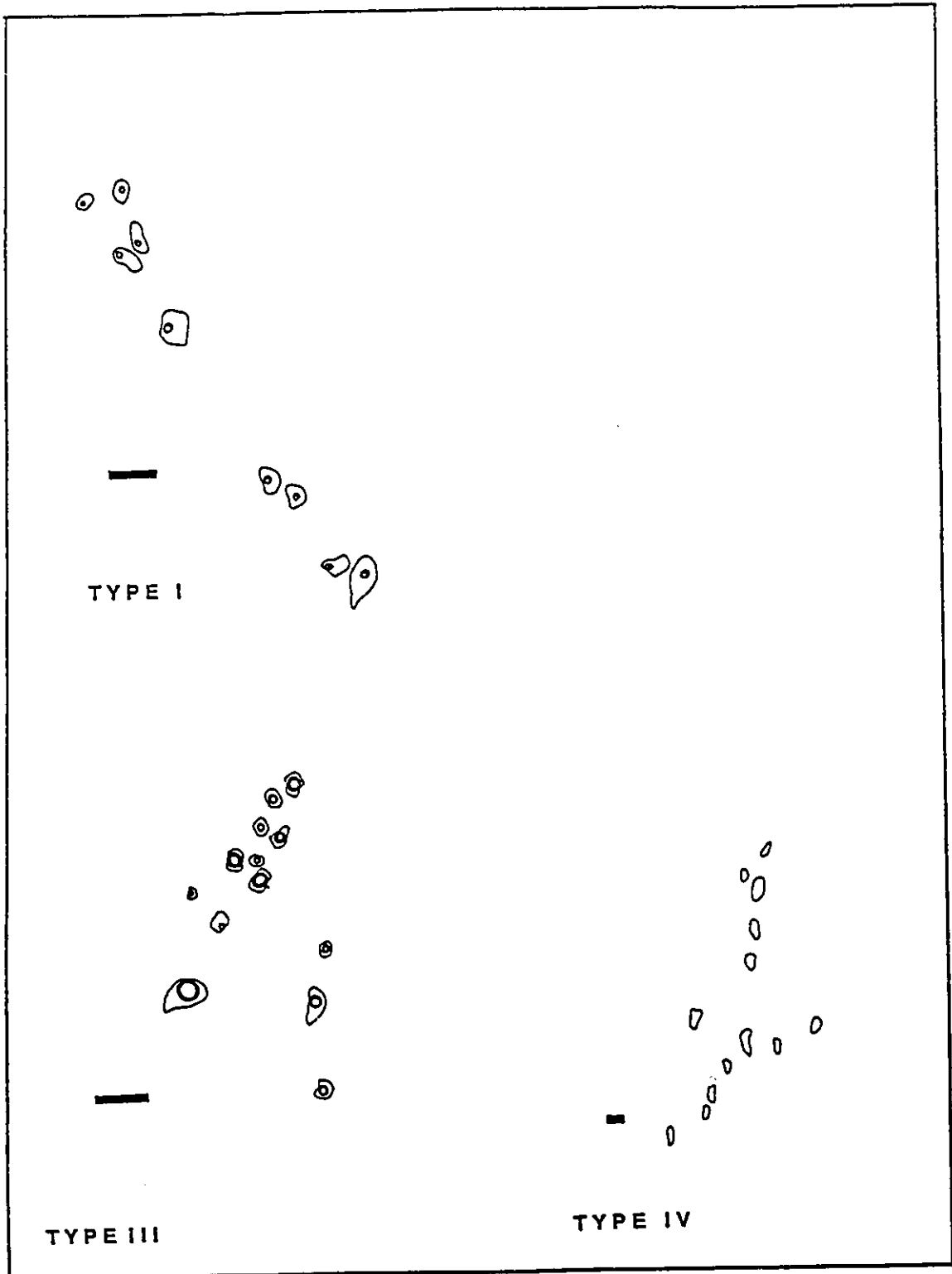


Figure 20 Fluid inclusions in Vein Set 2. Scale bars are 10 μm in length.

liquid-only inclusions (Type 4) are rare, and have only been observed along secondary planes in vein set 2.

Microthermometry, laser-excited Raman microprobe spectroscopy and quadrupole mass spectrometry have been utilized to ascertain the composition of the fluids trapped in the secondary inclusions.

Microthermometric measurements were made using a programmable Linkam TH600 heating-freezing stage. The heating-freezing stage provides microthermometric analysis of fluid inclusions over a range of temperatures from -180° to $+600^{\circ}\text{C}$ (Shepherd, 1981). The stage was calibrated using standard organic and inorganic liquids and solids (Macdonald and Spooner, 1981). The microthermometric results are displayed in Tables 1 and 2.

Laser Raman microprobe spectroscopy was used to identify the major volatiles within individual fluid inclusions in the quartz. A Jobin-Yvon U 1000 Raman spectrometer fitted with a 3 W Spectra Physics Ar ion laser was used to analyze individual inclusions. Spectra were collected through a Nacet microscope using a x80 objective, an excitation wavelength of 514.5 nm (200-300 mW), monochromator slit widths of 300 μm , a stepping interval of 1 cm^{-1} and an integration time of 1 second.

Quadrupole mass spectrometry was carried out at the University of Michigan in order to characterize the volatiles present in the inclusions. Several sand-sized grains of vein quartz were crushed and the released gases

were fed directly into a V G quadrupole mass spectrometer. A data-reduction program developed at the University of Michigan compares mass spectra obtained on gases to gas mixtures of known composition.

5.3 Fluid Inclusion Compositions

5.3.1 Aqueous, Liquid-Vapour Inclusions (Type 1)

Type 1 inclusions are aqueous, liquid-vapour inclusions which homogenize to the liquid phase. Type 1 inclusions in both vein sets displayed a wide range of homogenization temperatures (T_h) from 114° to 459°C (Figure 20). Final ice-melting temperatures (T_{mICE}) ranged from -9.4° to 0.0°C (Figure 21).

Data points and error bars on Figure 21 represent average values and one standard deviation, respectively obtained from groups of co-genetic fluid inclusions. Data points on the far left and upper right represent data for which only T_{mICE} or T_h , respectively, were obtained.

No data is available on the nature of the major cations dissolved in the inclusion fluids. Initial ice melting temperatures (T_e) range from -45° to -19°C. Eutectic temperatures of less than -23° cannot be explained with aqueous-salt systems such as NaCl-H₂O or NaCl-KCl-H₂O. Estimates of salinity must be based on the presence of additional salts such as FeCl₂, MgCl₂ and CaCl₂. Available experimental data (Oakes et al., 1990) allow estimation of the salinity of inclusions in the NaCl-CaCl₂-H₂O system (which has a eutectic temperature of -52°C).

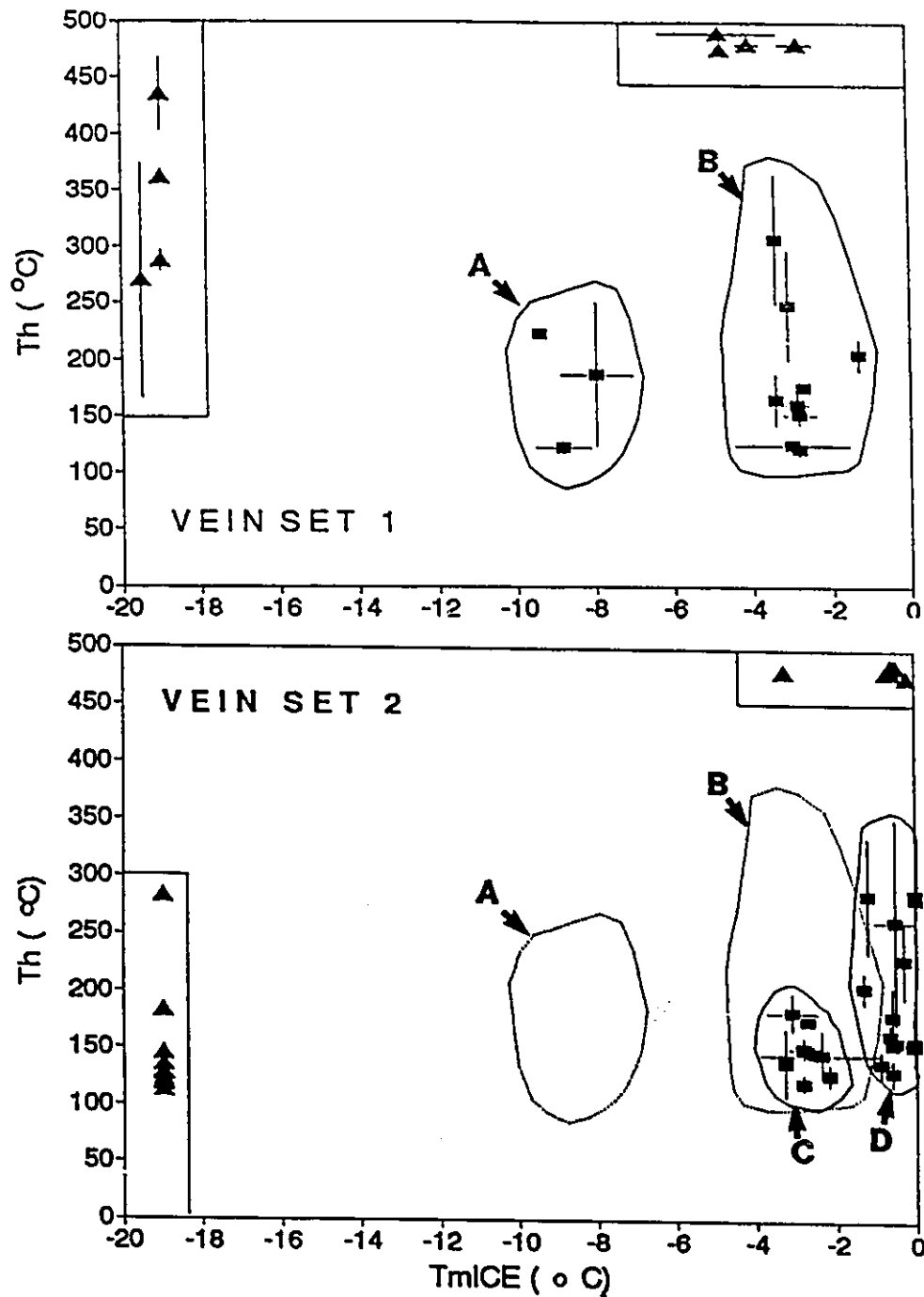


Figure 21 Th vs TmICE diagram for aqueous, Type 1 inclusions in vein sets 1 and 2. Field A and Field B represent the distinct groups of high and low salinity aqueous inclusions in vein set 1. Field C and Field D represent the distinct groups of moderate salinity and low salinity aqueous inclusions in vein set 2.

The salinity estimated for a given T_{mICE} value is the median value for that isotherm (the T_{mICE} value) in the NaCl-CaCl₂-H₂O system. T_{mICE} values from the two vein sets differ. In vein set 1, there are two aqueous fluids with salinities that range from 12 to 14 (Group A) and 4 to 8 (Group B) equiv. wt. % NaCl + CaCl₂ (Figure 21). Salinity values of Type 1 inclusions in the second vein set suggest the presence of two distinct fluids with values of 4 to 8 (Group C) and 0 to 3 (Group D) equiv. wt. % NaCl + CaCl₂ (Figure 21).

5.3.2 Vapour-rich Inclusions (Type 2)

Type 2 inclusions are vapour-rich. They are dark, generally opaque inclusions, which restricted the observation of phase changes that could have been used to determine their composition. Raman Spectroscopic analysis did not indicate the presence of CO₂, CH₄ or N₂. These inclusions most likely represent low density aqueous fluids.

5.3.3 Aqueous-Carbonic Inclusions (Type 3)

These inclusions contain an inner CO₂-rich (carbonic) phase and an outer, aqueous H₂O phase. During cooling, to temperatures as low as -190°, the carbonic phase nucleated a vapour bubble and the CO₂ froze between -94° and -110°C. On subsequent heating, the carbonic phase melted (T_{mCO_2}) between -56.6° to -58.6°C (Figure 22). The values below -56.6°C indicate the presence of additional gases such as CH₄ or N₂. Final ice melting temperatures of the aqueous phase could not be obtained from these inclusions.

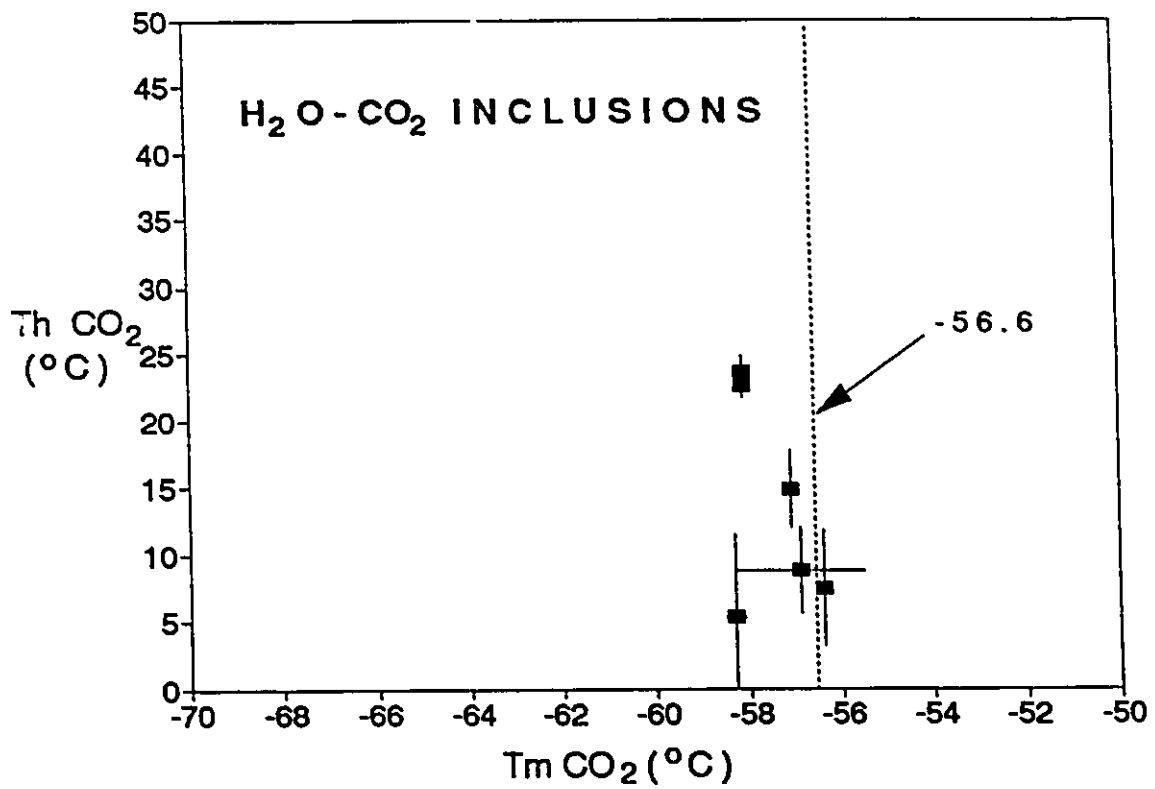


Figure 22 ThCO₂ vs TmCO₂ diagram for mixed H₂O-CO₂, Type 3 inclusions.

Clathrate melting temperatures were observed in only a small number of inclusions and ranged from 5.9° to 11.0°C. H₂O-CO₂ inclusions have an invariant clathrate melting temperature of 10°C. Deviation of the clathrate melting temperature from this value indicates the presence of additional components. The addition of NaCl or CH₄ shift the clathrate melting temperature to lower and higher temperatures respectively (Burruss, 1981). The minimum salinities of the aqueous phase in the Type 3 inclusions, calculated using the equation of Bozzo et al. (1973), range from 1.4 to 4.5 equivalent wt % NaCl.

Homogenization temperatures of the carbonic phase (ThCO₂) ranged from -0.1° to 25.4°C (Figure 22). In all cases, homogenization was to the liquid phase, in the absence of clathrate. All of the aqueous-carbonic inclusions decrepitated prior to total homogenization.

Several of the Type 3 inclusions provided Raman peaks for CO₂. CH₄ and N₂ were not detected in any of the inclusions. This may be the result of the low concentrations of these species in the carbonic fluid or the small size of the inclusions. However, the concentrations of these gases may be estimated using microthermometric data.

As the binary CO₂-CH₄ and CO₂-N₂ systems have similar properties and phase relationships (Arai et al., 1971; Touret, 1982; Ramboz et al., 1985), the mole fraction of CH₄ and N₂ can be expressed in terms of equivalent mole

fraction of CH_4 ($X_{\text{equiv. CH}_4}$).

In such inclusions, $X_{\text{equiv. CH}_4}$ can be calculated using $T_m\text{CO}_2$, $T_h\text{CO}_2$ and an $X\text{CH}_4$ -molar volume polythermal projection for the CO_2 - CH_4 system (Burruss, 1981; Heyen et al., 1982) (Figure 23). However, in H_2O -bearing inclusions, such as the Type 3 inclusions, if clathrate forms on cooling, the composition and molar volumes of the carbonic phase, can only be calculated using a graphical method developed by Seitz et al. (1987). This method requires the measurement of $T_h\text{CO}_2$ both in the presence and in the absence of clathrate. If $T_m\text{CO}_2$ and only one $T_h\text{CO}_2$ value (in the presence or absence of clathrate) are used to calculate $X\text{CH}_4$, the estimated $X\text{CH}_4$ values may be 0.05 to 0.08 too low. This is because CH_4 is preferentially partitioned into the clathrate over CO_2 , thus altering the composition of the residual fluid.

$T_m\text{CO}_2$ in the presence of clathrate and $T_h\text{CO}_2$ in the absence of clathrate were measured for Type 3 inclusions. As a result, the Seitz et al. (1988) method could not be used to determine $X\text{CH}_4$ values for the Type 3 inclusions. However, minimum concentrations of CH_4 can be calculated using the Heyen et al. (1982) method. Calculated minimum $X\text{CH}_4$ equiv. values for the carbonic phase of Type 3 inclusions range from 0 to 0.12 (Figure 23). As noted above, these values may be on the order of 0.05 to 0.1 too low. Calculated molar volumes range from 60 to 90 cm^3/mole (Figure 23).

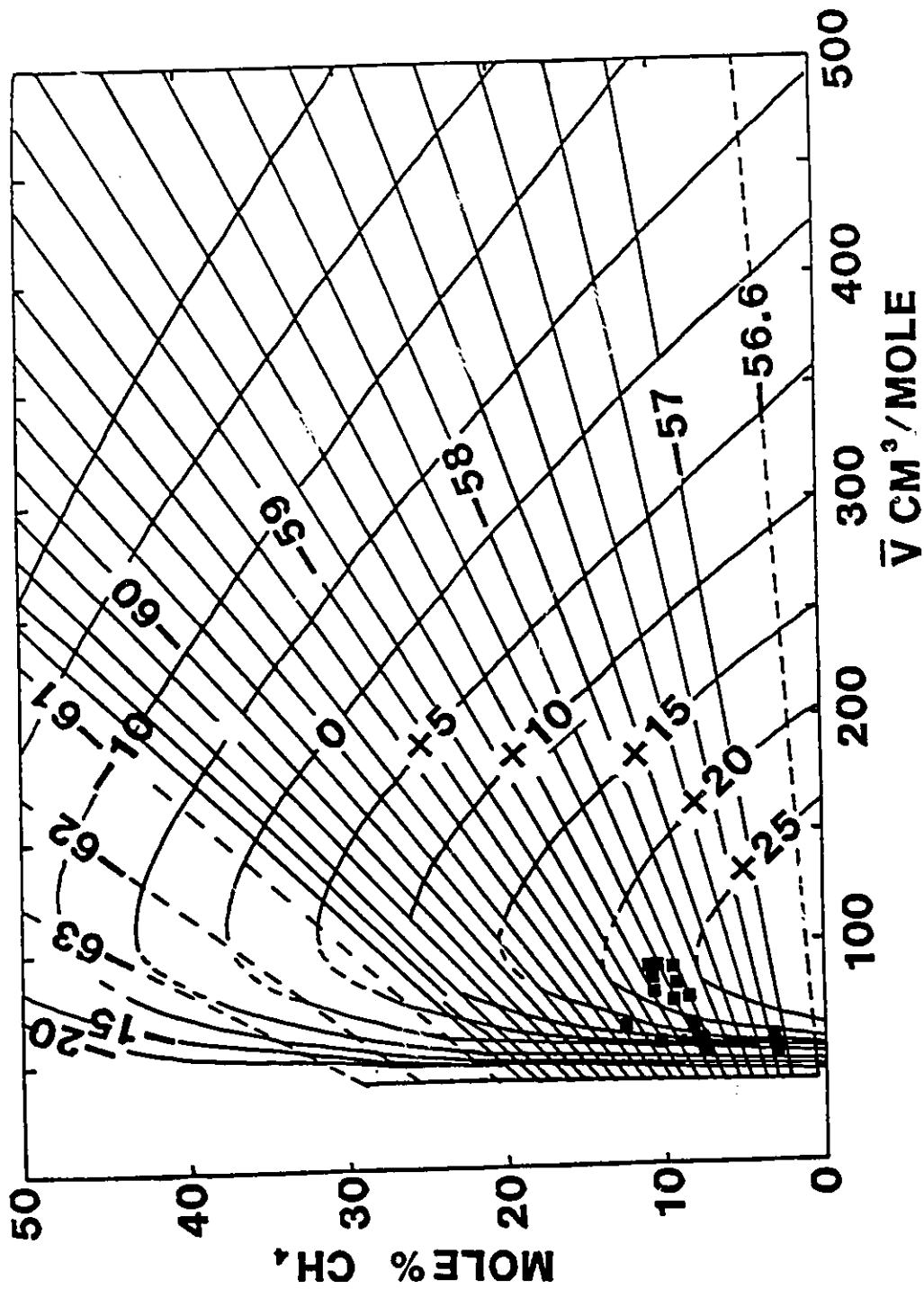


Figure 23 Estimates of X_{CH_4} in mixed H_2O-CO_2 , Type 3 inclusions using the diagram of Heyen et al. (1982).

An estimate of the bulk composition and bulk molar volume of the inclusions was determined by calculating the ratio of the aqueous and carbonic phases, X_{CH_4} of the carbonic phase, and the molar volumes of the phases.

Relative volumes of the aqueous and carbonic phases were calculated by determining the two dimensional area of individual phases at room temperature (Samson and Williams-Jones, 1991). These areas were measured with a dot planimeter and precise drawings produced with a drawing tube. Volumes were calculated assuming the spherical or semi-spherical shape of the carbonic phase as the third dimension. Mole fractions of H_2O , CO_2 and CH_4 were calculated using equations 1 through 4 in Table 2.

Microthermometric data were obtained on only a few groups of Type 3 inclusions because the small size (less than 10 μm) of the inclusions made observations of the phase changes difficult. X_{H_2O} values range from 0.20 to 0.71, X_{CO_2} values range from 0.30 to 0.80 and X_{CH_4} equiv. values range from 0 to .03 (Table 1).

The few analyses obtained on bulk crushes using quadrupole mass spectrometry compare favorably with the above results for individual fluid inclusion groups. Three reliable analyses indicate that the fluids are dominated by H_2O (45 to 50 %) and CO_2 (35 to 45 %) with low concentrations of both CH_4 (< 3 %) and N_2 (< 6 %) (Table 3). Methane and nitrogen in vein set 1 (1.79 to 4.12 %; Table 3) obtained by quadrupole mass spectrometry are similar to the

TABLE 1 Bulk Compositions of the Aqueous-Carbonic Inclusions

Sample #	Type	Vaq	TmCO2	TmICE	Tmclath	sal	Th	ZCO2	ZCH4	MVc	dH2O	MW
FM 88-21-01	L-L	0.30	-58.3	-	9.3	1.43	5.4	0.93	0.08	52.0000	1.0014	18.5785
FM 88-21-01	L-L	0.35	-58.1	-	7.7	4.50	22.5	0.91	0.09	78.0000	1.0256	19.8222
FM 88-27-02B	L-L	0.08	-56.4	-	8.0	3.95	23.6	1.00	0.00	60.1631	1.0212	19.5973
FM 88-27-02B	L-L	0.26	-56.4	-	7.7	4.51	7.4	1.00	0.00	49.9978	1.0256	19.8222

Sample #	nH2O	nCO2	nCH4	XH2O	XCO2	XCH4
FM 88-21-01	0.0162	0.0129	0.0010	0.54	0.43	0.03
FM 88-21-01	0.0179	0.0081	0.0008	0.67	0.30	0.03
FM 88-27-02B	0.0042	0.0154	0.0000	0.21	0.79	0.00
FM 88-27-02B	0.0135	0.0151	0.0000	0.47	0.53	0.00

results obtained by microthermometry (0 to 3 %; Table 1).
 Quadrupole data of vein set 2 indicate higher concentrations
 of methane and nitrogen (8.52 %, Table 3). However, there
 is no microthermometry data for the sample FM CH 2-1.

TABLE 2

Equations for Calculating Bulk Compositions Of Mixed
 Aqueous-Carbonic Inclusions (Type 3); Samson and William-Jones (1988)

$$n_{H_2O} = (V_1 \cdot d_1) / MW_1 \quad (1)$$

$$n_{CO_2} = (V_v \cdot Z_{CO_2}) / \bar{V}_v + n_{H_2O} \cdot Z'_{CO_2} \quad (2)$$

$$n_{CH_4} = (V_v \cdot Z_{CH_4}) / \bar{V}_v \quad (3)$$

$$X_i = (n_i) / \sum_i n_i \quad (4)$$

n_i = number of moles of species i in inclusion

X_i = mole fraction of species i in inclusion

Z_i = mole fraction of species i in non-aqueous part of
 the Type 3 inclusions

Z'_i = mole fraction of species i in aqueous part of
 Type 3 inclusions

V_1 = volume of aqueous part of the inclusions

V_v = volume of non-aqueous part of the inclusions

d_1 = density of aqueous part of inclusion

MW_1 = molecular weight of aqueous part of the inclusion

\bar{V}_v = molar volume of non-aqueous part of inclusion

TABLE 3 Quadrupole Mass Spectrometry Analysis
of Vein Quartz

	Vein Set 1		Vein Set 2
	FM 21-01	FM 21-01	FM CH 2-1
Water	45.57 %	46.97 %	50.16 %
Propane	0.08 %	0.0 %	0.05 %
Methane	1.18 %	1.12 %	2.81 %
Ethane	0.0 %	0.40 %	0.28 %
Hydrogen Sulphide	0.28 %	0.05 %	0.04 %
Sulfur Dioxide	0.34 %	0.13 %	0.17 %
Oxygen	28.32 ppm	0.0 %	0.0 %
Carbon Dioxide	43.83 %	42.79 %	37.35 %
Carbon Monoxide	7.91 %	5.309 %	3.15 %
Argon	0.21 %	0.17 %	0.19 %
Nitrogen	0.61 %	3.0 %	5.81 %
Nitrogen + Methane	1.79 %	4.12 %	8.62 %

5.3.4 Aqueous, Liquid-only inclusions (Type 4)

Type 4 inclusions nucleated a vapour bubble during cooling at temperatures of less than -100°C . On subsequent heating, they homogenize to the liquid phase (Th) between 33° and 52°C (Figure 24). Final ice melting temperatures range from -47° to -43°C (Figure 24) and initial ice melting temperatures range from -75° to -88°C . Such low initial and final ice melting temperatures indicate that the fluid contains salts in addition to NaCl. Salinities estimated using the $\text{H}_2\text{O}-\text{NaCl}-\text{CaCl}_2$ system for the Type 4 inclusions range from 29.0 to 30.3 equiv. wt. % NaCl + CaCl_2 .

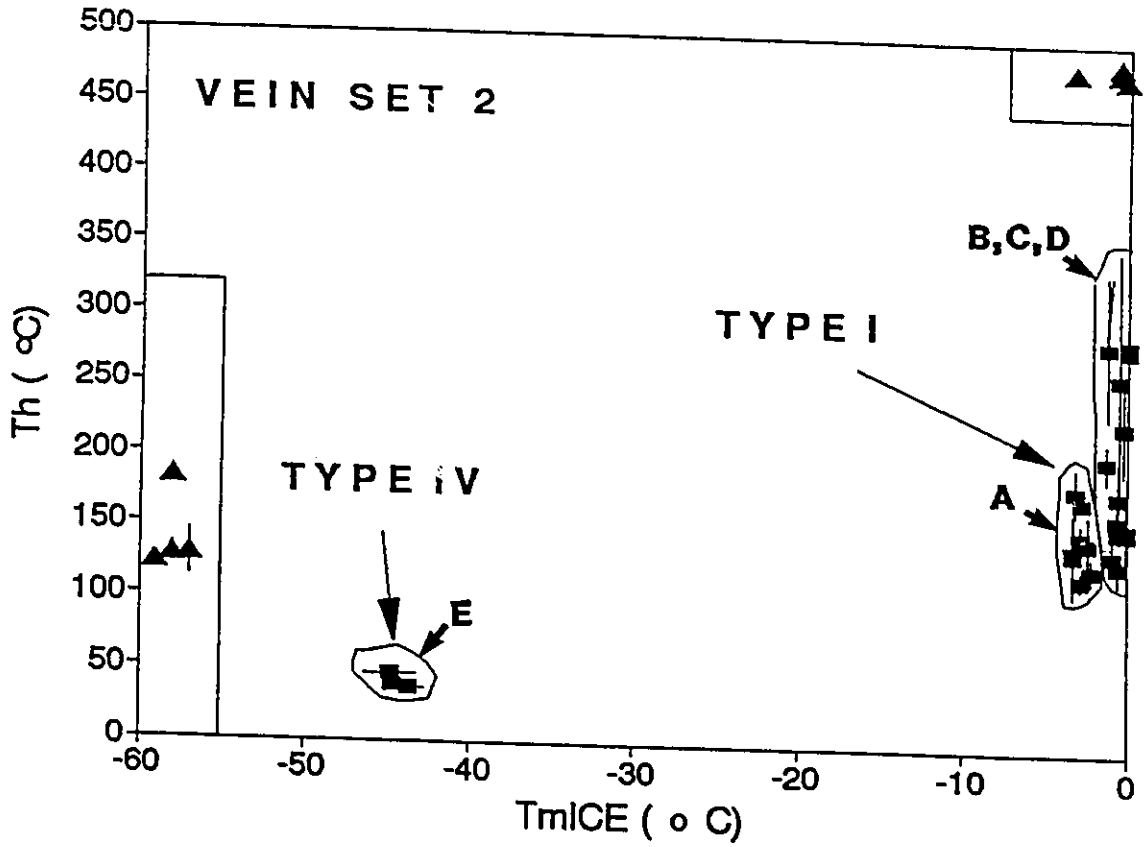


Figure 24 Th vs TmICE diagram for aqueous, Type 4 inclusions in vein set 2.

5.4 Fluid Evolution

Although no primary inclusions have been identified, the distribution and composition of the secondary inclusions provide information on fluid evolution in the Finlay McKinlay shear zone (Figure 25).

The data on the aqueous, liquid-vapour inclusions (Type 1) indicate that moderate salinity aqueous fluids (Group A in Figure 21) were trapped in vein set 1 prior to the formation of vein set 2. Such fluids have not been observed in vein set 2. Lower salinity fluids (Groups B and C in Figure 21) are present in both vein sets. The lowest salinity fluids are present only within vein set 2 (Group D, Figure 21) and therefore post-date vein set 2 or are contemporaneous with it. Therefore, the lowest salinity inclusions in vein set 2 represent later fluids, and the salinity of the aqueous fluids decreased over time.

The restriction of the lowest salinity inclusions to vein set 2 may indicate that they are related to its formation. This could, however, be an artifact of sampling.

The significance of the vapour-rich inclusions (Type 2) is not known because of the lack of compositional data. These fluids appear, however, to be abundant only within the first vein set and may represent an early vapour-rich aqueous fluid.

Aqueous-carbonic fluids, represented by the Type 3 inclusions, which contain H_2O , CO_2 with minor CH_4 and N_2 , have been recognized within both vein sets. This suggests

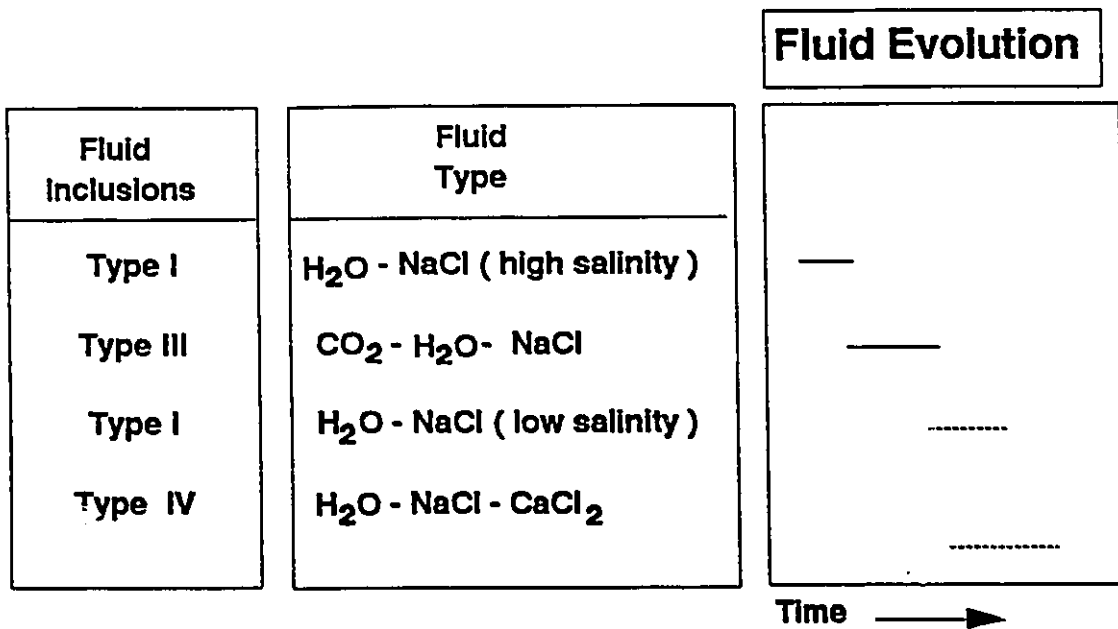


Figure 25 Evolution of fluids in the Finlay McKinlay shear zone.

as with the low salinity Type 1 inclusions, that these fluids post-date vein set 2.

The high salinity aqueous, liquid-only inclusions (Type 4) are present only within vein set 2 and must therefore also post-date vein set 2 or be contemporaneous with it (Group E, Figure 21). In this case, the restriction of the Type 4 inclusions to vein set 2 may indicate that they are related to its formation. This could, however, be an artifact of sampling because, even within vein set 2, they are rare.

Isochores for the aqueous inclusions were calculated in the H_2O -NaCl system using the equation of state of Brown and Lamb (1989) and the Flincor computer program (Brown, 1989). Isochores were constructed for the high and low salinity Type 1 inclusions using the maximum and minimum Th values from the two vein sets (Figure 25). For a given homogenization temperature, the slope of the isochores will be slightly shallower than if $CaCl_2$ were included in the system (Zhang and Frantz, 1987).

Isochores were also constructed for the aqueous-carbonic inclusions (Figure 26) utilizing the equation of state of Brown and Lamb (1989) and the Flincor computer program (Brown, 1989). The isochores calculated by Brown and Lamb (1986) in the H_2O - CO_2 -NaCl system are a best fit between isochores calculated for the H_2O -NaCl system (Zhang and Frantz, 1987) and for CO_2 (Kerrick and Jacobs, 1981).

Isochores constructed for the aqueous, Type 4 inclusions (in the H_2O -NaCl system) are distinct from the

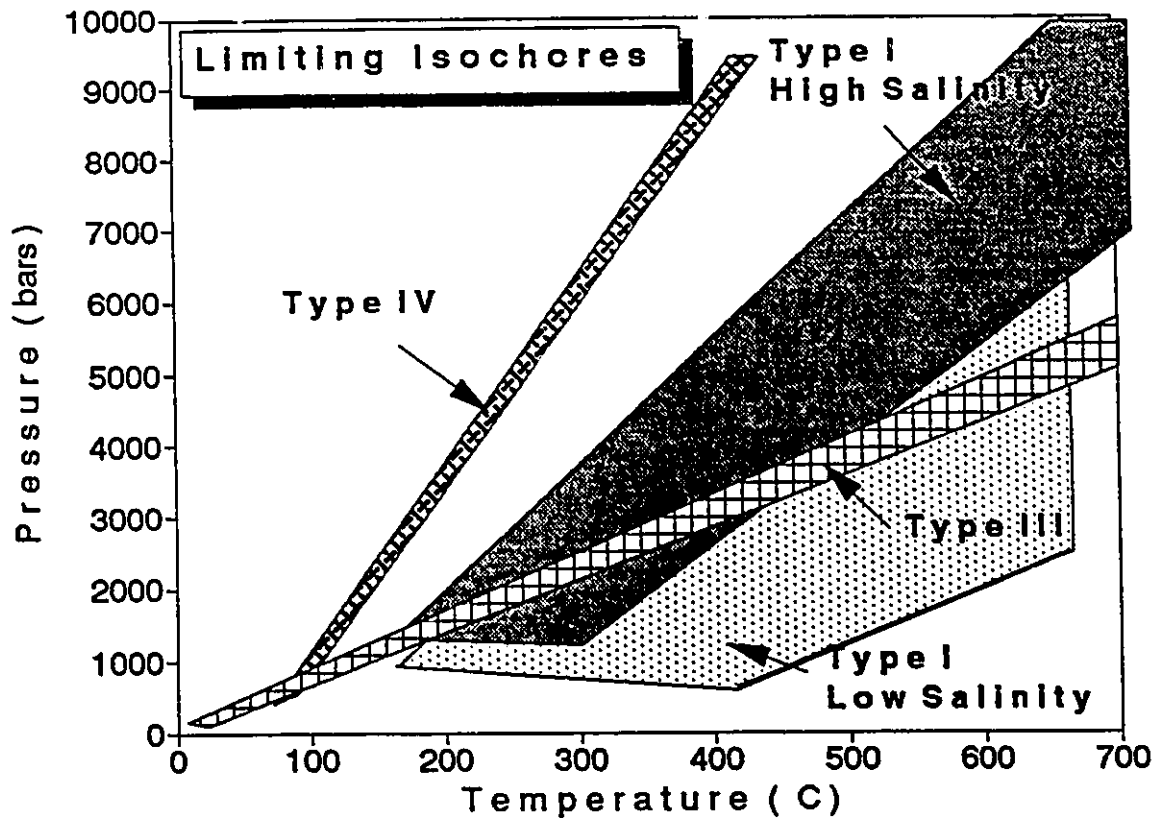


Figure 26 Limiting isochores of the fluid inclusions in the Finlay McKinlay shear zone.

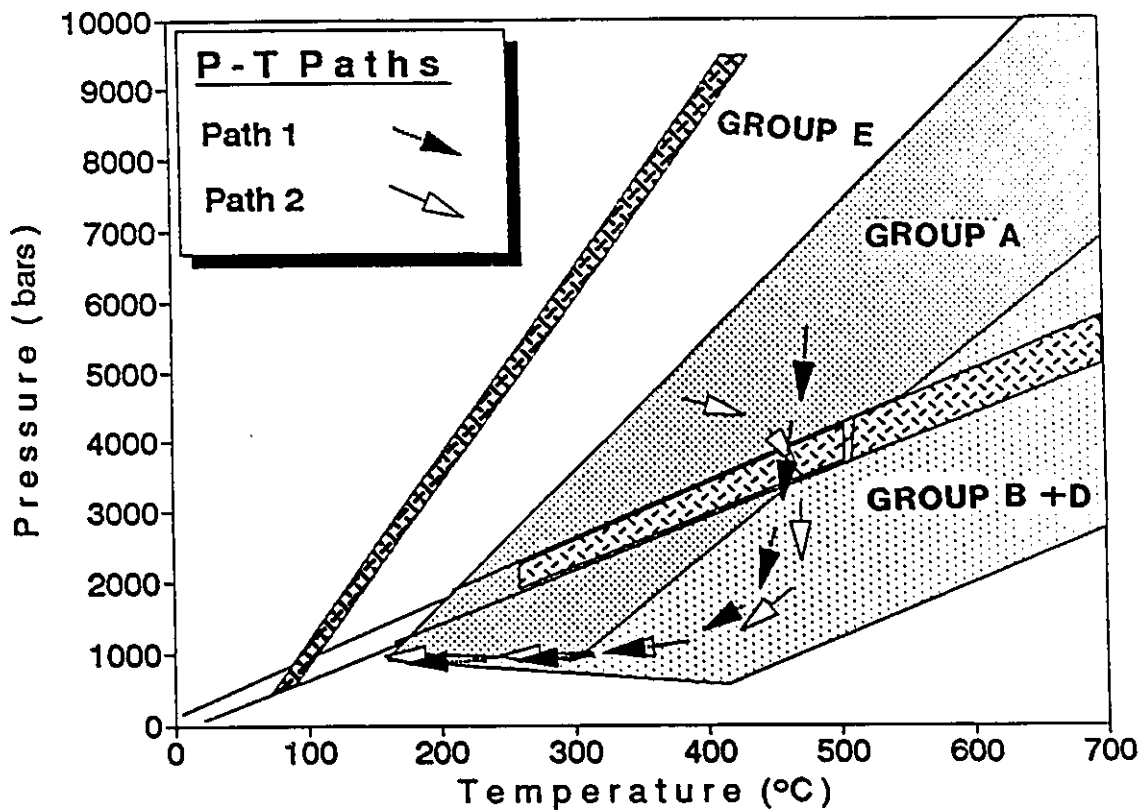


Figure 27 Pressure-Temperature paths of fluids in the Finlay McKinlay shear zone.

other aqueous inclusions, and define a narrow field that does not overlap the isochores for the other aqueous inclusions (Figure 26).

The progression from mylonites, to quartz veins, to faults with pseudotachylyte indicates that deformation progressed from ductile through brittle-ductile to brittle deformation. This suggests that during the development of the shear zone, pressures and temperatures decreased with time, possibly as a result of uplift. The fluid inclusion data indicate early high salinity aqueous fluids (Type 1; Group A) and later low salinity aqueous fluids (Type 1; Group B,C,D), H₂O-CO₂ (Type 3) and high salinity aqueous fluids (Type 4; Group E). Such an evolution and the positioning of the isochores for the fluid inclusions require either a decrease in pressure (Path 1, Figure 27), possibly due to uplift, and/or an increase in temperature (Path 2, Figure 27). An increase in temperature would require intrusive activity; however, no late intrusions have been recognized in the Gemmell Lake area.

The low salinity aqueous fluids (Type 1), the mixed aqueous-carbonic fluids (Type 3) and the high salinity aqueous fluids (Type 4) are all candidates for the gold mineralizing fluids as all these fluid post-date the precipitation of vein set 2 quartz. The mixed aqueous-carbonic fluid inclusions occur in both vein sets 1 and 2 and, in fact, appears to be more abundant in vein set 1. The lack of gold in vein set 1 therefore suggests that these

fluids were not responsible for the gold mineralization. The lowest salinity aqueous fluid (Group D) and the high salinity aqueous fluid (Group E) are the only fluids which are unique to vein set 2. The abundance of Group D inclusions in vein set 2 and the rarity of Group E inclusions suggests that the low salinity aqueous fluids (Group D) is the mineralizing fluid.

CHAPTER 6

DISCUSSION

6.1 Gold Transport Mechanisms

In order to evaluate potential reasons for gold deposition in the Finlay McKinlay shear zone, we first have to consider how gold is transported. Gold can only be transported in significant concentrations in aqueous solutions as complexes (Helegeson, 1969; Seward, 1984). Hydroxide, chloride, bromide, iodide, sulphide, sulphate, cyanide, arsenic, antimony and telluride complexes have all been postulated as possible transporting agents for gold (Romberger, 1984). However, available experimental and thermodynamic data indicate that sulphide and chloride complexes are the most important.

6.1.1 Sulphide Complexes

Based on a study of mercury deposits in California, the solubility of gold as a sulphide complex was postulated as early as 1887 by Becker. Studies on the aqueous solubility of gold-bisulphide complexes include those by Ogryzlo (1935), Smith (1943), Krauskopf (1951), Weisberg (1971), Seward (1973, 1979, 1984), and Shenberger and Barnes (1989).

Seward (1973) evaluated the solubility of gold in aqueous bisulphide solutions as a function of temperature, pH, pressure and sulphide concentration. Seward (1973) indicated that $\text{Au}_2(\text{HS})_2\text{S}^{2-}$, AuHS^0 and most importantly, $\text{Au}(\text{HS})_2^{1-}$ are the dominant sulphide complexes.

The solubility of gold-sulphide complexes increases with increasing temperature and reaches a maximum under near neutral to slightly alkaline conditions at approximately 300°C (Seward, 1973, Shenberger and Barnes, 1989).

The solubility of gold-bisulphide complexes are very sensitive to changes in the activity of oxygen and sulphur. An increase in oxygen activity decreases the aqueous solubility of gold as a result of the oxidation of reduced sulfur (HS^- or H_2S to sulphate). If there is a decrease in the activity of HS^- , the solubility of gold decreases.

Gold-bisulphide complexes generally dominate in reducing conditions at neutral to slightly alkaline pH values, high activity of H_2S and moderate temperatures (< 300°C). If gold is transported as a sulphide complex then the most important mechanisms for deposition from solution are oxidation and a decrease in H_2S or HS^- activity, less important are changes in pH and a decrease in temperature.

6.1.2 Chloride Complexes

The solubility of gold-chloride complexes was first experimentally measured using various chloride solutions by Stokes (1905) and Lenher (1918), and later verified by a number of authors including Ogryzlo (1935), Helgeson and Garrels (1968) and Henley (1973).

The solubility of gold as a chloride complex increases rapidly with increasing temperature and decreasing pH (Henley, 1973). The dominant chloride complexes are generally considered to be AuCl_2^- or AuCl_4^- (Henley, 1973).

Chloride complexes dominate in oxidizing, acidic, high temperature fluids (250° to 350°C). The most important mechanisms for gold precipitation from gold-chloride complexes are decreases in temperature, pH and the activity of chloride ions in solution (Helgeson and Garrels, 1968; Henley, 1973).

6.2 Mechanisms of Gold Deposition

1) Wall Rock Interaction

Fluid-wallrock interactions involving solutions carrying gold complexes may cause gold precipitation. Hydrothermal reactions destabilize the gold-transporting complex and gold is deposited from solution.

The veins in the Finlay McKinlay shear zone are associated with very limited hydrothermal alteration. Further, gold mineralization appears to post-date the vein-related hydrothermal alteration. Thus, wall rock interaction in the Finlay McKinlay shear zone does not appear to be a viable mechanism for gold precipitation.

2) Solution Mixing

Solution mixing of surface-derived fluids with deeper fluids has been postulated as a possible mechanism for gold deposition. Mixing of appropriate fluids could bring about a decrease in temperature and the activity of sulfur, and an increase in oxygen activity.

If solution mixing was the cause of gold deposition in the Finlay Mckinlay zone, then fluid inclusion compositions may reveal contemporaneous end-member fluids and any mixed

fluids. However, based on the fluid inclusion data, there is apparently no evidence of solution mixing in the Finlay McKinlay shear zone.

3) Boiling

In many gold deposits, CO₂ effervescence in aqueous-carbonic fluids has been proposed as the cause of gold deposition. Boiling or CO₂ effervescence can result in increases in pH and oxygen activity in the residual fluid, depending on the initial composition of the solution. Volatile species such as CO₂, H₂S, CH₄, and H₂ are partitioned into the vapour phase during boiling. Given that the mineralizing fluids in the Finlay McKinlay shear zone appear to be a low salinity aqueous fluids, CO₂ effervescence is probably not a viable mechanism for gold precipitation.

In conclusion, no viable depositional mechanism appears to have operated in this part of the Finlay McKinlay shear zone.

6.3 Comparison of Gold Mineralization in the Finlay McKinlay Occurrence and the Agassiz Metallotect

The Agassiz metallotect, located in the northern part of the Lynn Lake greenstone belt, hosts a sequence of dominantly mafic metavolcanic rocks that have been traced along strike for 70 km (Fedikow et al., 1986; Parbary, 1989; Gagnon, 1991). Significant gold mineralization has been discovered at the MacLellan and Farley Lake deposits.

6.3.1 The MacLellan Deposit

The MacLellan deposit is located approximately 7 km northeast of the town of Lynn Lake, Manitoba (Figure 28). Gold mineralization at the MacLellan Mine is hosted by a shear zone which occurs within an interlayered sequence of northeast striking, north-dipping, mafic to ultramafic metavolcanic flows and clastic and chemical metasedimentary rocks (Milligan 1960; Fox and Johnson, 1980; Gagnon, 1991) (Figure 29). The geological setting of the deposit has been previously described by numerous authors including Milligan (1960), Koo (1976), Fox and Johnson (1980), Fedikow and Gale (1982), Fedikow (1986), Fedikow et al. (1986) and Gagnon (1991).

The MacLellan deposit comprises three geologically distinct ore bodies, referred to as the East, Main and West zones, which form a laterally discontinuous series of mineralized zones up to 1500 m in length, (Fedikow, 1986; Gagnon, 1991) (Figure 29).

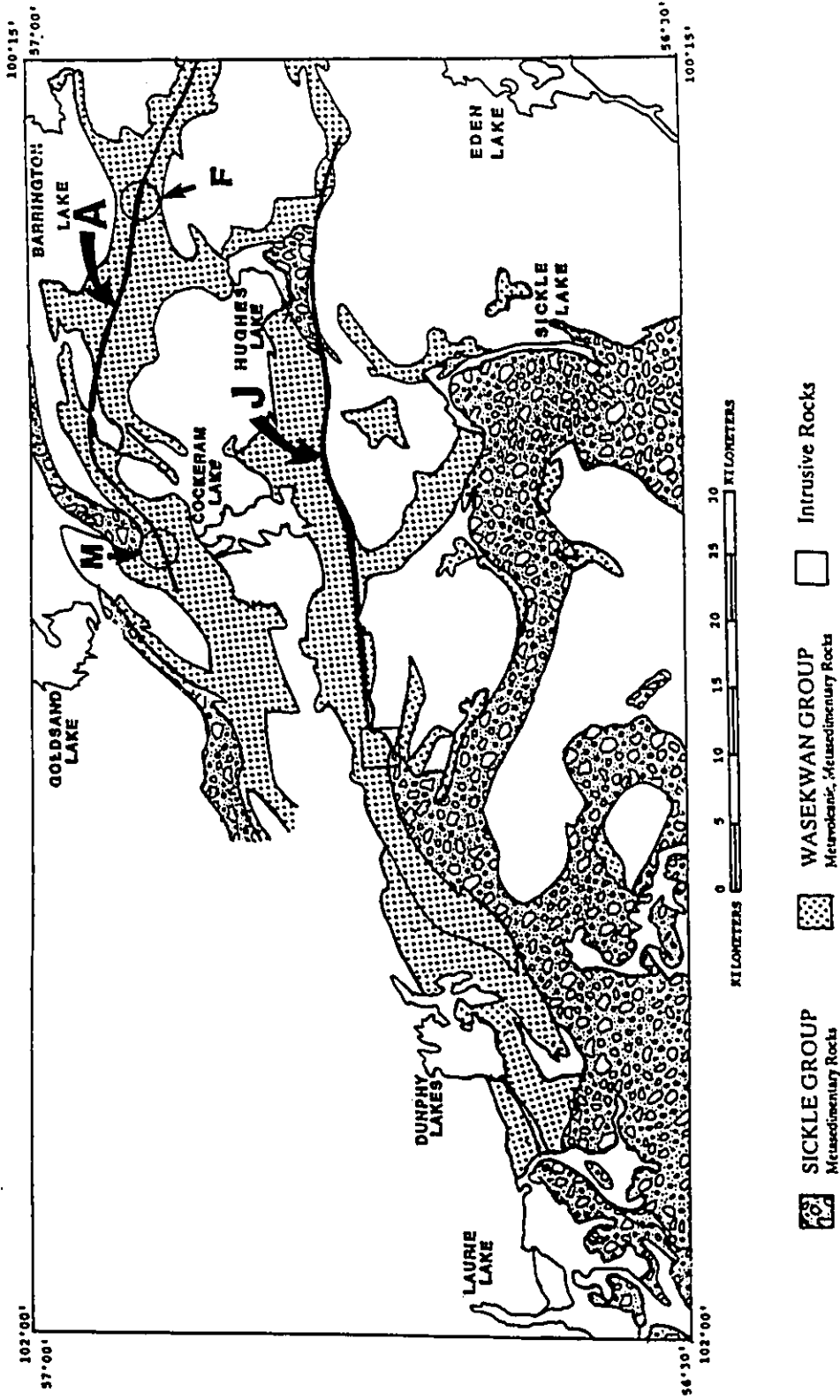


Figure 28 Location of the Maclellan (M) and the Farley Lake (F) deposits along the Agassiz metallotect (A) relative to the Johnson shear zone (J) and study area (Square).

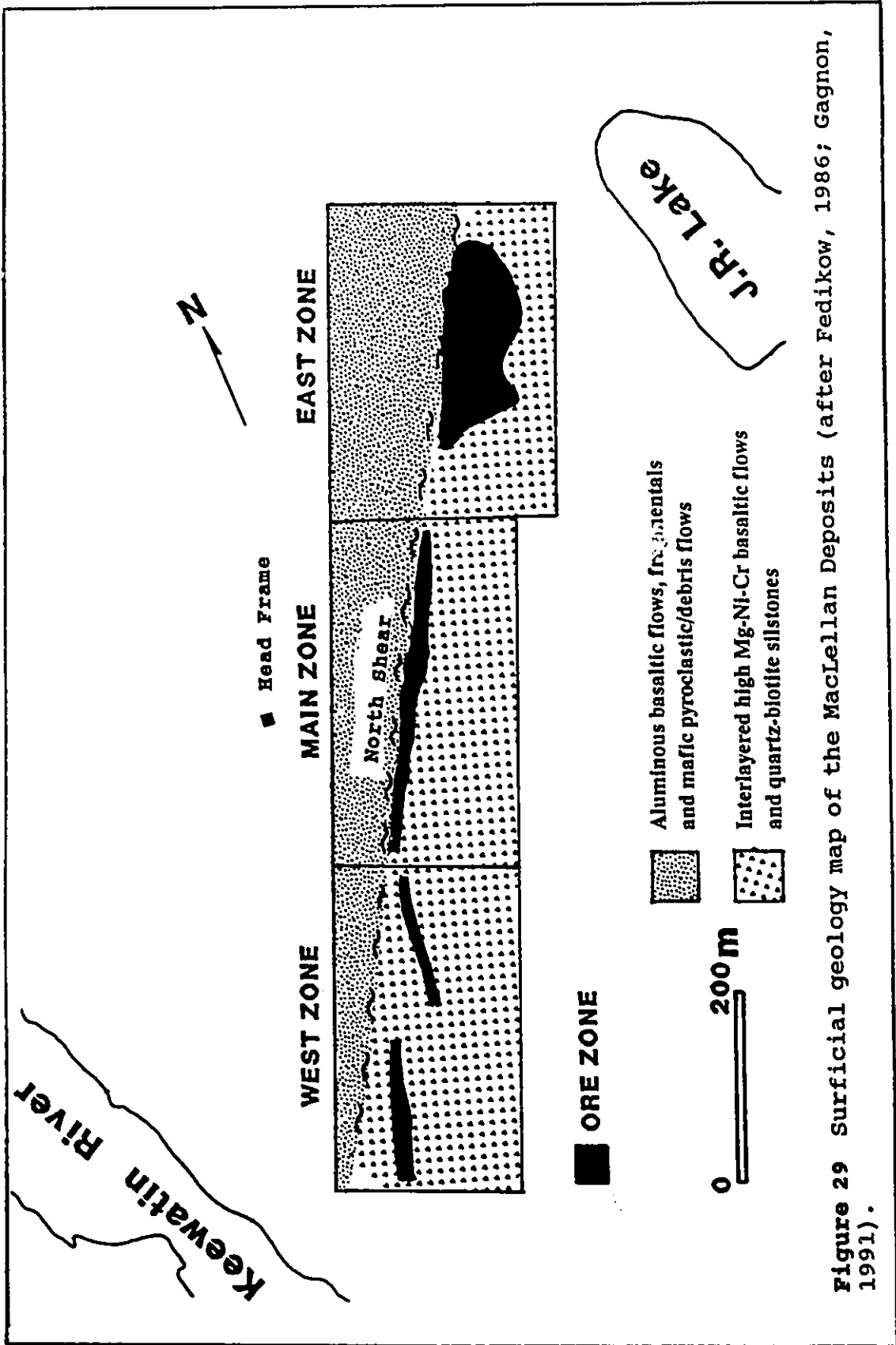


Figure 29 Surficial geology map of the MacLellan Deposits (after Fedikow, 1986; Gagnon, 1991).

The Main zone attains a maximum thickness of 10 to 20 m and can be followed along strike for approximately 400 m (Richardson and Ostry, 1987). Host rocks in this zone comprise chlorite-hornblende and biotite-plagioclase schists which formed during upper greenschist to lower amphibolite facies regional metamorphism and deformation (Gagnon, 1991). Most of the gold mineralization in the Main zone is hosted by quartz-arsenopyrite replacement veins in the biotite-plagioclase schists (Gagnon and Samson, 1989; Gagnon, 1991). These replacement veins are post-metamorphic, formed after ductile deformation but prior to late faulting. Wall rock alteration associated with the veins is dominated by silicification and the development of staurolite, cordierite, andalusite ± sillimanite alteration mineral assemblages, which indicate that the replacement veins formed at high temperatures, above 500°C. Gagnon (1991) suggests that gold mineralization in the Main zone was most likely controlled by sulphidation of the iron-rich wall rocks.

Another, later, veining event occurs at the MacLellan Mine which cross-cuts the replacement bodies (Gagnon, 1991). These veins comprise predominantly quartz with minor amounts of galena, sphalerite, pyrite and arsenopyrite and have no obvious wallrock alteration. In the MacLellan deposits, the later veins only contain significant gold concentrations when they cross-cut the earlier quartz-arsenopyrite replacement veins (Gagnon, 1991).

6.3.2 Farley Lake Deposits

The Farley Lake deposits are located approximately 40 km east of the town of Lynn Lake, Manitoba (Figure 26). Gold mineralization at Farley Lake is associated with an oxide-facies iron formation, interlayered with Wasekwan Group metasedimentary and metavolcanic rocks (Richardson and Ostry, 1986). The following description of the Farley Lake deposits is based on the work of Richardson and Ostry (1986).

The Farley Lake deposits comprise three mineralized zones and associated hydrothermal alteration. Individual mineralized zones consist of gold and sulphide-bearing iron formation. These comprise interbedded layers of pyrrhotite-magnetite and chert within subparallel alteration zones characterized by silicification, chloritization and sulphidization. The alteration zones cross-cut the layering in the iron formation.

The Farley Lake deposits are considered to be epigenetic deposits formed by the selective replacement of oxide facies iron formation by gold and sulphur-rich fluids (Richardson and Ostry, 1987). Similar deposits have been observed at the Water Tank Hill deposits in Nevada, Australia (Phillips et al., 1984) and Carshaw and Malga deposits in Timmins, Ontario (Fyon et al., 1983).

6.3.3 Discussion

The quartz-arsenopyrite replacement veins associated with high temperature alteration assemblages in the McLellan deposits are distinctly different from any other gold-bearing veins observed in the Lynn Lake greenstone belt including the Finlay McKinlay shear zone. However, gold mineralization in the MacLellan and the Farley Lake deposits are hosted by iron-rich wallrocks which appear to have controlled gold deposition.

The late veins in the MacLellan Mine are similar to many veins hosting gold mineralization in the Finlay McKinlay and Johnson shear zones. However, there is very little evidence of wallrock alteration associated with the late veins in the MacLellan deposit, Finlay McKinlay or Johnson shear zone. This suggests that wallrock alteration was not effective in these later veins and that gold mineralization is controlled by a different depositional mechanism.

6.4 Gold Mineralization in the Central Metavolcanic Belt, LaRonge Domain

Approximately 80 gold occurrences have been discovered in the Central Metavolcanic Belt of the LaRonge domain; the western portion of the LaRonge-Lynn Lake domain. This belt comprises a westward-dipping assemblage of ultramafic to felsic metavolcanic rocks which have been intruded by numerous syn- to late-kinematic elliptical plutons (Coombe et al., 1986). Regional metamorphism in the belt varies

from upper greenschist to lower amphibolite facies and the regional foliation is generally developed parallel to bedding. Northeast to northwest-striking shear zones with mylonitic rocks have been well documented in the Central Metavolcanic Belt (Poulsen, 1986; Poulsen et al., 1986).

Gold occurrences in the Central Metavolcanic Belt have been subdivided into stratiform and vein-type gold deposits (Coombe et al., 1986). Approximately 90 % of the gold occurrences in the Central Metavolcanic belt are vein-type deposits and the remainder are stratiform-type deposits (Coombe et al., 1986). Stratiform-type deposits occur within mafic metavolcanic rocks and stratiform carbonaceous sediments, chert and iron formations. Native gold occurs with pyrite and arsenopyrite and is locally accompanied by variable amounts of pyrrhotite, chalcopyrite, galena and sphalerite. Vein-type deposits comprise discrete quartz veins and stockworks hosting native gold with variable amounts of pyrite, galena, pyrrhoitite, chalopyrite, sphalerite and rare molybdenite, stibnite, marcasite, hematite, magnetite and tellurides. (Coombe et al., 1986).

6.4.1 Star Lake Lode Gold Deposits

The Star Lake pluton, located in the Central Metavolcanic Belt, is an elliptical pluton comprising an outer dioritic margin, an inner monzodiorite and a monzonite-granite core. The Star Lake deposits comprise auriferous quartz veins hosted by subordinate, northeast-

striking shear zones which vary in width from a few meters to several tens of meters (Poulsen, 1986). These northeast-striking shear zones are characterized by protomylonites and mylonites, penetrative foliations, and quartz veins. Native gold is intimately associated with pyrite, chalcopyrite, pyrrhotite, and minor amounts of arsenopyrite, molybdenite, chalcocite, bornite and trace amounts of scheelite and tellurides (Poulsen, 1986; Ibrahim and Kyser, 1991). Pyrite is the main sulphide mineral in the veins and it generally forms aggregates or euhedral grains filling fractures within the vein quartz (Ibrahim and Kyser, 1991).

Recent investigations of fluid inclusions in the Star Lake deposit by Ibrahim and Kyser (1991) indicated that the mineralizing fluid is characterized by H₂O-CO₂-NaCl fluids with relatively low density CO₂. The depositional mechanism operating at Star Lake was probably fluid immiscibility of the H₂O-CO₂-NaCl fluids (Ibrahim and Kyser, 1991).

6.4.2 Discussion

The style of gold mineralization in the Central Metavolcanic belt is very similar to that in the Lynn Lake greenstone belt which suggests that similar processes, such as wallrock interaction or fluid immiscibility, controlled gold deposition throughout the LaRonge-Lynn Lake domain.

The stratiform deposits in the Central metavolcanic belt display many similarities to the MacLellan Mine and Farley Lake deposits, in terms of geologic setting, host rocks, mineralogy, and wallrock alteration. Gold

mineralization in these stratiform deposits appears to be strongly controlled by iron-rich host rocks.

The vein-type gold deposits in both the Central Metavolcanic Belt and the Lynn Lake belt are very similar, in terms of mineralogy, vein textures and relative timing of the veins to deformation in the shear zones. Gold deposition in these deposits may be controlled by fluid immiscibility of a mixed H₂O-CO₂ fluid such as those postulated for the Star Lake deposits. If fluid immiscibility was the primary depositional mechanism in all these vein-type deposits, then it is unlikely that there is significant gold mineralization in the Finlay McKinlay shear zone because the mineralizing fluids appear to be low salinity, aqueous fluids.

CHAPTER 7
CONCLUSIONS

Detailed study of two deformation zones in the Gemmell Lake area allow the following conclusions to be made.

1) The Prospector deformation zone is a 75 m wide east-west striking zone of ductile to brittle deformation which occurs within the Wasekwan Group. This zone may represent the westward extension of the Johnson shear zone through the Gemmell Lake area.

2) The Finlay McKinlay deformation zone is a 10 m wide, northeast-striking, brittle-ductile shear zone hosted by a Pre-Sickle, tonalite intrusion approximately 300 m to the south of the Prospector zone. Kinematic indicators in the mylonites indicate that the ductile deformation was most likely the result of sinistral, reverse-oblique displacement.

3) Both the Prospector and Finlay McKinlay zones are characterized by post-metamorphic ductile deformation, quartz veins and late faults. Gold mineralization occurred after the peak of regional metamorphism and ductile deformation but prior to late, brittle faulting.

4) Two vein sets have been recognized in the Finlay McKinlay shear zone. Gold mineralization occurs in quartz veins characterized by vein breccia, vein ribbons and veinlets. Native gold occurs on fractures within the veins and is associated with quartz, carbonate, muscovite, pyrite, chalcopyrite, galena, hessite and tellurobismuth.

5) Four types of fluids infiltrated the Finlay McKinlay shear zone. These are 1) low density aqueous vapour; 2) moderate to low salinity aqueous fluid; 3) low salinity H₂-CO₂ fluid with minor CH₄ and N₂ (less than 12 mole % CH₄ equiv.) and 4) high salinity, aqueous fluid (29 to 30 wt. % equiv. NaCl + CaCl₂).

6) Fluid inclusion data indicate that moderate salinity aqueous fluids 12 to 14 wt% NaCl + CaCl₂ were trapped in vein set 1; lower salinity aqueous fluids (4 to 8 wt% equiv. NaCl + CaCl₂) occur in both vein sets and the lowest salinity aqueous fluid (0 to 3 wt % equiv. NaCl + CaCl₂) occur only in vein set 2. This suggests that the salinity of the aqueous fluids decreased.

7) A low salinity aqueous fluid (0 to 3 wt % equiv. NaCl + CaCl₂), mixed H₂O-CO₂ fluid with minor CH₄ and N₂ and a high salinity aqueous fluid (30 wt % equiv. NaCl + CaCl₂) are all possible candidates for the mineralizing fluids. However, the mineralizing fluid is most likely the low salinity aqueous fluids.

8) The depositional mechanisms, such as wallrock interaction and fluid immiscibility, which are normally called upon to explain gold deposition, both in the LaRonge-Lynn Lake domain, and in other terranes, do not appear to have been important in the Finlay McKinlay shear zone. Therefore it is unlikely that significant gold mineralization occurs in this part of the Finlay McKinlay shear zone.

REFERENCES

- Arai, Y., Kaminishi, G.I., and Saito, S., 1971. The experimental determination of the P-V-T-X relations for the carbon dioxide-nitrogen and carbon dioxide-methane systems. *Journal Chemical Engineering Japan*, v. 4, pp. 113-122.
- Baldwin, D.A., 1986. Gold mineralization associated with the Johnson shear zone. In *Manitoba Mineral Resources Division, Report of Field Activities, 1987, GS-1*, pp. 7-11.
- Baldwin, D.A., Syme, E.C., Zwanzig, H.V., Gordon, T.M., Hunt, P.A., and Stevens, R.D., 1987. U-Pb zircon ages from the Lynn Lake and Rusty Lake metavolcanic belts, Manitoba. two ages of Proterozoic magmatism. *Canadian Journal of Earth Sciences*, v.24, pp 1053-1063.
- Bateman, J.D., 1945. McVeigh Lake area, Manitoba. *Geological Survey of Canada Paper 45-14*, 34p.
- Beach, A., 1976. The interactions of fluid transport, deformation, geochemistry and heat flow in early Proterozoic shear zones in the Lewisian complex. *Phil. Trans. R. Soc. Lond. A*. 280, pp 569-604.
- Becker, G.F., 1887, Natural solutions of cinnabar, gold, and associated sulphides. *American Journal of Science*, v. 33, pp. 199-209.
- Berthe, D., Choukroune, P., and Jegouzo, P., 1979. Orthogneiss, mylonite and non-coaxial deformation of

- granites. the example of the South American Shear Zone. *Journal of Structural Geology*, Volume 1, pp. 31-42.
- Bowers, T.S. and Helgeson, H.C., 1983. Calculation of the thermodynamic and geochemical consequences of non-ideal mixing in the system H_2O-CO_2-NaCl on phase relations in geologic systems. Equation of state for H_2O-CO_2-NaCl fluids at high pressures and temperatures. *Geochimica et Cosmochimica Acta*, Volume 47, pp. 1247-1275.
- Bozzo, A.T., Chen, J.R., Kass, J.R., and Barduhun, A.J., 1973. The properties of the hydrates of chlorine and carbon dioxide. International Symposium on Fresh Water from the Sea, Amaraoussion, Greece, 1973, Proc., v. 3, pp. 437-451.
- Brown, P.E., 1985. Au-only and Au-Ag-base metal ores of the Sioux Lookout-Sturgeon Lake area, NW Ontario - A comparison [abstract]. p. 533 in Abstracts with Programs, Geological Society of America, Volume 17, pp. 772.
- Brown, P.E., and Lamb, W.M., 1986. Mixing of H_2O-CO_2 in fluid inclusions. geobarometry and Archean gold deposits. *Geochimica et Cosmochimica Acta*, Volume 50, pp. 847-852.
- Burruss, R.C., 1981. Analysis of phase equilibria in C-O-H-S fluid inclusions. Mineralogical Association of Canada Short Course Handbook, v. 6, pp. 39-74.

- Colvine, A.C., Fyon, J.A., Heather, K.B., Marmont, S.,
Smith, P.M., and Troop, D.G., 1988. Archean lode gold
deposits in Ontario. Ontario Geological Survey
Miscellaneous Paper, 139, 210 p.
- Coombe, W., Lewry, J.F., and Macdonald, R., 1986. Regional
Geologic setting of gold in the La Ronge Domain,
Saskatchewan. In Gold in the Western Shield, CIM
Special Volume 38, pp. 26-55.
- English, P.J., 1981. Gold-quartz veins in metasediments of
the Yellowknife Supergroup, Northwest Territories. A
fluid inclusion study. Unpublished M.Sc. thesis,
University of Alberta, Edmonton, Alberta, 108 p.
- Fedikow, M.A.F. and Gale, G.H., 1982. Mineral deposits
studies in the Lynn Lake are. In Manitoba Mineral
Resources Division, report of Field Activities, pp. 44-
54.
- Fedikow, M.A.F., 1986. Geology of the Agassiz (MacLellan)
stratabound Au-Ag deposit, Lynn Lake, Manitoba.
Manitoba Energy and Mines, Geological Services Branch,
Open File Report OF85-5, 80p.
- Fedikow, M.A.F., Baldwin, D.A., and Taylor, C., 1986. Gold
mineralization associated with the Agassiz metatect
and the Johnson shear zone, Lynn Lake greenstone belt,
Manitoba. In Gold in the Western Shield, CIM Special
Volume 38, pp. 361-378.
- Ferreira, K., 1986. Geological investigations in the Foster
Lake-Wasekwan Lake area. In Manitoba Mineral Resources

- Division, Report of Field Activities, 1986, pp. 13-17.
- Fox, J.S. and Johnson. W.G.Q., 1980. Komatiites, "boninites", and theolitic picrites in the central LaRonge metavolcanic belt, Saskatchewan and Manitoba and their possible economic significance. Saskatchewan Department of Mineral Resources, Publication No.G-741-1-G-80, 51 p.
- Fyon, J.A., Schwarz, H.P. and Crockett, J.H., 1984. Carbonatization and gold mineralization in the Timmins area, Abitibi greenstone belt: genetic links with Archean CO₂ degassing and lower crustal granulitization. Geological Association of Canada Program with Abstracts, v. 9, p. 65.
- Gagnon, J.E. and Samson, I.M., 1989 Geology, mineralization and alteration in the MacLellan Au-Ag deposit, Lynn Lake, Manitoba. In Manitoba Energy and Mines, Minerals Resource Division, Report of Field Activities, 1989, pp. 13-15
- Gagnon, J.E., 1991. Geology, Geochemistry, and Genesis of the Proterzoic MacLellan Au-Ag Deposit, Lynn Lake Greenstone Belt, Manitoba. Unpublished M.Sc. thesis, University of Windsor, 275 p.
- Gilbert, H.P., Syme, E.C., and Zwanzig, H.V., 1980. Geology of the metavolcanic and volcanoclastic metasedimentary rocks in the Lynn Lake area. Manitoba Energy and Mines, Geological Paper GP80-1, 118p.

- Green, A.G., Hajnal, Z., and Weber, W., 1985. An evolutionary model of the western Churchill province and western margin of the Superior province of Canada and the north-central United States. *Tectonophysics*, v. 116, pp. 281-322.
- Guha, J., Gauthier, A., Vallee, M., Descarreaux, J., and Lange-Brard, F., 1982. Gold mineralization patterns at the Doyon Mine (Silverstack), Bousquet, Quebec. pp. 50-57. In *Geology of Canadian Gold Deposits*, edited by R.W. Hodder and W. Petruk, Canadian Institute of Mining and Metallurgy, Special Volume 24, 286 p.
- Harper, C., Thomas, D. and Watters, B., 1986. Geology and petrochemistry of the Star Lake-Waddy Lake area, Saskatchewan. In *Gold in the Western Shield*, L.A. Clark, ed., CIM Spec. Vol.38. pp. 57-85.
- Helgeson, H.C., and Garrels, R.M., 1968. Hydrothermal transport and deposition of gold. *Economic Geology*, v. 63, pp. 622-635.
- Henley, R.W., 1973. Solubility of gold in hydrothermal chloride solutions. *Chemical Geology*, v. 11, pp. 73-87.
- Heyen, G., Ramboz C., and Dubessy, J., 1982. Simulation des equilibres de phases dans systeme $\text{CO}_2\text{-CH}_4$ en dessous de 50°C et de 500 bar. Application aux inclusion fluides. *C. R. Acad. Sc. Paris, Ser. II v 294*, 203-206.
- Ho, S.E., Groves, D.I., and Phillips, G.N., 1985. Fluid inclusions as indicators of the nature and source of

ore fluids and ore depositional conditions for Archean gold deposits of the Yilgarn block, Western Australia. Geological Society of South America, Transactions, Volume 88, pp. 149-158.

- Hoffman, P.F., 1989. Precambrian geology and tectonic history of North America. In Bally, A.W., and Palmer, A.R. (eds.), The Geology of North America - An overview. The Geology of North America, Geological Society of America, Boulder, Colorado, v. A, pp. 447-512.
- Hollister, L.S., and Burreuss, R.C., 1976. Phase equilibria in fluid inclusions from the Khtada Lake metamorphic complex. Geochimica et Cosmochimica Acta, v. 40, pp. 163-175.
- Ibrahim, M.S. and Kyser, T.K., 1991. Fluid inclusion and isotope systematics of high-temperature Proterozoic Star Lake gold deposit, northern Saskatchewan, Canada. Economic Geology, v. 86, pp. 1468-1490.
- Kenlay, D.S., 1982. Petrology, geochemistry and economic geology of selected gold claims in rocks of the Wasekwan Lake area, Lynn Lake District, Manitoba, Canada. M.Sc. thesis, University of North Dakota, 306 p.
- Kerrick, D.M., and Jacobs, G.K., 1981. A modified Redlich-Kwong equation for H₂O, CO₂, and H₂O-CO₂ mixtures at elevated pressures and temperatures. American Journal of Science, v. 281, pp. 735-767.

- Koo, J., 1976. Evaluation of massive sulphide environments in the Lynn Lake-Leaf Rapids region. Manitoba Mineral Resources Division, Report of Field Activities, pp. 14-16.
- Krauskopf, K.B., 1951. The solubility of gold. *Economic Geology*, v. 46, pp. 858-870.
- Krupka, K.M., Ohmoto, H., and Wickman, F.E., 1977. A new technique in neutron activation analysis of Na/K ratios of fluid inclusions and its application to the gold-quartz veins at the O'Brien Mine, Quebec, Canada. *Canadian Journal of Earth Sciences*, Volume 14, pp. 2760-2770.
- Lakind, J.S., and Brown, P.E., 1984. Characterization of the gold-bearing fluid at Red Lake, Ontario [abstract]. p. 80. In Program with Abstracts, Geological Association of Canada - Mineralogical Association of Canada, Volume 9, 127 p.
- Lenher, V., 1918. Further studies on the deposition of gold in nature. *Economic Geology*, v. 13, pp. 161-184.
- Lewry, J.F., 1981. La Ronge Project. II. Geology of the Stanley Shear Zone. In Summary of Investigations 1981, Saskatchewan Geological Survey. Saskatchewan Mineralogical Resources Misc. Report 81-4, pp. 28-33.
- Lewry, J.F., Stauffer, M.R., and Fumerton, S., 1981. A Cordilleran-type batholithic belt in the Churchill province in northern Saskatchewan. *Precambrian Research*, v.14, pp. 277-313.

- Lewry, J.F., and Sibbald, T.I.I., 1980. Thermotectonic Evolution of the Churchill Province in Northern Saskatchewan. In *Tectonophysics*, v. 68, pp. 45-82.
- Lister, G.S., and Snoke, A.W., 1984. S - C Mylonites. *Journal of Structural Geology*, Volume 6, pp. 617-638.
- Macdonald, R., 1987. Update on the Precambrian geology and domainal classification of northern Saskatchewan. In *Summary of Investigations 1987*, Saskatchewan Geological Survey. Saskatchewan Energy and Mines, Miscellaneous Report 87-4.
- Macdonald, A.J., and Spooner, E.T.C., 1981. Calibration of a Linkam TH 600 programmable heating-cooling stage for microthermometric examination of fluid inclusions. In *Economic Geology*, v. 76, pp. 1248-1258.
- Milligan, G.C., 1960. *Geology of the Lynn Lake District*. Manitoba Mines Branch, Publication 57-1, 317 p.
- Norman, G.W.H., 1933. Granville Lake district, northern Manitoba. *Geological Survey of Canada, Summary Report, Part C*, pp. 23-41.
- Oakes, C.S., Bodnar, R.J., and Simonson, J.M., 1990. The system $\text{NaCl-CaCl}_2\text{-H}_2\text{O}$: I. The ice liquidus at 1 atm total pressure. In *Geochimica et Cosmochimica Acta*, v. 54, pp. 603-610.
- Ogryzlo, S.P., 1935. Hydrothermal experiments with gold. *Economic Geology*, v. 30, pp. 400-424.
- Parbery, D., 1988. Investigation of volcanic stratigraphy and iron formation occurrences, Lynn Lake area.

- Manitoba Energy and Mines, Minerals Division, Report of Field Activities 1988, pp. 12-15.
- Peck, D.C., 1984. An investigation of gold mineralization at Cartwright Lake, Manitoba. Manitoba Mineral Resources Division Report of Field Activities, pp. 25-28.
- Peck, D.C., 1985. Geological investigations at Cartwright Lake, Manitoba. Manitoba Mineral Resources Division Report of Field Activities, pp. 37-40.
- Peck, D.C., 1986. The geology and geochemistry of the Cartwright Lake area. Lynn Lake greenstone belt, northern Manitoba. M.Sc. thesis, University of Windsor, 271 p.
- Phillips, G.N., Groves, D.I. and Martin, J.E., 1984. An epigenetic origin for Archean banded iron-formation-hosted gold deposits. *Economic Geology*, v. 79, pp. 162-171.
- Pinsent, R.H., 1980. Nickel-copper mineralization in the Lynn Lake gabbro. Manitoba Department of Energy and Mines, Mineral Resources Division, *Economic Geology Report ER79-3*, 138 p.
- Poulsen, K.H., Ames, K.E., Lau, S. and Brisbin, W.C., 1986. Preliminary report on the structural setting of gold in the Rice Lake area, Uchi Subprovince, southeastern Manitoba. In *Current Research, Part A, Geological Survey of Canada, Paper 86-1A*, pp. 213-220.

- Ramboz, C., Schnapper, D., and Dubessy, J., 1985. The P-V-T-X-fo₂ evolution of H₂O-CO₂-CH₄-bearing fluid in a wolframite vein. Reconstruction from fluid inclusion studies. *Geochimica et Cosmochimica Acta*, v. 49, pp. 205-219.
- Ramsay, J.G., 1980. Shear zone geometry. a review. *Journal Structural Geology*, v. 2, pp. 83-89.
- Ramsay, J.G., and Huber, M.I., 1987. The techniques of modern structural geology, volume I. strain analysis. Academic Press, Orlando, 307 p.
- Ramsay, J.G., and Huber, M.I., 1987. The techniques of modern structural geology, volume II. folds and fractures. Academic Press, Orlando, 700 p.
- Ray, G.E., and Wanless, R.K., 1980. The age and geological history of the Wollaston, Peter Lake, and Rottenstone domains in northern Saskatchewan. *Canadian Journal of Earth Sciences*, v. 17, pp. 333-347.
- Robert, F., and Kelly, W.C., 1987. Ore-forming fluids in Archean gold-bearing quartz veins at the Sigma Mine, Abitibi greenstone belt, Quebec, Canada. *Economic Geology*, Volume 82, pp. 1464-1482.
- Roedder, E., 1984. Fluid inclusion evidence on the environments of gold deposition. pp. 129-163 in *Proceedings of Gold '82: the Geology, Geochemistry, and Genesis of Gold Deposits*. Geological Society of Zimbabwe, Special Publication 1, 753 p.

- Romberger, S.B., 1984. Mechanisms of deposition of gold in low temperature hydrothermal systems. Association of Exploration Geochemists Abstracts with Program, Reno, Nevada, p. 26.
- Romberger, S.B., 1986. The solution chemistry of gold applied to the origin of hydrothermal deposits. pp. 168-186. In Gold in the Western Shield, edited by Lloyd A. Clark, Canadian Institute of Mining and Metallurgy, Special Volume 38, 537 p.
- Richardson, D.J. and Ostry, G., 1987. Gold deposits of Manitoba. Manitoba Energy and Mines, Minerals Division, Economic Geology Report ER86-1, 91 p.
- Samson, I.M. and Williams-Jones, A.E., 1988. Fluid compositions associated with syn-contact metamorphic copper mineralization, Mine Madeleine, Quebec, Canada [abstract]. Geological Society of America Programs with Abstracts, v. 20, p. A282.
- Samson, I.M. and Williams-Jones, A.E., 1991. C-O-H-N-salt fluids associated with contact metamorphism, McGerrigle Mountains, Quebec. A Raman spectroscopic study. Geochimica et Cosmochimica Acta, Vol. 55, pp. 169-177.
- Seward, T.M., 1973. Thio complexes of gold and the transport of gold in hydrothermal ore solutions. Geochimica et Cosmochimica Acta, 37, pp. 370-399.
- Seward, T.M., 1984. The transport and deposition of gold in hydrothermal systems. In Foster, R.P. (ed.), Gold '82. The Geology, Geochemistry and Genesis of Gold Deposits.

- A.A. Balkema, pp. 165-181.
- Shenberger, D.M., and Barnes, H.L., 1989. Solubility of gold in aqueous sulphide solutions from 150 to 350° C. *Geochimica et Cosmochimica Acta*, v. 53, pp. 269-278.
- Shepherd, T., 1981. Temperature-programmable, heating-freezing stage for microthermometric analysis of fluid inclusions. In *Economic Geology*, v. 76, pp. 1244-1247.
- Sherman, G.R., Samson, I.M. and Holm, P.E., 1988. Preliminary observations of a detailed geological investigation of the Gemmell Lake area, Lynn Lake. report of Field Activities 1988, Manitoba Energy and Mines, GS-3 pp. 16-19.
- Sibbald, T.I.I., 1980. NEA/IAEA test area. subAthabasca basement geology. In *Summary of Investigations 1980*, Saskatchewan Geological Survey. Saskatchewan Mineral Resources, Misc. Report 80-4, pp. 57-58.
- Sibson, R.H., 1975. Generation of pseudotachylite by ancient seismic faulting. *Geophysical Journal of the Royal Astronomical Society*, v. 43, pp. 775-794.
- Sibson, R.H., 1977. Fault rocks and fault mechanisms. *Journal Geological Society of London*, vol. I33, pp. 191-213.
- Sietz, J.C., Pasteris, J.D., and Wopenka, B, 1987. Characterization of CO₂-CH₄-H₂O fluid inclusions by microthermometry and laser Raman microprobe spectroscopy. Inferences for clathrate and fluid equilibria. *Geochimica et Cosmochimica Acta*, Vol. 51,

- pp. 1651-1664.
- Simpson, C., 1986. Determination of movement sense in mylonites. *Journal of Geological Education*, Volume 34, pp. 246-260.
- Smith, F.G., 1943. The alkali sulphide theory of gold deposition. *Economic Geology*, v. 38, pp. 561-590.
- Smith, T.J., Cloke, P.L., and Kesler, S.E., 1984. Geochemistry of fluid inclusions from the McIntyre-Hollinger gold deposit, Timmins, Ontario, Canada. *Economic Geology*, Volume 79, pp. 1265-1285.
- Stauffer, M.R., 1984. Manikewan. An Early Proterozoic ocean in central Canada, its igneous history and orogenic closure. *Precambrian Research*, v. 25, pp. 257-281.
- Steeves, M.A., and Lamb, C.F., 1972. Geology of the Issett-Opachuanau-Pemichigamau-Earp Lakes area. Manitoba Mines Branch, Publication 71-2F, 56 pp.
- Stokes, H.N., 1905. Experiments on the solution, transportation, and deposition of copper, gold, and silver. *Economic Geology*, v. 1, pp. 644-650.
- Syme, E.C., 1985. Geochemistry of metavolcanic rocks in the Lynn Lake belt. Manitoba Energy and Mines, Geological Report GR84-1, 84 p.
- Thomas, D.J. 1984. Geological mapping in the Star Lake area (part of NTS 73P-16 and 74A-1). In Summary of Investigations 1984, Saskatchewan Geological Survey, Saskatchewan Energy and Mines, Misc. Report. 84-4, pp.

21-31.

- Touret, J., 1982. An empirical phase diagram for a part of the N_2 - CO_2 system at low temperature. *Chemical Geology*, v. 37, pp. 49-58.
- Van Schmus, W.R., Persons, S.S., MacDonald, R., and Sibbald, T.I.I., 1986. Preliminary results from U-Pb zircon geochronology of the Uranium City region, northwest Saskatchewan. In *Summary of Investigations 1986, Saskatchewan Geological Survey. Saskatchewan Energy and Mines, Misc. Report. 86-4*, pp. 108-111.
- Williams-Jones, A.E., and Samson, I.M., 1990. Theoretical estimation of halite solubility in the system $NaCl$ - $CaCl_2$ - H_2O . Applications to fluid inclusions. *Canadian Mineralogist*, Vol. 28, pp. 299-304.
- Wood, P.C., Burrows, D.R., Thomas, A.V., and Spooner, E.T.C., 1986. The Hollinger-McIntyre Au-quartz vein system, Timmins, Ontario, Canada: geologic characteristics, fluid properties and light stable isotope geochemistry. In MacDonald, A.J. (ed.), *Proceedings Gold '86*. Konsult International Toronto, pp. 56-80.
- Zhang, Y.G., and Frantz, J.D., 1987. Determination of the homogenization temperatures and densities of supercritical fluids in the system $NaCl$ - KCl - $CaCl_2$ - H_2O using synthetic fluid inclusions. *Chemical Geology*, 64, pp. 335-350.

APPENDIX A
STRUCTURAL MEASUREMENTS

TABLE 1 Structural Measurements from the Wasekwan and Sickie Groups

Sickle Group				Wasekwan Group				F2 Folds			
Foliation (S1)		Lineation (L1)		Foliation (S1)		Lineation (L1)		Fold Axis		Axial Plane	
Strike	Dip	Trend	Plunge	Strike	Dip	Trend	Plunge	Trend	Plunge	Strike	Dip
250	75	65	50	305	88						
261	74	33	71	260	78						
248	74	348	74	250	78	7	76				
280	90	35	85	236	85	9	78				
280	90	35	85	242	72	335	70			25	63
283	82	15	82	243	73	21	71				
265	80	16	78	238	84						
265	73	15	72	240	84	10	72				
265	74	13	63	250	76						
264	63	22	59	225	75	355	71				
253	70	10	70	265	72						
267	60	26	56	240	78	355	88				
261	72	348	69	258	78						
248	65	25	63	235	83						
239	74	6	66	237	75	3	68				
245	75	25	74	242	78	8	72				
248	73	348	72	245	81						
261	67	38	65	231	78	5	75				
262	75	28	74	240	82	5	77			29	64
266	76	9	71	270	86	34	75			29	55
255	68	4	63	241	73	38	62	23	28		
265	70	2	69	228	78	355	71				
273	60	25	59	265	81	10	73				
280	83	14	75	253	82						
				233	83	330	83				
				240	74	335	74				
				245	61						
				245	72	345	72				
				253	77	355	77				
				270	80						
				255	68	21	66				
				247	65	0	64				
				245	74	10	71				
				245	80	10	68				
				243	78						
				230	74	4	72	10	52	15	78
				235	78	340	72	10	69	15	90
				275	74						
				220	82						
				240	78	7	66				
				241	71	0	66				
				285	87						
				245	77						

NOTE: Foliations are measured using the right hand rule

TABLE 1 (Contd) Structural Measurements from the Wasekwan and Sickle Groups

Sickle Group		Wasekwan Group				F2 Folds					
Foliation (S1)		Lineation (L1)		Foliation (S1)		Lineation (L1)		Fold Axis		Axial Plane	
strike	dip	trend	plunge	Strike	Dip	Trend	Plunge	Trend	Plunge	Strike	Dip
				238	77	280	63			9	77
				255	78	39	79				
				240	76	347	71				
				265	78	35	76				
				260	83	32	78				
				305	85						
				245	83						
				244	74	37	55				
				253	73						
				255	74	13	73				
				227	76						
				255	77						
				255	68						
				235	85						
				235	15	15	73				
				244	79						
				237	79	349	75				
				241	81	24	74				
				207	85	347	82				
				235	80	303	80				
				240	88	35	88				
				231	82						
				241	79	354	78				
				231	82	65	80				
				235	89	330	86				
				234	81	354	79				
				228	81	1	70				
				246	85	8	83				
				246	86	13	84				
				232	75	335	75				
				227	77	313	73				
				240	78	21	77				
				237	66	3	60				
				227	73	10	68				
				239	86	351	81				
				223	83						

NOTE: Foliations are measured using the right hand rule

TABLE 2 Structural Measurements in the Prospector Deformation Zone

Foliation (S1)		Lineation (L1)		Foliation (S2)		F2 Fold Axis		F2 Folds		Axial Plane		Faults		Pseudotachylite Injection Veins	
Strike	Dip	Trend	Plunge	Strike	Dip	Trend	Plunge	Strike	Dip	Strike	Dip	Strike	Dip	Strike	Dip
58	84	83	82	213	85	14	53	210	70	235	78	303	72		
42	68	103	50	214	85	2	68	204	79	232	66	324	87		
54	76			200	88	210	61	26	65	216	68	252	83		
51	86			242	90	28	69	207	63	196	64	245	83		
256	86	24	76	238	88	10	69			186	67	235	85		
263	89	31	81	210	81	30	70	25	73	232	83	340	65		
235	78	339	69	265	78	19	71	38	78	234	52	355	79		
237	80	3	72	263	81	19	58	38	70	234	76	350	79		
236	81	336	80			17	64			234	78	248	74		
239	87	356	83			16	68			234	72	275	75		
241	83	2	73			23	63			234	65	272	72		
238	83	6	77			34	70			225	72	310	81		
229	84	328	81			27	63	214	78	234	76	345	88		
232	84	353	82			14	70			216	75	280	84		
222	77	357	76			10	78			222	72	325	78		
224	85	348	83			11	64			241	75				
225	84	344	84			356	71			238	83				
222	86	16	84			1	65			230	87				
229	79	6	71			345	58			225	69				
220	83	2	75			353	77			241	81				
218	83	356	74			1	59	182	67	210	86				
224	85	5	84			348	68			223	89				
220	84	354	81			359	66			271	73				
231	85	344	78			24	85	26	88	271	81				
232	81	337	80			21	37			225	74				

NOTE: Foliations, axial planes, and faults are measured using the right hand rule
 Fault measurements include pseudotachylite fault veins

TABLE 2 (Cont'd) Structural Measurements in the Prosperor Deformation Zone

Foliation (S1)		Lineation (L1)		Foliation (S2)		F2 Folds			Faults		Pseudotachylyte Injection Veins		
Strike	Dip	Trend	Plunge	Strike	Dip	Trend	Plunge	Strike	Dip	Strike	Dip	Strike	Dip
231	72	341	71			26	60			223	83		
246	86	21	72			16	59			220	80		
212	88					18	20			226	78		
240	87					6	76	12	89	237	74		
238	83	351	83			7	67	22	74	220	71		
233	85	23	81			12	68			196	65		
235	75	22	67			12	63			210	68		
235	79	16	73			14	73			216	60		
250	82					12	58			238	69		
262	83					10	78			225	65		
242	88					359	69			221	70		
228	88					13	63			221	75		
226	86	4	77			23	63			232	79		
213	83	350	80			12	58			230	73		
224	81	1	78			13	67			212	69		
247	90	27	88			17	66			224	77		
221	85	16	83			16	78			234	79		
231	78	339	64			18	79			227	83		
207	74					41	52			214	80		
207	85					21	64			213	80		
214	82	310	80			39	70			229	81		
213	82					3	78						
231	78	339	68			8	78						
215	80	295	78			10	79						
212	64	356	60			27	69						
220	64	334	53			22	72						

NOTE: Foliations, axial planes, and faults are measured using the right hand rule
 Fault measurements include pseudotachylyte fault veins

TABLE 2 (Contd) Structural Measurements in the Prospector Deformation Zone

Foliation (S1) Strike	Lineation (L1)		Foliation (S2)		F2 Fold Axis		F2 Folds		Axial Plane		Faults		Pseudotachylyte Injection Veins	
	Dip	Trend	Plunge	Dip	Trend	Plunge	Strike	Dip	Strike	Dip	Strike	Dip	Strike	Dip
221	84	344	79		24	60								
216	71	354	63		21	64					210		86	
225	76	14	79		9	71					205		78	
228	79				8	71					214		78	
243	82	355	60		4	68					218		79	
228	77	347	72		7	76					219		71	
211	79	347	72		22	79					226		78	
205	83	356	81		22	64					230		80	
225	77	357	86		24	82					210		75	
222	88	359	88		20	58					213		74	
216	82	346	81		31	68					214		78	
220	84	353	74		45	64		230			226		67	
224	82	12	72		30	63		34			180		85	
223	77	346	72		41	58		31			164		80	
224	78	348	74		24	69		10			240		75	
216	69	356	67		18	71		6			225		78	
217	82	357	73		21	58					269		82	
233	67	329	65		4	71		31			241		83	
210	77	348	64		16	67		31			218		89	
265	80	359	75		14	68					240		72	
234	86	3	82		347	72		214						
249	87	323	85		5	75								
224	84				355	79		37			246		76	
242	85	343	76											
243	67	4	57											

NOTE: Foliations, axial planes, and faults are measured using the right hand rule
 Fault measurements include pseudotachylyte fault veins

TABLE 2 (Contd) Structural Measurements in the Prospector Deformation Zone

Foliation (S1)		Lineation (L1)		Foliation (S2)		F2 Folds			Pseudotachylyte Injection Veins		
Strike	Dip	Trend	Plunge	Strike	Dip	Trend	Plunge	Strike	Dip	Strike	Dip
240	75	0	66								
231	76	347	70								
236	78	351	69								
235	77	344	73								
230	76							245	82		
250	81	24	69					19	83		
185	78							226	86		
186	85							245	75		
262	68	16	62								
239	73										

NOTE: Foliations, axial planes, and faults are measured using the right hand rule
 Fault measurements include pseudotachylyte fault veins

TABLE 3 Structural Measurements in the Finlay McKinlay Deformation Zone

Foliation (S3)		Lineation (L3)		Quartz Vein		Fault	
Strike	Dip	Trend	Plunge	Strike	Dip	Strike	Dip
242	72			165	86		
250	65			181	86		
220	75			197	80		
220	81			358	83		
261	71			183	81		
236	52			220	76		
245	57			182	81		
235	66			203	85		
247	83			187	88		
233	73			188	85		
				187	80		
				317	38		
				187	84		
				183	84		
				173	76		
				142	51		
				181	80		
				174	84		
				205	81		
				206	78		
				215	73		

NOTE: Foliations, vein orientations and faults were measured using the right hand rule
Lineations do not correspond with adjacent foliations

TABLE 3 Structural Measurements in the Finlay McKinlay Deformation Zone

Foliation (S3)		Lineation (L3)		Quartz Vein		Fault	
Strike	Dip	Trend	Plunge	Strike	Dip	Strike	Dip
238	70	348	66	173	79		
236	70	5	56	212	78		
234	72	352	64	216	79		
223	71	344	50	215	84		
225	66	2	64	206	81		
234	67	5	56	221	81		
242	57	2	55	185	76		
236	66	1	63	176	78		
240	64	10	67	181	89		
239	67	359	77	181	81		
241	60	357	58	352	83		
249	57	355	62	319	80		
231	64	357	60	183	76		
226	68	341	60	228	76		
227	77	344	77	155	72		
228	61	357	65	231	84		
210	71	347	70	215	66		
217	68	355	65	185	74		
219	65	354	70	184	78		
219	82	348	68	175	78		
212	80	355	58	185	77		
211	76	353	58	187	70		
212	77	359	70	188	79		
212	70	25	61	181	79		
223	70	356	65	174	74		
226	78	3	55	181	89		
224	72	342	60	187	78		
230	66			191	86		
235	69	251	68	183	85		
235	70	344	73	219	82		
241	60	6	68	225	85		
239	75	16	70	212	79		
267	66	21	49	215	76		
244	78	346	81	354	77		
265	59	2	42	192	81		
271	62	7	60	176	80		
261	79	4	78	176	80		
248	72	33	65	191	73		
264	75	12	53	165	78		
250	78	331	61	182	81		
263	79	9	73	190	75		
263	56	355	71	190	73		
230	84			212	82		
241	45			194	88		

NOTE: Foliations, vein orientations and faults were measured using the right hand rule
Lineations do not correspond with adjacent foliations

TABLE 3 Structural Measurements in the Finlay McKinlay Deformation Zone

Foliation (S3)		Lineation (L3)		Quartz Vein		Fault	
Strike	Dip	Trend	Plunge	Strike	Dip	Strike	Dip
295	75	3	59	200	78	235	90
247	72	335	64	217	69	275	90
253	72	335	71	353	74	255	90
260	78	350	56	200	79	226	80
251	73	16	63	354	81	229	84
250	71	355	76	140	83	221	73
246	83	345	79	180	85	202	64
239	64	11	73	196	68	226	90
227	81	348	62	180	79	213	90
235	79	334	54	215	76	227	90
238	73	11	61	220	75	215	76
235	71	3	68	190	88	216	71
251	55	6	74	185	75	260	73
232	66	20	79	215	76	218	69
265	68	5	51	205	75	223	73
261	74	343	78	200	74	226	76
264	80	355	80	204	68		
244	67	349	71	325	90		
230	80	333	71	330	81		
231	84	355	64	205	64		
236	80	9	71	115	87		
230	72	347	70	184	71		
233	82	337	54	194	85		
251	66	0	56	205	61		
265	75	357	53	213	67		
211	82	356	62	184	87		
215	76	338	51	185	87		
216	54	355	59	345	74		
228	59	358	72	170	85		
238	55	347	73	175	77		
225	73	358	75	180	73		
225	64	352	62	205	73		
231	68	5	76	215	68		
232	80	11	74	193	73		
247	73	9	74	215	74		
244	77	9	66	225	69		
230	68	347	60	180	71		
234	82	345	68	210	76		
230	74	18	74	183	85		
230	85	358	66	175	74		
241	79	358	65	195	82		
234	74	358	63	175	68		
228	70	11	62	194	90		

NOTE: Foliations, vein orientations and faults were measured using the right hand rule
Lineations do not correspond with adjacent foliations

APPENDIX B
MICROTHERMOMETRY OF FLUID INCLUSIONS

**TABLE 1 Microthermometry of Aqueous Inclusions from Vein Set 1
Finlay McKinlay deformation zone**

Sample	Frag.	Incl.	Type	Origin	Te	Tm Ice	Th	V/L
FM88-06-21-01	A1.1	1.1	V-L	S	-	-	363	L
		1.2	V-L	S	-	-	368	L
FM88-06-21-01	A1.2	1.1	L-V	S	< -40	-4.0		
		1.2	L-V	S	< -50	-4.5		
		1.3	L-V	S	< -40	-4.5		
FM88-06-21-01	A2	1.1	L-V	S	-53.0	-7.0	390	L
		1.2	L-V	S	< -45	-6.4	276	L
		1.3	L-V-S	S	-43.0	-15.5	265	L
		1.4	L-V	S	-	-	227	L
		1.5	L-V	S	-	-	263	L
		1.6	L-V-S	S	-	-	275	L
		1.7	L-V	S	-	-	307	L
		1.8	L-V	S	-	-	333	L
		1.9	L-V	S	-	-	341	L
		2.1	L-V	S/PS	-46.0	-3.0	-	-
		2.2	L-V	S/PS	-	-3.1	-	-
		2.3	L-V	S/PS	-45.0	-3.6	175	L
		2.4	L-V	S/PS	-	-	151	L
		2.5	L-V	S/PS	-	-	151	L
2.6	L-V	S/PS	-	-	164	L		
FM88-06-21-01	A3.1	3.1	L-V	S	-23.0	-5.0	-	-
		1.1	L-V	S/PS	< -40	-3.8	199	L
		1.2	L-V	S/PS	-	-3.8	155	L
		1.3	L-V	S/PS	< -30	-3.7	151	L
		1.4	L-V	S/PS	-	-3.7	154	L
		3.1	L-V	S	-	-0.6	349	L
		3.2	L-V	S	-	-0.8	-	-
		3.3	L-V	S	-	-	409	L
		4.1	L-V	S/PS	-	-3.7	255	L
		4.2	L-V	S/PS	-	-	303	L
FM88-06-21-01	A3.2	4.3	L-V	S/PS	-	-	371	L
		1.1	L-V	S/PS	< -45	-8.9	-	-
		1.2	L-V	S/PS	-	-9.2	-	-
		1.3	L-V	S/PS	-	-8.2	289	L
		1.4	L-V	S/PS	-	-7.3	-	-
		1.5	L-V	S/PS	-	-7.1	142	L
		1.6	L-V	S/PS	-	-	155	L
		1.7	L-V	S/PS	-	-	137	L
		1.8	L-V	S/PS	-	-	213	L
		2.1	L-V	S	< -30	-9.3	120	L
2.2	L-V	S	< -30	-9.5	-	-		
2.3	L-V	S	< -30	-8.2	127	L		
2.4	L-V	S	-	-	114	L		
2.5	L-V	S	-	-	122	L		

TABLE 1 Microthermometry of Aqueous Inclusions from Vein Set 1
Finlay McKinlay deformation zone

Sample	Frag.	Incl.	Type	Origin	Te	Tm Ice	Th	V/L
FM88-06-21-01	A3.4	2.1	L-V	S/PS	< -30	-5.9		
		2.2	L-V	S/PS	-	-6.0		
		2.3	L-V	S/PS	< -30	-2.2		
		2.4	L-V	S/PS	< -30	-5.2		
		2.5	L-V	S/PS	< -45	-6.0		
		2.6	L-V	S/PS	-	-5.2		
		3.1	L-V	S/PS	-25.0	-2.8		
		3.2	L-V	S/PS	-	-3.4		
FM88-06-21-01	A3.5	2.1	L-V	S/PS	-27.2	-4.6	125	L
		2.2	L-V	S/PS	< -30	-1.4	115	L
		2.3	L-V	S/PS	< -30	-4.7	125	L
		2.4	L-V	S/PS	< -30	-3.5	125	L
		2.5	L-V	S/PS	< -30	-2.5	125	L
		2.6	L-V	S/PS	-	-	125	L
		3.1	L-V	S/PS	-	-3.5	288	L
		3.2	L-V	S/PS	-	-	176	L
		3.3	L-V	S/PS	-	-	263	L
		3.4	L-V	S/PS	-	-	271	L
FM88-06-21-01	A3.8	1.1	L-V	S		-2.8		L
		1.2	L-V	S	-27	-2.9	145	L
		1.3	L-V	S		-3.1		L
		1.4	L-V	S		2.9	158	L
FM88-06-21-01	A3.9	1.1	L-V	S	-	-1.7	215	L
		1.2	L-V	S	-	-1.7	195	L
		1.3	L-V	S	-	-1.7	-	-
		1.4	L-V	S	-	-1.7	-	-
FM88-06-21-01	A4.1	1.1	L-V	S/PS	-	-	154	L
		1.2	V-L	S/PS	-	-	303	L
		1.3	V-L	S/PS	-	-	358	L
		1.4	V-L	S/PS	-	-	393	V
FM88-06-21-01	B1.2	1.1	L-V	S	-	-	278	L
		1.2	L-V	S	-	-	295	L
		1.3	V-L	S	-	-	294	L
FM88-06-21-01	G-1	1.1	L-V	S	-	-3	175	L
		1.2	L-V	S	-	-3		
		1.3	L-V	S	-	-3		
		1.4	L-V	S	-	-3.1		
		3.1	L-V	S	-	-3.1		
		3.2	L-V	S	-	-3.1		
		3.3	L-V	S	-	-3.3		
		3.4	L-V	S	-	-3.1	115	L
3.5	L-V	S	-	-	125	L		

**TABLE 2 Calibrated Microthermometry of Aqueous Inclusion from Vein Set 1
Finlay McKinlay deformation zone**

Sample	Frag.	Incl.	Type	Origin	Te	Tm Ice	Th	V/L		
FM88-06-21-01	A1.1	1.1	V-L	S	-	-	359.3	L		
		1.2	V-L	S	-	-	364.2	L		
FM88-06-21-01	A1.2	1.1	L-V	S	< -40	-3.7				
		1.2	L-V	S	< -50	-4.2				
		1.3	L-V	S	< -40	-4.2				
FM88-06-21-01	A2	1.1	L-V	S	-53.8	-6.8	385.9	L		
		1.2	L-V	S	< -45	-6.1	273.7	L		
		1.3	L-V-S	S	-43.5	-15.4	262.9	L		
		1.4	L-V	S	-	-	225.5	L		
		1.5	L-V	S	-	-	260.9	L		
		1.6	L-V-S	S	-	-	272.7	L		
		1.7	L-V	S	-	-	304.2	L		
		1.8	L-V	S	-	-	329.8	L		
		1.9	L-V	S	-	-	337.7	L		
		2.1	L-V	S/PS	-46.6	-2.7	-	-		
		2.2	L-V	S/PS	-	-2.8	-	-		
		2.3	L-V	S/PS	-45.6	-3.3	174.3	L		
		2.4	L-V	S/PS	-	-	150.7	L		
		2.5	L-V	S/PS	-	-	150.7	L		
		2.6	L-V	S/PS	-	-	163.5	L		
		3.1	L-V	S	-23.1	-4.7	-	-		
		FM88-06-21-01	A3.1	1.1	L-V	S/PS	< -40	-3.5	197.9	L
				1.2	L-V	S/PS	-	-3.5	154.6	L
				1.3	L-V	S/PS	< -30	-3.4	150.7	L
				1.4	L-V	S/PS	-	-3.4	153.7	L
				3.1	L-V	S	-	-0.2	345.5	L
3.2	L-V			S	-	-0.4	-	-		
3.3	L-V			S	-	-	404.6	L		
4.1	L-V			S/PS	-	-3.4	253.0	L		
4.2	L-V			S/PS	-	-	300.3	L		
4.3	L-V			S/PS	-	-	367.2	L		
FM88-06-21-01	A3.2	1.1	L-V	S/PS	< -45	-8.7	-	-		
		1.2	L-V	S/PS	-	-9.0	-	-		
		1.3	L-V	S/PS	-	-8.0	286.5	L		
		1.4	L-V	S/PS	-	-7.1	-	-		
		1.5	L-V	S/PS	-	-6.9	141.8	L		
		1.6	L-V	S/PS	-	-	154.6	L		
		1.7	L-V	S/PS	-	-	136.9	L		
		1.8	L-V	S/PS	-	-	211.7	L		
		2.1	L-V	S	< -30	-9.1	120.2	L		
		2.2	L-V	S	< -30	-9.3	-	-		
		2.3	L-V	S	< -30	-8.0	127.1	L		
		2.4	L-V	S	-	-	114.3	L		
		2.5	L-V	S	-	-	122.2	L		

**TABLE 2 Calibrated Microthermometry of Aqueous Inclusions from Vein Set 1
Finlay McKinlay deformation zone**

Sample	Frag.	Incl.	Type	Origin	Te	Tm Ice	Th	V/L
FM88-06-21-01	A3.4	2.1	L-V	S/PS	< -30	-5.6		
		2.2	L-V	S/PS	-	-5.7		
		2.3	L-V	S/PS	< -30	-1.8		
		2.4	L-V	S/PS	< -30	-4.9		
		2.5	L-V	S/PS	< -45	-5.7		
		2.6	L-V	S/PS	-	-4.9		
		3.1	L-V	S/PS	-25.1	-2.5		
		3.2	L-V	S/PS	-	-3.1		
FM88-06-21-01	A3.5	2.1	L-V	S/PS	-27.2	-4.3	125.1	L
		2.2	L-V	S/PS	< -30	-1.0	115.3	L
		2.3	L-V	S/PS	< -30	-4.4	125.1	L
		2.4	L-V	S/PS	< -30	-3.2	125.1	L
		2.5	L-V	S/PS	< -30	-2.2	125.1	L
		2.6	L-V	S/PS	-	-	125.1	L
		3.1	L-V	S/PS	-	-3.2	285.5	L
		3.2	L-V	S/PS	-	-	175.3	L
		3.3	L-V	S/PS	-	-	260.9	L
		3.4	L-V	S/PS	-	-	268.8	L
FM88-06-21-01	A3.8	1.1	L-V	S		-2.5		L
		1.2	L-V	S	-27.2	-2.6	144.8	L
		1.3	L-V	S		-2.8		L
		1.4	L-V	S		3.4	157.6	L
FM88-06-21-01	A3.9	1.1	L-V	S	-	-1.3	213.7	L
		1.2	L-V	S	-	-1.3	194.0	L
		1.3	L-V	S	-	-1.3	-	-
		1.4	L-V	S	-	-1.3	-	-
FM88-06-21-01	A4.1	1.1	L-V	S/PS	-	-	153.7	L
		1.2	V-L	S/PS	-	-	300.3	L
		1.3	V-L	S/PS	-	-	354.4	L
		1.4	V-L	S/PS	-	-	388.8	V
FM88-06-21-01	B1.2	1.1	L-V	S	-	-	275.7	L
		1.2	L-V	S	-	-	292.4	L
		1.3	V-L	S	-	-	291.4	L
FM88-06-21-01	G-1	1.1	L-V	S	-	-2.7	174.3	L
		1.2	L-V	S	-	-2.7		
		1.3	L-V	S	-	-2.7		
		1.4	L-V	S	-	-2.8		
		3.1	L-V	S	-	-2.8		
		3.2	L-V	S	-	-2.8		
		3.3	L-V	S	-	-3.0		
		3.4	L-V	S	-	-2.8	115.3	L
3.5	L-V	S	-	-	125.1	L		

**TABLE 3 Summary of Microthermometry of Aqueous Type 1 Inclusions from VeinSet 1
Finlay McKinlay deformation zone**

Sample	Frag. Group	TYPE	Origin	Te		Tm Ice		Th		V/L
				#	aver.	#	aver.	#	aver.	
FM88-06-21-01	A3.2	1	S/PS	-	-	5	-7.94	5	186.3	L
FM88-06-21-01	A3.4	1	S/PS	1	-25.1	2	-2.8	2	63.46	L
FM88-06-21-01	A3.1	1	S/PS	-	-	1	-3.4	3	306.8	L
FM88-06-21-01	A3.1	1	S/PS	-	-	4	-3.45	4	164.2	L
FM88-06-21-01	A2	1	S/PS	2	-45.5	3	-2.9	4	22.5	L
FM88-06-21-01	A3.5	1	S/PS	-	-	1	-3.1	4	159.8	L
FM88-06-21-01	A3.5	1	S/PS	1	-27.2	5	-3.02	4	247.6	L
FM88-06-21-01	A3.4	1	S/PS	-	-	6	-4.77	6	123.5	L
FM88-06-21-01	A3.2	1	S	-	-	3	-8.8	4	121.5	L
FM88-06-21-01	A2	1	S	2	-48.0	3	-9.4	12	221.8	L
FM88-06-21-01	B1.2	1	S	-	-	-	-	3	286.5	L
FM88-06-21-01	A4.1	1	S/PS	-	-	-	-	3	269.5	L
FM88-06-21-01	A2	2	S	1	-23.1	1	-4.7	-	-	-
FM88-06-21-01	A3.1	2	S	-	-	2	-0.3	2	375.1	L
FM88-06-21-01	A1.1	2	S	-	-	-	-	2	361.8	L
FM88-06-21-01	A1.2	2	S	-	-	3	-4.0	2	-	-
FM88-06-21-01	A3.9	1	S	-	-	4	-1.3	2	204	L
FM88-06-21-01	A3.8	1	S	1	-27.2	4	-2.83	2	151.2	L
FM88-06-21-01	G-1	1	S	-	-	4	-2.73	1	174.3	L
FM88-06-21-01	G-1	3	S	-	-	4	-2.85	2	120.2	L

**TABLE 4 Microthermometry of Aqueous Inclusions from Vein Set 2
Finlay McKinlay deformation zone**

Sample	Frag.	Incl.	Type	Origin	Te	Tm Ice	Th	V/L
FM88-06-21-03	1.0	1.1	L-V	S	-	-0.4	285	L
		2.1	L-V	S	-	-0.6	248	L
		2.2	L-V	S	-	-0.6	-	-
		2.3	L	S	-	-1.5	-	-
		2.4	L-V	S	-	-	143	L
		2.5	L-V	S	-	-	312	L
FM88-06-21-03	2.0	2.6	L-V	S	-	-	354	L
		1.1	L-V	S	-22	-1.6	313	L
		1.2	L-V	S	< -30	-1.8	372	L
		1.3	L-V	S	-	-1.4	225	L
		1.4	L-V	S	-	-	255	L
		1.5	L-V	S	-	-	265	L
FM88-06-21-03	3.0	1.6	L-V	S	-	-	296	L
		1.1	L-V	S	-35	-3.5	184	L
		1.2	L-V	S	-35	-3.4	193	L
		1.3	L-V	S	-	-3.4	212	L
		1.4	L-V	S	-	-3.4	176	L
		1.5	L-V	S	-	-3.4	-	-
FM88-06-21-03	4.0	1.6	L-V	S	-	-3.4	-	-
		1.7	L-V	S	-	-	162	L
		1.8	L-V	S	-	-	175	L
		1.1	L-V	S	-27	-0.6	269	L
		1.2	L-V	S	-	-0.4	-	-
		1.3	L-V	S	-	-0.5	156	L
FM88-06-21-03	6.0	1.4	L-V	S	-	-	152	L
		1.5	L-V	S	-	-	285	L
		2.1	L-V	S	-	-0.9	158	L
		2.2	L-V	S	-	0.5	142	L
		2.3	L-V	S	> -30	-0.9	-	-
		2.4	L-V	S	-	-	152	L
FM88-06-21-03	7.0	2.5	L-V	S	-	-	163	L
		2.6	L-V	S	-	-	183	L
		1.1	L-V	S	-	-0.4	152	L
		1.2	L-V	S	-	-0.6	184	L
		1.3	L-V	S	-22	-0.4	-	-
		1.4	L-V	S	-19	-0.5	172	L
		1.5	L-V	S	-20	-0.4	181	L
		1.6	L-V	S	-	-0.4	-	-
		1.7	L-V	S	-	-0.5	-	-
		1.8	L-V	S	-	-0.4	153	L
		1.9	L-V	S	-	-0.4	153	L
1.10	L-V	S	-	-	126	L		
1.11	L-V	S	-	-	134	L		

**TABLE 4 Microthermometry of Aqueous Inclusions from Vein Set 2
Finlay McKinlay deformation zone**

Sample	Frag.	Incl.	Type	Origin	Te	Tm Ice	Th	V/L
FM88-06-21-03	7.0	3.1	L-V	S	-	-	255	L
		3.2	L-V	S	-	-0.4	-	-
		3.3	L-V	S	-	-	322	L
FM88-06-21-03	8.0	1.1	L-V	S	-30	-0.7	195	L
		1.2	L-V	S	-	-0.6	226	L
		1.3	L-V	S	< -20	-0.5	-	-
		1.4	L-V	S	-25	-0.9	-	-
		1.5	L-V	S	-	-0.8	225	L
		1.6	L-V	S	-	-	195	L
		1.7	L-V	S	-	-	262	L
		1.8	L-V	S	-	-	275	L
FM88-06-21-06	2	1.1	L-V	S	-	-0.7	162	L
		1.2	L-V	S	-	-1.2	-	-
		1.3	L-V	S	-	-0.8	-	-
		1.4	L-V	S	-	-	151	L
	3	1.1	L-V	S	-	-3.6	135	L
		1.2	L-V	S	-	-3.7	-	-
		1.3	L-V	S	-	-3.5	-	-
		2.1	L-V	S	-	-2.5	-	-
	6	2.2	L-V	S	-	-	116	L
		2.3	L-V	S	-	-	131	L
		2.4	L-V	S	-	-	135	L
		3.1	L-V	S	-	-2.9	-	-
		3.2	L-V	S	-	-	140	L
		3.3	L-V	S	-	-	151	L
FM88-06-27-02b	1.1	3.4	L-V	S	-	-	152	L
		1.1	L-V	S	-19.0	-1.0	135	L
		1.2	L-V	S	-	-	142	L
		1.3	L-V	S	-	-	118	L
		1.4	L-V	S	-	-	128	L
		1.5	L-V	S	-	-	123	L
		1.6	L-V	S	-	-	123	L
		1.7	L-V	S	-	-	123	L
		1.8	L-V	S	-	-	124	L
		1.9	L-V	S	-	-	125	L
1.10	L-V	S	-	-	156	L		
FM88-06-27-02b	1.1	2.1	V-L	S	-26.0	-3.6	-	-
FM88-06-27-02b	1.2	1.1	L-V	S	-21.0	-3.6	-	-
		1.2	L-V	S	-19.0	-	181	L
		1.3	L-V	S	-	-	137	L
		1.4	S	S	-	-	111	L
		1.5	S	S	-	-	125	L

**TABLE 4 Microthermometry of Aqueous Inclusions from Vein Set 2
Finlay McKinlay deformation zone**

Sample	Frag.	Incl.	Type	Origin	Te	Tm Ice	Th	V/L
FM88-06-27-02b	1.5	1.1	L-V	S	-	-	124	L
		1.2	L-V	S	-	-	128	L
		1.3	L-V	S	-	-	138	L
		1.4	L-V	S	-	-	135	L
		1.5	L-V	S	-	-	124	L
FM88-06-27-02b	1.6	1.6	L-V	S	-	-	118	L
		2.1	L-V	S	-15.0	-1.1	147	L
		2.2	L-V	S	-	-1.5	145	L
		2.3	L-V	S	-	-	133	L
		2.4	L-V	S	-	-	135	L
		2.5	L-V	S	-	-	145	L
		2.6	L-V	S	-	-	129	L
		2.7	L-V	S	-	-	135	L
		2.8	L-V	S	-	-	114	L
		2.9	L-V	S	-	-	142	L
FM88-06-27-02b	1.7	2.10	L-V	S	-	-	156	L
		3.1	L-V	S	-	-1.0	155	L
		1.4	L-V	S	-	-	114	L
		1.6	L-V	S	-	-2.7	155	L
		1.7	L-V	S	-	-0.8	161	L
FM88-06-27-02b	2.2	1.9	L-V	S	-	-3.8	136	L
		1.10	L-V	S	-	-9.2	163	L
		1.1	L-V	S	-29.0	-0.9	213	L
		1.2	L-V	S	-22.0	-0.9	155	L
		1.3	L-V	S	-	-1	203	L
		1.4	L-V	S	-	-1.2	163	L
		1.5	L-V	S	-	-1	165	L
FM88-06-27-02b	2.3	2.1	L-V	S	-	-	125	L
		2.2	L-V	S	-	-	125	L
		2.5	L-V	S	-	-	123	L
		2.6	L-V	S	-	-	115	L
		2.1	L	S	-88	-44	45	L
		2.2	L	S	-84	-46.8	44.8	L
		2.3	L	S	-	-43.6	-	L
		2.4	L	S	-84	-43.2	50	L
		2.5	L	S	-75	-43	42	L
		2.6	L	S	-85	-45.9	46	L
		2.7	L	S	-75	-43.2	46	L
2.8	L	S	-	-	43	L		
3.1	L-V	S	-	-1.0	-	-		
3.2	L-V	S	-	-0.9	-	-		
4.1	L-V	S	-	-0.6	-	-		

**TABLE 4 Microthermometry of Aqueous Inclusions from Vein Set 2
Finlay McKinlay deformation zone**

Sample	Frag.	Incl.	Type	Origin	Te	Tm Ice	Th	V/L
		6.1	L	S		-43.9	32	L
		6.2	L	S		-43.9	38	L
		6.3	L	S	-	-44.3	44	L
		6.4	L	S	-	-	34	L
		6.5	L	S	-	-43.9		
		6.6	L	S	-	-	37	L
		6.7	L	S	-	-43.9		
		6.8	L	S	-	-43.9		
		8.1	L	S	-	-42.5	38	L
		8.2	L	S	-	-43.8		
		8.3	L	S	-		32	L
FM88-06-27-02b	2.5	1.1	L-V	S			115	L
		1.2	L-V	S			115	L
		1.3	L-V	S			129	L
		1.4	L-V	S			128	L
		1.5	L-V	S			155	L
		2.1	L-V	S		-1	176	L
		2.2	L-V	S		-1.1	165	L
		2.3	L-V	S		-1		
		2.4	L-V	S		-1.1		
		2.5	L-V	S			155	L
		2.6	L-V	S			155	L

**TABLE 5 Microthermometry of Aqueous Inclusions from Vein Set 2
Finlay McKinlay deformation zone**

Sample	Frag.	Incl.	Type	Origin	Te	Tm Ice	Th	V/L
FM88-06-21-03	1.0	1.1	L-V	S	-	-0.0	282.6	L
		2.1	L-V	S	-	-0.2	246.2	L
		2.2	L-V	S	-	-0.2	-	-
		2.3	L	S	-	-1.1	-	-
		2.4	L-V	S	-	-	142.8	L
		2.5	L-V	S	-	-	309.1	L
FM88-06-21-03	2.0	2.6	L-V	S	-	-	350.5	L
		1.1	L-V	S	-22.1	-1.2	310.1	L
		1.2	L-V	S	< -30	-1.4	368.2	L
		1.3	L-V	S	-	-1.0	223.5	L
		1.4	L-V	S	-	-	253.0	L
		1.5	L-V	S	-	-	262.9	L
FM88-06-21-03	3.0	1.6	L-V	S	-	-	293.4	L
		1.1	L-V	S	-35.4	-3.2	183.2	L
		1.2	L-V	S	-35.4	-3.1	192.0	L
		1.3	L-V	S	-	-3.1	210.7	L
		1.4	L-V	S	-	-3.1	175.3	L
		1.5	L-V	S	-	-3.1	-	-
FM88-06-21-03	4.0	1.6	L-V	S	-	-3.1	-	-
		1.7	L-V	S	-	-	161.5	L
		1.8	L-V	S	-	-	174.3	L
		1.1	L-V	S	-27.2	-0.2	266.8	L
		1.2	L-V	S	-	-0.0	-	-
		1.3	L-V	S	-	-0.1	155.6	L
FM88-06-21-03	6.0	1.4	L-V	S	-	-	151.7	L
FM88-06-21-03	6.0	1.5	L-V	S	-	-	282.6	L
FM88-06-21-03	6.0	2.1	L-V	S	-	-0.5	157.6	L
		2.2	L-V	S	-	0.9	141.8	L
		2.3	L-V	S	> -30	-0.5	-	-
		2.4	L-V	S	-	-	151.7	L
		2.5	L-V	S	-	-	162.5	L
		2.6	L-V	S	-	-	182.2	L
FM88-06-21-03	7.0	1.1	L-V	S	-	-0.0	151.7	L
		1.2	L-V	S	-	-0.2	183.2	L
		1.3	L-V	S	-22.1	-0.0	-	-
		1.4	L-V	S	-19.0	-0.1	171.4	L
		1.5	L-V	S	-20.0	-0.0	180.2	L
		1.6	L-V	S	-	-0.0	-	-
		1.7	L-V	S	-	-0.1	-	-
		1.8	L-V	S	-	-0.0	152.7	L
		1.9	L-V	S	-	-0.0	152.7	L
		1.10	L-V	S	-	-	126.1	L
		1.11	L-V	S	-	-	134.0	L

**TABLE 5 Microthermometry of Aqueous Inclusions from Vein Set 2
Finlay McKinlay deformation zone**

Sample	Frag.	Incl.	Type	Origin	Te	Tm Ice	Th	V/L
FM88-06-21-03	7.0	3.1	L-V	S	-	-	253.0	L
		3.2	L-V	S	-	-0.0	-	-
		3.3	L-V	S	-	-	319.0	L
FM88-06-21-03	8.0	1.1	L-V	S	-30.3	-0.3	194.0	L
		1.2	L-V	S	-	-0.2	224.5	L
		1.3	L-V	S	< -20	-0.1	-	-
		1.4	L-V	S	-25.1	-0.5	-	-
		1.5	L-V	S	-	-0.4	223.5	L
		1.6	L-V	S	-	-	194.0	L
		1.7	L-V	S	-	-	259.9	L
		1.8	L-V	S	-	-	272.7	L
FM88-06-21-06	2	1.1	L-V	S	-	-0.3	161.528	L
		1.2	L-V	S	-	-0.8	-	-
		1.3	L-V	S	-	-0.4	-	-
		1.4	L-V	S	-	-	150.70	L
	3	1.1	L-V	S	-	-3.3	134.96	L
		1.2	L-V	S	-	-3.4	-	-
		1.3	L-V	S	-	-3.2	-	-
		2.1	L-V	S	-	-2.2	-	-
	6	2.2	L-V	S	-	-	116.26	L
		2.3	L-V	S	-	-	131.05	L
		2.4	L-V	S	-	-	134.96	L
		3.1	L-V	S	-	-2.6	-	-
FM88-06-27-02b	1.1	3.2	L-V	S	-	-	139.88	L
		3.3	L-V	S	-	-	150.70	L
		3.4	L-V	S	-	-	151.69	L
		1.1	L-V	S	-19.0	-0.6	135.0	L
		1.2	L-V	S	-	-	141.8	L
		1.3	L-V	S	-	-	118.2	L
		1.4	L-V	S	-	-	128.1	L
		1.5	L-V	S	-	-	123.2	L
		1.6	L-V	S	-	-	123.2	L
		1.7	L-V	S	-	-	123.2	L
FM88-06-27-02b	1.1	1.8	L-V	S	-	-	124.1	L
		1.9	L-V	S	-	-	125.1	L
FM88-06-27-02b	1.2	1.10	L-V	S	-	-	155.6	L
		2.1	V-L	S	-26.2	-3.3	-	-
		1.1	L-V	S	-21.1	-3.3	-	-
		1.2	L-V	S	-19.0	-	180.2	L
		1.3	L-V	S	-	-	136.9	L
FM88-06-27-02b	1.2	1.4	S	S	-	-	111.3	L
		1.5	S	S	-	-	125.1	L

**TABLE 5 Microthermometry of Aqueous Inclusions from Vein Set 2
Finlay McKinlay deformation zone**

Sample	Frag.	Incl.	Type	Origin	Te	Tm Ice	Th	V/L
FM88-06-27-02b	1.5	1.1	L-V	S	-	-	124.1	L
		1.2	L-V	S	-	-	128.1	L
		1.3	L-V	S	-	-	137.9	L
		1.4	L-V	S	-	-	135.0	L
		1.5	L-V	S	-	-	124.1	L
		1.6	L-V	S	-	-	118.2	L
FM88-06-27-02b	1.6	2.1	L-V	S	-14.9	-0.7	146.8	L
		2.2	L-V	S	-	-1.1	144.8	L
		2.3	L-V	S	-	-	133.0	L
		2.4	L-V	S	-	-	135.0	L
		2.5	L-V	S	-	-	144.8	L
		2.6	L-V	S	-	-	129.1	L
		2.7	L-V	S	-	-	135.0	L
		2.8	L-V	S	-	-	114.3	L
		2.9	L-V	S	-	-	141.8	L
		2.10	L-V	S	-	-	155.6	L
		3.1	L-V	S	-	-0.6	154.6	L
FM88-06-27-02b	1.7	1.4	L-V	S	-	-	114.3	L
		1.6	L-V	S	-	-2.7	154.6	L
		1.7	L-V	S	-	-0.8	160.5	L
		1.9	L-V	S	-	-3.8	135.9	L
FM88-06-27-02b	2.2	1.10	L-V	S	-	-9.2	162.5	L
		1.1	L-V	S	-29.2	-0.5	211.7	L
		1.2	L-V	S	-22.1	-0.5	154.6	L
		1.3	L-V	S	-	-0.6	201.9	L
		1.4	L-V	S	-	-0.8	162.5	L
		1.5	L-V	S	-	-0.6	164.5	L
		2.1	L-V	S	-	-	125.1	L
FM88-06-27-02b	2.3	2.2	L-V	S	-	-	125.1	L
		2.5	L-V	S	-	-	123.2	L
		2.6	L-V	S	-	-	115.3	L
		2.1	L	S	-89.5	-44.6	46.4	L
		2.2	L	S	-85.4	-47.4	46.2	L
		2.3	L	S	-	-44.2	-	L
		2.4	L	S	-85.4	-43.7	51.3	L
		2.5	L	S	-76.2	-43.5	43.4	L
		2.6	L	S	-86.5	-46.5	47.4	L
		2.7	L	S	-76.2	-43.7	47.4	L
		2.8	L	S	-	-	44.4	L
3.1	L-V	S	-	-0.6	-	-		
3.2	L-V	S	-	-0.5	-	-		
4.1	L-V	S	-	-0.2	-	-		

**TABLE 5 Microthermometry of Aqueous Inclusions from Vein Set 2
Finlay McKinlay deformation zone**

Sample	Frag.	Incl.	Type	Origin	Te	Tm Ice	Th	V/L
		6.1	L	S		-44.5	33.6	L
		6.2	L	S		-44.5	41.0	L
		6.3	L	S	-	-44.9	45.4	L
		6.4	L	S	-	-	35.6	L
		6.5	L	S	-	-44.5		
		6.6	L	S	-	-	38.5	L
		6.7	L	S	-	-44.5		
		6.8	L	S	-	-44.5		
		8.1	L	S	-	-43.0	39.5	L
		8.2	L	S	-	-44.4		
		8.3	L	S	-		33.6	L
FM88-06-27-02b	2.5	1.1	L-V	S			115.3	L
		1.2	L-V	S			115.3	L
		1.3	L-V	S			129.1	L
		1.4	L-V	S			128.1	L
		1.5	L-V	S			154.6	L
		2.1	L-V	S		-0.6	175.3	L
		2.2	L-V	S		-0.7	164.5	L
		2.3	L-V	S		-0.6		
		2.4	L-V	S		-0.7		
		2.5	L-V	S			154.6	L
		2.6	L-V	S			154.6	L

TABLE 6 Summary of Microthermometry of Aqueous Inclusions from VeinSet 2
Finlay McKinlay deformation zone

Sample	Frag.	Group	TYPE	Origin	Te		Tm Ice		Th		V/L				
					#	aver.	sd.	#	aver.	sd.		#	aver.	sd.	
FM88-06-21-03	7.0	2.0	1/4	S	-	-	-	-	1	182.2	-	L			
FM88-06-21-03	7.0	3.0	2/4	S	-	-	-	1	0.00	-	-	L			
FM88-06-21-03	6.0	1.0	1	S	-	-	-	-	-	1	282.6	L			
FM88-06-21-03	6.0	2.0	1	S	-	< -30	-	3	-0.03	0.81	-	L			
FM88-06-21-03	3.0	1.0	1	S	2	-34.4	0.0	6	-3.1	0.64	4	153.4	8.91	L	
FM88-06-21-03	2.0	1.0	1	S	1	-22.1	-	3	-1.2	0.2	4	182.8	17.0	L	
FM88-06-21-03	7.0	1.0	1	S	3	-20.3	1.58	9	-0.04	0.07	6	285.2	50.83	L	
FM88-06-21-03	8.0	1.0	1	S	2	-27.7	3.6	4	-0.3	0.16	8	156.5	20.63	L	
FM88-06-21-03	4.0	1.0	2	S	1	-27.2	-	3	-0.1	0.10	6	228.0	32.7	L	
FM88-06-21-03	1.0	2.0	2	S	-	-	-	3	-0.5	0.52	2	153.7	2.76	L	
FM88-06-21-03	1.0	1.0	2	S	-	-	-	1	0	-	4	262.2	90.39	L	
FM88-06-21-06	2	1	1	S	-	-	-	3	-0.5	0.26	1	282.6	-	L	
FM88-06-21-06	3	1	1	S	-	-	-	3	-3.3	0.1	2	156.1	7.64	L	
FM88-06-21-06	3	2	1	S	-	-	-	1	-2.2	-	1	140	-	L	
FM88-06-21-06	6	3	1	S	-	-	-	1	-2.6	-	3	127.5	9.8	L	
FM88-06-27-02B	1.1	1.0	1.0	S	1	-19	-	1	-0.6	-	3	147.4	6.54	L	
		2.0	2.0	S	1	-26.2	-	1	-3.3	-	10	129.8	11.35	L	
FM88-06-27-02B	1.2	1.0	1.0	S	2	-20.1	1.48	1	-3.3	-	4	138.4	29.78	L	
FM88-06-27-02B	1.5	1.0	1.0	S	-	-	-	-	-	-	6	127.8	7.15	L	
FM88-06-27-02B	1.6	1.0	1.0	S	1	-14.9	-	2	-0.9	0.28	10	138.0	11.44	L	
		3.0	3.0	S	-	-	-	1	-0.6	-	1	154.6	-	L	
FM88-06-27-02B	1.7	1.0	1.0	S	-	-	-	3	-2.4	1.52	5	145.6	20.39	L	
FM88-06-27-02B	2.2	1	1	S	2	-25.7	5.02	5	-0.6	0.122	5	179	25.8	L	
FM88-06-27-02B	2.2	2	2	S	-	-	-	-	-	-	4	122.2	4.67	L	
FM88-06-27-02B	2.3	2	2	S	6	-83.2	5.63	7	-44.8	1.54	7	46.6	2.54	L	
FM88-06-27-02B	2.3	3	3	S	-	-	-	2	-0.55	0.071	-	-	-	-	-
FM88-06-27-02B	2.3	4	4	S	-	-	-	1	-0.2	-	-	-	-	-	-
FM88-06-27-02B	2.3	6	6	S	-	-	-	6	-44.6	0.163	5	38.8	4.63	L	
FM88-06-27-02B	2.3	8	8	S	-	-	-	2	-43.7	0.99	2	36.6	4.27	L	
FM88-06-27-02B	2.5	1	1	S	-	-	-	4	-0.65	0.058	5	128.5	16	L	
FM88-06-27-02B	2.5	2	2	S	-	-	-	4	-0.65	0.058	4	162.3	9.87	L	

TABLE 7 Microthermometry of Mixed Aqueous-Carbonic Inclusions from Vein Set 1
Finlay McKinlay deformation zone

Sample	Frag.	Incl.	Type	Origi	Tm CO2	Tm Clat	Th CO2	V/L	Tm Ice	Th	V/L	Td	
FM88-06-21-01	A3.4	4.1	L	S	-57.2	8.0	1.8	L	-	-	-	-	
		4.2	L-L	S	-57.2	8.3	8.9	L	-	-	-	-	
		4.3	L-L	S	-57.3	9.6	-0.5	L	-	-	-	-	
		4.4	L-L	S	-57.7	8.8	0.9	L	-	-	-	-	
		4.5	L-L	S	-57.6	-	13.4	L	-	-	-	-	
		A3.5	5.1	L-L	S	-57.3	8.3	21.3	L	-	-	-	-
			5.2	L-L-V	S	-57.2	-	22.8	L	-	-	-	-
			5.3	L-L	S	-57.1	-	22.8	L	-	-	-	-
			5.4	L-L	S	-57.2	-	22.0	L	-	-	-	-
			5.5	L-L	S	-57.3	-	-	-	-	-	-	-
5.6	L	S	-57.1	-	20.8	L	-	-	-	-			
5.7	L-L	S	-57.2	-	20.8	L	-	-	-	-			
5.8	L-L	S	-57.1	-	-	-	-	-	-	-			
5.9	L-L	S	-57.4	-	21.0	L	-	-	-	-			
5.10	L-L	S	-56.9	6.0	-	-	-	-	-	-			
FM88-06-21-01	A3.8	6.1	L	S	-57.1	-	22.0	L	-	-	-	-	
		6.2	L	S	-57.1	-	21.3	L	-	-	-	-	
		6.3	L-L	S	-57.1	-	23.4	L	-	-	-	-	
		6.4	L	S	-57.3	-	21.5	L	-	-	-	-	
		6.5	L-L	S	-57.2	-	24.5	L	-	-	-	-	
		6.6	L-L	S	-57.2	-	23.3	L	-	-	-	-	
		1.1	L-L	S	-57.2	8.4	10.5	L	-	-	-	-	
		1.2	L-L	S	-55.5	-	-	-	-	-	-	-	
		1.3	L	S	-55.5	-	-	-	-	-	-	-	
		1.4	L-L	S	-	-	6.0	-	-	-	-	-	
FM88-06-21-01	G-1	2.1	L-L	S	-56.3	-	13.3	L	-	-	-	295	
		2.2	L-L	S	-56.3	-	14.3	L	-	-	-	295	
		2.3	L-L	S	-56.4	-	13.1	L	-	-	-	-	
		2.4	L-L	S	-56.3	-	8.6	L	-	-	-	305	
		2.5	L-L	S	-56.3	-	17.1	L	-	-	-	305	
		2.6	L-L	S	-56.3	-	13.2	L	-	-	-	-	
		2.7	L-L	S	-	-	18.7	L	-	-	-	-	
2.8	L-L	S	-	-	15.9	L	-	-	-	-	295		
2.9	L-L	S	-	-	16.4	L	-	-	-	-	-		

TABLE 8 Calibrated Microthermometry of Mixed Aqueous-Carbonic Inclusions from Vein Set 1
Finlay McKinlay deformation zone

Sample	Frag.	Incl.	Type	Origl	Tm	CO ₂	Tm	Clat	Th	CO ₂	V/L	Tm	Ice	Th	V/L	Td	
FM88-06-21-01	A3.4	4.1	L	S	-58.1	8.6		2.2			L						
		4.2	L-L	S	-58.1	8.9		9.5			L						
		4.3	L-L	S	-58.2	10.2		-0.1			L						
		4.4	L-L	S	-58.6	9.4		1.3			L						
		4.5	L-L	S	-58.5	-		14.1			L						
	A3.5	5.1	L-L	S	-58.2	8.9		22.2			L						
		5.2	L-L-V	S	-58.1	-		23.7			L						
		5.3	L-L	S	-58.0	-		23.7			L						
		5.4	L-L	S	-58.1	-		22.9			L						
		5.5	L-L	S	-58.2	-		-			L						
FM88-06-21-01	A3.8	5.6	L	S	-58.0	-		21.7		L							
		5.7	L-L	S	-58.1	-		21.7		L							
		5.8	L-L	S	-58.0	-		-			L						
		5.9	L-L	S	-58.3	-		21.9			L						
		5.10	L-L	S	-57.7	6.5		-			L						
		6.1	L	S	-58.0	-		22.9			L						
		6.2	L	S	-58.0	-		22.2			L						
		6.3	L-L	S	-58.0	-		24.3			L						
		6.4	L	S	-58.2	-		22.4			L						
		6.5	L-L	S	-58.1	-		25.4			L						
FM88-06-21-01	A3.8	6.6	L-L	S	-58.1	-		24.2		L							
		1.1	L-L	S	-58.1	9.0		11.1			L						
		1.2	L-L	S	-56.3	-		-			L						
		1.3	L	S	-56.3	-		-			L						
FM88-06-21-01	G-1	1.4	L-L	S	-	-		6.5		L							
		2.1	L-L	S	-57.1	-		14.0		L						292.4	
		2.2	L-L	S	-57.1	-		15.0		L						292.4	
		2.3	L-L	S	-57.2	-		13.8		L						-	
		2.4	L-L	S	-57.1	-		9.2		L						302.24	
		2.5	L-L	S	-57.1	-		13.8		L						302.24	
		2.6	L-L	S	-57.1	-		13.9		L						-	
2.7	L-L	S	-	-		19.5		L						-			
2.8	L-L	S	-	-		16.7		L						292.4			
2.9	L-L	S	-	-		17.2		L						-			

**TABLE 9 Microthermometry of Mixed Aqueous-Carbonic Inclusions from Vein Set 2
Finlay McKinlay deformation zone**

Sample	Frag.	Incl.	Type	Origl	Tm CO2	Tm Clat	Th CO2	V/L	Tm Ice	Th	V/L	Td
FM88-06-27-02b	1.3	1.1	L-L	S	-55.6	7.8	3.1	L
		1.2	L-L	S	-55.5	5.7	4.5	L
		1.3	L-L	S	-55.6	5.4	1.9	L
		1.4	L-L	S	-55.5	6.1	4.4	L
		1.5	L-L	S	-55.6
		1.6	L-L	S	-55.6	6.8	7.4	L
		1.7	L	S
		1.8	L	S
		1.9	L-L	S	-55.6	.	13.0	L
		1.10	L	S
		1.11	L-L	S	-55.6	.	8.2	L
		1.12	L-L	S	-55.6	10.4	12.5	L

TABLE 10 Calibrated Microthermometry of Mixed Aqueous-Carbonic Inclusions from Vein Set 2
Finlay McKinlay deformation zone

Sample	Frag.	Incl.	Type	Origi	Tm CO2	Tm Ciat	Th CO2	V/L	Tm Ice	Th	V/L	Td
FM89-06-27-02b	1.3	1.1	L-L	S	-56.4	9.0	3.6	L
		1.2	L-L	S	-56.3	6.2	5.0	L
		1.3	L-L	S	-56.4	5.9	2.3	L
		1.4	L-L	S	-56.3	6.6	4.9	L
		1.5	L-L	S	-56.4
		1.6	L-L	S	-56.4	7.4	8.0	L
		1.7	L	S
		1.8	L	S
		1.9	L-L	S	-56.4	.	13.7	L
		1.10	L	S
		1.11	L-L	S	-56.4	.	8.8	L
		1.12	L-L	S	-56.4	11.0	13.2	L

TABLE 11 Summary of Mixed Aqueous-Carbonic Inclusions

Sample	Carbonic Inclusions	Frag. Incl.	Tm CO ₂		Tm Clath.		Th CO ₂	V/L	Td				
			# aver.	sd.	# aver.	sd.				# aver.	sd.		
FM88-06-21-01	A3.4	4.0	5	-58.3	0.23	4	9.3	0.7	5	5.4	6.12	L	
FM88-06-21-01	A3.5	5.0	10	-58.1	0.16	2	7.7	1.7	7	22.5	0.89	L	
FM88-06-21-01	A3.5	6.0	6	-58.1	0.08	-	-	-	6	23.6	1.26	L	
FM88-06-21-01	A3.9	1.0	3	-56.9	1.39	1	9.0	-	2	8.8	3.25	L	
FM88-06-21-01	G-1	2	6	-57.1	0.04	-	-	-	9	14.8	2.88	L	
FM88-06-27-02B		1.3	1.0	10	-56.4	0.04	6	7.7	1.97	8	7.44	4.28	L

GEORGE R. SHERMAN

EDUCATION:

Undergraduate University of Windsor
Honours Bachelor of Science Degree - Geology

Thesis: Mineralization and alteration associated with
Rook Lake Deformation Zone, Mishibishu Lake
greenstone belt, Wawa, Ontario

Graduate University of Windsor
Masters of Science Degree - Geology

Thesis: Geology, hydrothermal activity and gold
mineralization in the Gemmell Lake area of
the Early Proterozoic, Lynn Lake
greenstone belt, Manitoba

EMPLOYMENT:

April 1991 to January 1992	Geologist The Dragun Corporation 30445 Northwestern Hwy. Suite 260 Farmington Hills, MI 48334
September 1990 to April 1991 September 1989 to August 1990 September 1988 to April 1989	Graduate Assistant University of Windsor
May to August 1990 May to August 1989	Research Assistant University of Windsor
May to September 1988	Geologist Lynngold Resources Inc. Lynn Lake, Manitoba
June to September 1987	Junior Assistant Ontario Geological Survey 77 Grenville, Toronto, Ontario
June to September 1986	Junior Assistant Ontario Geological Survey 77 Grenville, Toronto, Ontario

PUBLICATIONS:

Government Reports:

Sherman, G.R., Samson, I.M. and Holm, P.E., 1988, Preliminary observations of a detailed geological investigation of the Gemmell Lake area, Lynn Lake. Report of Field Activities 1988, Manitoba Energy and Mines, GS-3, pp. 16-19.

Sherman, G.R., Samson, I.M. and Holm, P.E., 1989, Deformation, veining and gold mineralization along part of the Johnson Shear Zone, Lynn Lake Greenstone Belt, Manitoba; Report of Field Activities 1989, Manitoba Energy and Mines, GS-3, pp. 16-18.

Abstracts:

Sherman, G.R., Holm, P.E. and Samson, I.M., 1990, Vein textures and pseudotachylite within an auriferous, Proterozoic, brittle-ductile shear zone, Lynn Lake greenstone belt, Manitoba, Canada: evidence of seismic pumping?; GSA 1990 abstr. with Prog. 1990, A40.

Sherman, G.R., Samson, I.M. and Holm, P.E., 1990, Hydrothermal activity and Au-quartz veining within a brittle-ductile shear zone in the Proterozoic, Lynn Lake greenstone belt, Manitoba; GAC-MAC abstr. & Prog., 1990

Sherman, G.R. and Samson, I.M., 1990, Fluid Evolution in an auriferous, brittle-ductile shear zone in the Proterozoic, Lynn Lake greenstone belt, Manitoba: evidence from fluid inclusions in quartz veins; PACROFI III abstr. & Prog., 1990.